Saclay: Pollen and fungal spore monitoring

Finnian Neeson BSc, PGDip

Thesis Submitted for the MSc Degree

Supervisor:

Dr David O'Connor, Dublin City University

School of Chemical Sciences

January 2024

School of Chemical Sciences

Declaration

I hereby certify that this material, which I now submit for assessment on the programme of study leading to the award of MSc is entirely my own work, and that I have exercised reasonable care to ensure that the work is original, and does not to the best of my knowledge breach any law of copyright, and has not been taken from the work of others save and to the extent that such work has been cited and acknowledged within the text of my work.

Signed: Finnian Neeson 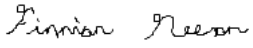

(Candidate) ID NO: 21270576

Date: 03/01/2024

Table of Contents

List of abbreviations and acronyms 4
List of Figures 5
List of Tables 9
Acknowledgements 10
Abstract 11
Chapter 1 - Introduction 12
1.1 Bioaerosols Overview 12
1.2 Release, Transport and Deposition 20
1.3 Chemical and Physical Properties of PBAPs 26
1.4 Impacts of Bioaerosols 29
1.4.1 Health 29
1.4.2 PBAPs Interaction with Air Pollution 35
1.4.3 Weather/ Climate 38
1.5 Bioaerosol Monitoring 39
1.5.1 Traditional 39
1.5.2 Real-Time 44
1.6 Modelling and Forecasting 50
References 58
Chapter 2 – Methodology 67
2.1 Sampling site 67
2.2 Instrumentation 68
2.2.1 Hirst type bioaerosol instrumentation 68
2.3 Data analysis 91
2.3.1 Geographical Origin Data 91
2.3.2 Meteorological Data 93
2.3.3 Clustering analysis procedure 93
References 95
Chapter 3 – Results & Discussion 104
3.1 Traditional monitoring of Pollen and Fungal spores 104
3.2 WIBS determination of ambient fluorescent particles 108
3.3 Hirst values versus WIBS 113
3.3.1. Comparison of Fungal Spore Concentrations with WIBS fluorescent categories 116
3.3.2. Comparison of Pollen Concentration with WIBS Fluorescent Categories 121
3.4 Impact of Meteorological Factors on PBAPs and their Geographic Source 123
3.5 K-Means Clustering 130
References 135
Chapter 4 - Conclusion 144

List of abbreviations and acronyms

AGL	Above Ground Level
CEA	Alternative Energies and Atomic Energy Commission
ARL	Association of Research Libraries
AF	Asymmetric Factor
COPD	Chronic Obstructive Pulmonary Disease
CCN	Cloud Condensation Nuclei
CFU	Colony-Forming Unit
CSV	Comma-Separated Values
CPC	Condensation Particle Counter
CW	Continuous Wave
CNN	Convolutional Neural Networks
CLC	Corine Land Cover
EPA	Environmental Protection Agency
EAACI	European Academy of Allergy and Clinical Immunology
EAN	European Aeroallergen Network
ECMWF	European Centre for Medium-Range Weather Forecast
FTP	File transfer protocol
FAP	Fluorescent Airborne Particle
GDAS	Global Data Analysis System
HVAC	Heating, Ventilation, and Air Conditioning
HM	Heavy Metals
HEPA	High-Efficiency Particulate Absorbing
HYSPLIT	Hybrid Single-Particle Lagrangian Integrated Trajectory
IN	Ice Nuclei
LIF	Laser-Induced Fluorescence
LED	Light-Emitting Diode
LDT	Long-Distance Transport
MPS	Major Pollen Season
NOAA	National Oceanic and Atmospheric Administration
NADH	Nicotinamide adenine dinucleotide
NWR	Non-parametric Wind Regression
OM	Organic Matter
OW	Organic Waste
PM	Particulate Matter
PMT	Photomultiplier Tube
PCR	Polymerase Chain Reaction
PTFE	Polytetrafluoroethylene
PBAP	Primary Biological Aerosol Particle
QGIS	Quantum Geographic Information System
RH	Relative Humidity
SBS	Sick Building Syndrome
SLPM	Standard Litres Per Minute
SWIM	Sustained Wind Incidence Method
SILAM	System for Integrated modeLling of Atmospheric Composition
VOC	Volatile organic compound
WIBS	Wideband Integrated Bioaerosol Sensor
WHO	World Health Organization

List of Figures

Figure 1.1. Schematic of PBAP properties (Zhang *et al.*, 2021). 13

Figure 1.2. Pollen calendar for Dublin (Markey et al., 2022). 23

Figure 1.3. The aerodynamic equivalent diameter of a particle with an irregular shape compared to one with a spherical shape (*Aerosol Technology: Properties, Behavior, and Measurement of Airborne Particles, 2nd Edition | Wiley*). 25

Figure 1.4. Morphological characteristics of Didymella (Latif *et al.*, 2021)..... 26

Figure 1.5. a. Agrocybe sp. b. Alternaria sp. c. Arthrinium sp. d. Beltrania sp. e. Cladosporium sp. f. Curvularia sp. g. Dreschslera sp. h. Epicoccum sp. i. Fusarium sp. j. Nigrospora sp. k. Leptosphaeria. l. Pithomyces sp. m. Pleospora sp. n. Puccinia sp. o. Tetraploa sp. p. Torula sp. q. Pisolithus sp. (Alzate et al., 2015) 27

Figure 1.6. a. Alnus glutinosa, b. Betula pendula, c. Corylus avellana, d. Quercus robur, e. Ambrosia artemisiifolia, f. Pinus sylvestris, g. Juglans regia, h. Acer sp., i. Poaceae, j. Taxus baccata, k. Ulmus sp. and l. Fagus sylvatica (Boldeanu et al., 2021)..... 28

Figure 1.7. Pollen type prevalence in Dublin (POMMEL). 31

Figure 1.8. Schematic of sampling head of the Rotorod (Huang *et al.*, 2015)..... 42

Figure 1.9. Andersen sampler Cascade Impactor Schematic. The diagram illustrates a 6-stage Andersen cascade impactor. Each stage is equipped with a Petri plate filled with nutrient agar. The stages are designed with progressively smaller nozzles, resulting in higher impaction velocities of particles onto the agar (Andersen, 1958). 43

Figure 1.10. WIBS instrument (image taken by author). 45

Figure 1.11. The measurement principle of the Swisens Poleno, provided by Swisens AG..... 48

Figure 1.12. The Rapid-E Intelligent Real-Time Bioaerosol Sensing, developed by Plair SA. ... 49

Figure 2.1. Site of sampling at CEA in Saclay (48.7247◦ N, 2.1488◦ E) (Source Google Earth). 68

Figure 2.2. Hirst volumetric sampler and impact unit schematic diagram (Hirst, 1952; Galán, González, et al., 2007). 69

Figure 2.3. Image of a drum being prepared for placement within spore watch sampling head (Lacey and West, 2006). 70

Figure 2.4. Images of the various stages of preparation of the spore watch drum for sampling (Lacey and West, 2006). 71

Figure 2.5. Images of the different stages in mounting the melinex tape (Lacey and West, 2006). 73

Figure 2.6. The analytical procedure of pollen grains collection and counting (Sarda Estève et al., 2018). 75

Figure 2.7. A one-day sample slide, including applying an identification label for optical counting and positioning the acetate ruler on top of the slide to obtain a daily sample (images taken by the author). 76

Figure 2.8. Internal and external parts of the WIBS instrument (Stanley, 2009). 78

Figure 2.9. Schematic of the central optical chamber of the WIBS (Stanley, 2009). 79

Figure 2.10. Particle type classification, as initially presented by Perring et al. (2015). 81

Figure 2.11. (A) The inlet of the WIBS4. (B) Oversize Particle Trap (OPT) within the inlet. (C) Inlet with OPT removed (Stanley, 2009). 82

Figure 2.12. Sectional view of WIBS4 chamber showing aerosol flow (Stanley, 2009) 83

Figure 2.13. Smoke visualisation of scattering volume and its surrounding clean sheath flow (Stanley, 2009)..... 84

Figure 2.14. illustrates the spatial geometry of the laser and xenon UV pulses as the particle passes through the scattering volume. (Stanley, 2009). 85

Figure 2.15. Schematic diagram showing the passage of a particle through the laser beam and then into the space below the laser beam where it is illuminated sequentially by the two xenon UV flashes. The accompanying oscilloscope plot shows the analogue signals resulting from this particle transit (Stanley, 2009). 86

Figure 2.16. Energy density profile of typical xenon UV flash. Dotted lines indicate the relative position of the sample airflow column (Kaye et al., 2005) 87

Figure 2.17. Graph showing calibration curve (dashed line) used in WIBS4 for particle size estimation (Stanley, 2009). 88

Figure 2.18. Example of the formation of a scattering pattern used to determine particle shape (Stanley, 2009)..... 89

Figure 2.19. Variety of different particles and sizes and their light-scattering patterns (Stanley, 2009). 90

Figure 3.1. Time-series data represents daily pollen and fungal spore concentration measurements obtained using the Hirst. The dataset has been refined to exclude days with missing WIBS data. 105

Figure 3.2. Distribution of Fungal Spore Types by Percentage..... 107

Figure 3.3. The distribution of WIBS particles categorized by the Perring nomenclature (% of total fluorescent particles) is illustrated as a pie chart..... 109

Figure 3.4. Particle type size distribution for each of the WIBS categories. 111

Figure 3.5. Asymmetry factor distribution for the most significant fluorescent particle distribution 112

Figure 3.6. Normalised Diurnal Fungal spore and WIBS categories plot. 115

Figure 3.7. Pearson correlation between fluorescent particle types and fungal spore concentrations. The colour bar indicates positive (blue) and negative (red) correlations. 118

Figure 3.8. (A) time series of Hirst fungal spore counts and WIBS A (9σ) type particles (Daily) and (B) Hirst fungal spore counts and WIBS A-type particles (Daily). 120

Figure 3.9. Pearson correlation between fluorescent particle types and pollen concentrations. The colour bar indicates positive (blue) and negative (red) correlations..... 121

Figure 3.10. Daily temporal progression and incorporated linear regression of Hirst aggregate pollen against WIBS particle concentrations featuring FL2 and FL3 intensities surpassing 1300. 122

Figure 3.11. Wind rose of prevailing winds during the sampling period. White circles represent a wind speed scale in kilometres per hour (4 km/h, 8 km/h, 12 km/h, 16 km/h). 126

Figure 3.12. Origin of Total pollen at the sampling site. The colour scale represents the estimated concentration (Pollen grains/m^3) white gridlines represent a wind speed scale in kilometres per hour (5 km/h, 10 km/h, 15 km/h,20 km/h). 127

Figure 3.13. Origin of Total fungal spores, Ascospores and Cladosporium, Alternaria and Basidiospores spores at sampling site. The colour scale represents the estimated concentration

(Spores/m^3) white gridlines represent a wind speed scale in kilometres per hour (5 km/h, 10 km/h, 15 km/h,20 km/h). 128

Figure 3.14. Landcover map of the 30km surrounding the sampling site (CLC, 2018). 129

Figure 3.15. Daily temporal trends of Hirst fungal spore concentrations compared to resultant WIBS K-means clusters (4 + 8). 130

Figure 3.16. illustrates the following daily time series comparisons: (A) The daily time series plots the Hirst fungal spore concentrations with corresponding WIBS K-means clusters (4 + 8). (B) The daily time series displays the Hirst tree pollen concentrations alongside the associated WIBS K-means clusters (1 + 3). (C) The daily time series showcases the Hirst grass/herb pollen concentrations in correlation with the WIBS K-means clusters (2). 133

List of Tables

Table 1.1. Fluorophore Excitation and Emission Wavelengths nm (Fennelly *et al.*, 2018)..... 46

Table 2.1. The WIBS channel annotation matrix associated channels with their respective excitation wavelengths and emission wavebands. 81

Table 3.1. Spearman´s rank Correlation between daily Pollen/Spore types, WIBS fluorescent category concentrations and Weather Parameters. 124

Table 3.2. Comparative Analysis of Outcomes from K-means Clustering and Particle Filtering Methods. 131

Acknowledgements

I want to express my sincere gratitude to my thesis advisor, Dr David O'Connor, for his guidance throughout the research process. His expertise, insight, and encouragement have been instrumental in shaping my ideas and helping me to develop as a researcher.

I would also like to thank my committee members for their valuable feedback and contributions to this project. Their insights and expertise have been invaluable in helping me refine my research and present my findings clearly and compellingly.

I am also grateful to the staff and faculty of the Department of Chemical Sciences at Dublin City University, who have provided a supportive and collaborative environment for my research. I want to extend a special thank you to the postgraduate student community, who have provided support throughout my time at the university.

Finnian Neeson

Saclay: Pollen and fungal spore monitoring

Abstract

In recent years, the real-time monitoring of primary biological aerosol particles (PBAP), like pollen and fungal spores, has gained significant attention due to their health and climactic effects. This study evaluates the efficacy of the WIBS in sampling and detecting comparisons of ambient fungal spore and pollen concentrations with the conventional Hirst volumetric method. While the total concentration of pollen and fungal spores is interesting, detecting specific allergenic pollen and fungal spore types is crucial. Results indicate that the WIBS detected and differentiated between total pollen ($R^2 = 0.6$) and total fungal spore ($R^2 = 0.8$) concentrations. The study also examines the correlation between ambient pollen/fungal spore concentrations and meteorological/air quality parameters. The temperature was the most influential parameter in pollen production and release, showing a strong positive correlation. Relative humidity had a strong negative correlation with pollen while showing a strong positive association with fungal spore concentrations. Wind data analysis provided geographic origin details of pollen and fungal spore concentrations, with fungal spores originating mainly from a westerly direction and pollen primarily from a North-easterly direction.

Chapter 1 - Introduction

1.1 Bioaerosols Overview

Aerosols play a crucial role in the Earth's atmosphere, exerting significant ecological, health, and climactic effects. They encompass a wide range of liquid or solid particles suspended in a gas, varying in physical diameter from "ultrafine" (less than 100 nm) to "super coarse" (larger than 10 μm) (Galán *et al.*, 2000, O'Connor *et al.*, 2014, O'Gorman and Fuller, 2008, Skjøth *et al.*, 2007). Aerosols are typically solid or liquid particles that are small enough to remain suspended in the atmosphere for a significant amount of time (days to weeks, depending on their aerodynamic diameter)(Gubanova *et al.*, 2021). This size distribution affects their behaviour in the atmosphere, which contributes to the overall atmospheric makeup, shaping the interactions and impacts within the environment (O'Gorman and Fuller, 2008). Aerosols vary widely, depending on their sources and the atmospheric processes exerted on them (Huffman *et al.*, 2013). They can comprise organic compounds, sulphate, black carbon (soot), mineral dust, nitrates, ammonium, and other chemical substances. These Aerosols can modify the Earth's radiative forcing by scattering and absorbing short and long-wave radiation. Aerosols encompass various processes that impact the microphysical properties, radiative characteristics, and lifespan of clouds. This is achieved by aerosols acting as cloud condensation nuclei (CCN) and ice nuclei (IN) (Zhang *et al.*, 2021). Figure 1.1 shows a schematic that illustrates the influence of PBAP properties and ageing processes on direct and indirect radiative effects. The figure is divided into three parts, each of which shows how different PBAP properties and ageing processes can affect different aspects of aerosol-cloud interactions and optical properties. Part A of the figure shows that direct radiative forcing can be influenced by PBAP concentration, diameter, refractive index, surface tension, and hygroscopicity at relative humidity (RH) less than 100%. Part B shows that PBAP concentration, diameter, surface tension, and hygroscopicity can affect CCN activity and properties of warm clouds. Lastly, Part C shows that PBAP concentration, diameter, and contact angle of ice germ on the particle can affect

the evolution of mixed-phase clouds. This figure highlights the complex ways in which PBAP properties and ageing processes can impact aerosol-cloud interactions and their optical properties.

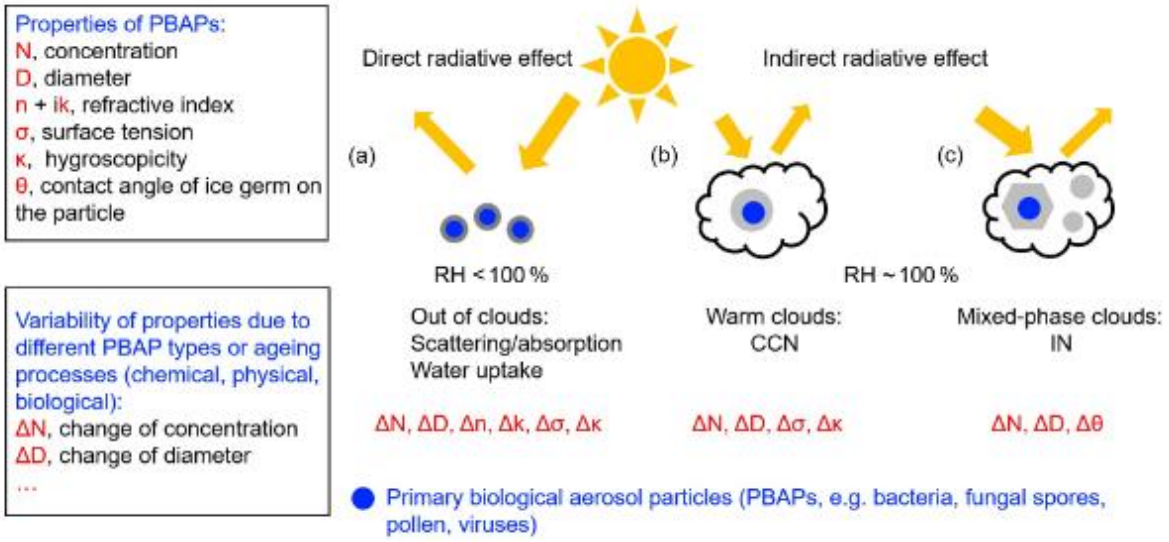

Figure 1.1. Schematic of PBAP properties (Zhang *et al.*, 2021).

Bioaerosols (a subset of aerosols), also known as Primary Biological Aerosol Particles (PBAPs), are equally as varied group of airborne particles. They include bacteria, fungi, pollen, viruses, and fragments of plants and animals. They are significant in various ecological processes and can negatively impact human health as a result of their inherent variability and complex nature. Understanding the relationship between different bioaerosols and their sources is crucial for effectively monitoring and managing their potential environmental and public health effects. They can be directly released from an organism or produced through the breakdown of organisms and organic matter (OM). bioaerosols also range from ultrafine to super-course, with the focus of this work on particles greater than 2 microns.

Fungal spores are the dormant form of bioaerosols in terms of particle number (in the size range from 2-100 microns) with concentrations ranging from 10,000–100,000 spores m^{-3} seen in specific locations (Fröhlich-Nowoisky *et al.*, 2009, Huffman, *et al.*, 2010, Li *et al.*, 2020). Pollen is generally seen to be larger than fungal spores ranging from 20-100 microns. Their concentrations

are also lower than fungal spores, with the mean pollen content outdoors being 100 to 1000 times less than fungal spores. The European Academy of Allergy and Clinical Immunology (EAACI) establishes criteria based on pollen concentrations in the air to determine the start of the pollen season and its impact on human health. For instance, the grass pollen season is deemed to commence when 5 out of 7 consecutive days register more than 10 grass pollen grains/m³ air, with the cumulative pollen count exceeding 100 grains/m³ air within these 5 days (Pfaar *et al.*, 2017). Hourly pollen concentrations can vary significantly, ranging from 0 to over 5000 grains/m³, depending on the specific location and the time of day. These fluctuations in pollen levels highlight the dynamic nature of airborne pollen and the influence of factors such as local vegetation, weather conditions, and diurnal patterns. Monitoring these variations in real-time provides a more comprehensive understanding of the daily and seasonal pollen distribution patterns, aiding in assessing and managing allergic reactions caused by pollen exposure (Skjøth *et al.*, 2021).

Moving to fungal spores in the Summer and Autumn months, Cladosporium species generally exhibit the highest concentrations among the identified spores (Patel *et al.*, 2018). Some studies suggest various concentration thresholds for Cladosporium spores, ranging between 2000–4000 spores/m³ (Targonski *et al.*, 1995; Hollins *et al.*, 2004a). However, more recent research has narrowed down the suggested values to a range of 500–1500 spores/m³ (Vélez-Pereira *et al.*, 2019). In the case of Alternaria spores, a threshold of 100 spores/m³ is commonly considered a high daily concentration (Gravesen, 1979).

Bacteria concentrations in the atmosphere can vary depending on location, time of year, weather conditions, and human activities. Some common bacterial genera detected in the atmosphere include Bacillus, Pseudomonas, Streptococcus, and Staphylococcus, among others. In African desert dust concentrations, a study identified 13 genera, with Bacillus comprising 32% of the dominant species, followed by Gordonia at 12% and Staphylococcus at 8% (Griffin *et al.*, 2006). The concentration of bacteria in the atmosphere tends to be higher in urban and industrial areas

compared to rural areas (Cho *et al.*, 2019). Human activities such as vehicle emissions, construction, and industrial pollution can contribute to releasing bacteria and other bioaerosols into the air (Madhwal *et al.*, 2020). Additionally, certain weather conditions like high humidity and wind can facilitate bacteria transport over long distances (Ruiz-Gil *et al.*, 2020).

Studies estimate that the global emissions of bacteria-containing particles into the atmosphere range from 7.6×10^{23} to 3.5×10^{24} per year. These emissions are primarily sourced from grasslands, shrubs, and crops. The mass of bacteria emitted annually is estimated to be between 40 and 1800 gigagrams (Gg), depending on the proportion of bacterial cells in the particles (Burrows *et al.*, 2009).

Bioaerosols can resist harsh environmental conditions as some PBAPs have evolved to withstand extreme temperatures, high or low humidity levels, UV radiation, and desiccation (Zhang *et al.*, 2021). Fungal spores have a protective biofilm when conditions become favourable, e.g. sufficient moisture and nutrients, which germinate and give rise to actively growing fungal cells which help the spores adhere to surfaces in species such as Aspergillus, Alternaria, Botrytis, Cladosporium, and Penicillium (Siqueira *et al.*, 2011). They consist of fungal cells embedded within an extracellular matrix of polysaccharides, proteins, and other substances produced by the fungi themselves that help shield them from desiccation, UV radiation, and other environmental challenges (Gollakota *et al.*, 2021).

There are several sources of bioaerosol from both natural and man-made origins. Natural sources comprise things like plants, which release pollen into the air. Pollen is a common bioaerosol consisting of small, lightweight reproductive structures produced by plants, especially those that rely on wind for pollination. Soil is another significant natural source of bioaerosols, especially when disturbed by wind, rain, or human activity. It can release bacteria, fungal spores, and other OM into the air. Bodies of water, including oceans, rivers, and lakes, can produce bioaerosols through the mechanical action of waves and wind; again, this can include bacteria but also algae

and fragments of aquatic organisms. Quantifying the exact flux of particles released from bodies of water is a complex task due to the dynamic and variable nature of the environment. The flux can differ significantly between different water bodies and vary seasonally and diurnally.

Studies have been conducted to estimate the flux of particles from bodies of water, including measurements of aerosol concentrations and modelling approaches. According to Burrows et al. (2009b), when foams or bubbles burst in water, many microorganisms can form and be propelled into the atmosphere by external forces such as wind and water currents. Cho and Hwang (2011) reported that the concentration of prokaryotes over the East Sea reached approximately 104–105 cells/m³. Similarly, Hu *et al.,* (2017) found that the airborne bacterial concentration over the Kuroshio Extension region of the northwest Pacific Ocean ranged from 104 to 105 cells/m³, with an average viability of 93%. These high concentrations of microorganisms in marine air primarily originate from the sea. Consequently, the presence of bacteria in Tokyo has been attributed to the influence of seawater from Tokyo Bay (Uetake *et al*., 2019).

Anthropogenic sources of bioaerosols include agricultural activities such as farming practices like ploughing and harvesting, which disturb the soil and release bioaerosols. Animal husbandry can also produce bioaerosols, such as bacteria and viruses, from the livestock waste produced or as a nutrient source for such biological organisms. Specific industrial processes can release bioaerosols. For instance, waste treatment facilities can produce bioaerosols such as Clostridium perfringens, Acinetobacter calcoaceticus and Aspergillus fumigatus from the handling and processing of organic waste (OW) (Franchitti *et al.*, 2020). According to Li *et al.,* (2015b), elevated bioaerosol concentration levels were observed during haze episodes in China, reaching approximately 2500 CFU/m³. The concentration levels of bioaerosols were found to vary significantly over time. In their studies, certain bacterial species dominated the bacterial community during these haze episodes.

Another study by Cao *et al.*, (2014) indicated that opportunistic fungi, such as Aspergillus fumigatus, showed elevated levels during haze episodes. This suggests that bacteria and certain fungi are affected by and present in higher concentrations during haze events. Furthermore, the level of endotoxin, a significant inflammation agent and a component of Gram-negative bacterial membranes, increased approximately twice during a haze episode in Beijing, as Wei *et al*., (2016) reported. This indicates the presence of potentially harmful components associated with bioaerosols.

These studies highlight the impact of haze episodes on bioaerosol concentrations, the dominance of specific microbial species, and the presence of inflammatory agents like endotoxin. Indoor environments, such as homes and offices, can be sources of bioaerosols as human occupants contribute to the presence of pollen and fungal spores in indoor workplaces by transporting PBAPs through their skin, footwear, and clothing. These particles become airborne and mix with particulate matter indoors, originating from floors and surfaces (D'Ovidio *et al.*, 2021). PBAPs have the potential to exert their influence over vast distances, as dust particles can carry biological material for thousands of kilometres from the source of emission (Smith *et al.*, 2013; Whitehead *et al.,* 2016). By assessing the impact of PBAPs in ambient environments, it is crucial to differentiate them from other particles in the atmosphere and assess their viability.

Healthcare settings such as hospitals and other healthcare settings can be significant sources of bioaerosols, particularly those containing pathogens. These can be generated through various activities, such as medical procedures, handling of waste, or simply through the presence of diseases. The issue of indoor air pollution is increasingly raising concerns (Cheek *et al.*, 2021; Guercio *et al.*, 2021; Luo *et al.*, 2021). According to the United States Environmental Protection Agency (EPA), indoor air pollution levels can be two to five times higher than outdoor air pollution

levels when ventilation is inadequate (Nevalainen *et al.*, 2015). In today's society, where individuals spend over 80% of their time indoors, the quality of indoor air plays a vital role in determining their health (Adams *et al.*, 2016). The types and concentrations of bioaerosols can vary widely depending on the specific source and environmental conditions. Perhaps, the most vital context for bioaerosols from a public health perspective is healthcare settings, as these bioaerosols can transmit diseases, underscoring the need for effective infection control measures. Healthcare environments can harbour pathogens on surfaces such as countertops, medical equipment, or patient care items. These surfaces can serve as reservoirs for bioaerosol generation through activities like touching, cleaning, or manipulating contaminated objects. For example, invasive fungal infection is a significant cause of morbidity and mortality in newborn babies, especially those with low birth weight. However, the extent to which fungi present in indoor air contribute to the incidence of mucocutaneous colonisation and the risk of invasive fungal infection in the population remains uncertain (Belizario *et al.*, 2021).

The sources of indoor bioaerosol pollution are diverse and encompass outdoor contaminants entering through windows, doors, and ventilation systems, as well as building materials, furnishings, occupants, pets, house plants, and organic waste (Nazaroff, 2016). Additionally, routine human activities like coughing, washing, toilet flushing, talking, walking, sneezing, and sweeping floors can generate bioaerosols (Chen and Hildemann, 2009).

Exposure to bioaerosols in occupational environments is linked to a wide range of health effects with significant public health implications. These effects include infectious diseases, acute toxicity, allergies, and cancer. Among the bioaerosol-associated health effects, respiratory symptoms and lung function impairment have been extensively studied and considered particularly important. Additionally, some research suggests that microbial exposure may have protective effects against atopy and atopic conditions (Douwes *et al.*, 2003). Occupational activities encompass a wide range

of sources for bioaerosol exposure, including waste sorting and composting, agricultural and food processing activities, and the livestock industry (Pearson *et al.*, 2015). Workers susceptible to such exposure have reported a variety of respiratory diseases or symptoms, including allergic asthma, rhinitis, and airway inflammation (Beck *et al.*, 2012). Bioaerosols have been estimated to contribute to approximately 5 to 34% of indoor particulate matter air pollution (Mandal and Brandl, 2011).

Epidemiological studies have established that air pollution is a leading cause of millions of premature deaths annually. Consequently, economic analyses indicate that air pollution carries a substantial economic burden, amounting to trillions of dollars each year. The diseases caused by biological air pollutants are of significant global concern due to their social and economic implications. Considering that individuals spend a considerable portion of their time indoors, exceeding 90% in some cases, it is crucial to prioritise research and development methods to remove indoor air pollutants effectively (Brągoszewska *et al.*, 2020). This pursuit is paramount for safeguarding public health and promoting overall well-being. New industrial activities have emerged in recent years that can lead to abundant exposure to bioaerosols. Examples of such activities include the waste recycling and composting industry, biotechnology industries producing highly purified enzymes, and the detergent and food industries utilising these enzymes. High levels of microbial bioaerosols, including pathogenic bacteria, fungi, fungal spores, and viruses, pose environmental and public health risks. These occurrences and exposures can contribute to the deterioration of environmental quality and have further implications for public health.

Establishing dose-response relationships for most biological agents and determining threshold values is challenging due to limited knowledge. While exposure limits have been defined for specific contaminants like wood dust, subtilisins (bacterial enzymes), and flour dust, proposed exposure limits for bacterial endotoxin exist (Douwes *et al.*, 2003). However, the lack of valid quantitative exposure assessment methods hinders practical risk assessment. Investigating the

potential protective effects of microbial exposures on atopy and atopic diseases requires understanding inter-individual susceptibility to biological exposures, exploring interactions between bioaerosols and non-biological agents, and investigating potential health effects such as skin and neurological conditions and birth effects. Respiratory symptoms and lung function impairment are extensively studied health effects associated with exposure to organic dust. These effects can vary in severity, ranging from mild conditions that initially have minimal impact on daily life to severe chronic respiratory diseases that necessitate specialized medical care. Respiratory symptoms related to occupational exposures are generally attributed to airway inflammation triggered by specific toxins, pro-inflammatory agents, or allergens. The development of these symptoms is often associated with the nature of the exposure and can lead to adverse respiratory outcomes requiring appropriate medical attention (Douwes *et al.*, 1999).

Understanding the origins of bioaerosols is not merely an academic exercise; it is a cornerstone for devising strategies to mitigate their potential adverse effects and harnessing their benefits. As we continue to alter our environment and climate, the narrative of bioaerosols will continue to unfold, demanding our attention and scientific curiosity.

1.2 Release, Transport and Deposition

The release of bioaerosols is a multifaceted process shaped by diverse mechanisms that span the biosphere (Xie *et al.*, 2020). They contribute to forming cloud droplets and ice crystals and act as regulators of precipitation, thereby influencing the hydrological cycle and climate patterns (Matthias-Maser *et al.*, 1996). The aerosolization process involved dispersing and suspending non-gaseous small particles in a gaseous medium, creating a colloidal dispersion.

PBAPs can be released actively or passively into the air. Passive release of PBAPs occurs when bioaerosols are released into the air through natural processes such as wind, air currents, or

turbulence. For example, pollen grains can be released from plants and carried passively by the wind over long distances. Mechanical Dispersal refers to the release of bioaerosols due to external factors such as physical disturbance or human/animal activities. For instance, walking through grass or brushing against plants can cause pollen to become airborne. Human activities can actively generate bioaerosols. Examples include industrial processes, agricultural practices (e.g., crop dusting), waste management, and activities like construction or demolition that can generate dust particles containing bioaerosols.

Passive release involves the natural dispersal of bioaerosols through wind or external factors, while active release refers to intentional or inherent mechanisms by which organisms or human activities actively generate and release bioaerosols into the air. The active release refers to a source's deliberate release of bioaerosols. In these cases, individuals actively expel respiratory droplets or aerosols into the air, potentially containing PBAPs. These releases occur through natural processes or environmental disturbances, such as when bioaerosols are dispersed due to air currents and wind. It can also happen when bioaerosols are released from contaminated surfaces, microbial growth on building materials, or sources such as decaying OM or wastewater. Typically, bioaerosol concentrations in wastewater treatment plants (WWTPs) range from 10^2 to 10^4 CFU/m^3, as Wlazło *et al.* (2002) reported. The release of high levels of bioaerosols is commonly observed in aerator tanks and residual sludge storage yards within WWTPs (Szyłak-Szydłowski *et al.,* 2016). Moreover, bioaerosol particles can be transported over long distances by wind, posing a health risk to on-site workers and nearby residents (Sanchez-Monedero *et al.,* 2008).

Dust particles in the air can also carry PBAPs for instance, a study conducted in Mali, West Africa, a known source region for dust storms, isolated fungi from air samples and found fungal counts ranging from 80 to 370 CFU/m containing Cladosporium, Aspergillus, and Alternaria (Kellogg *et al.*, 2004). Every year, a significant amount of African desert dust, amounting to millions of metric

tons, is carried across the Atlantic Ocean, forming a blanket over the Caribbean and the south-eastern United States. Previous research conducted in the Caribbean region has revealed that atmospheric samples collected during dust events contain viable microorganisms, including plant and opportunistic human pathogens. According to (Moulin *et al.*, 1997), it is believed that this particular source contributes approximately one billion metric tons of dust annually to the global atmosphere. To gain a deeper understanding of the potential impacts on public health and ecosystems downwind of these dust microbes, it is crucial to characterise the microbial population in the source region. Cladosporium and Penicillium are common fungi known to attack wooden building materials (Nevalainen *et al.,* 2015). In addition, fungi such as Aspergillus, Trichoderma, and Penicillium can infest acylated wood furniture, polyethylene composites, plywood, and modified wood products. Lakes, rivers, and oceans can release bioaerosols. Research has indicated that these water bodies can release bioaerosols This concentration was selected because it is achievable in all microbial harvesting runs, ranging between 7.0×10^7 - 1.0×10^8 CFU/mL through wave action, splashing, and bubble bursting (Kruglyakova *et al.*, 2022). The processes can potentially contribute to aerosolising water droplets and particles; wave action and bursting bubbles were significant factors in releasing bioaerosols from seawater. These droplets may contain bacteria, algae, viruses, or other microorganisms in the water. Indoor spaces can harbour bioaerosols from various sources. Outdoor air can introduce bioaerosols into indoor environments. Pollen, fungal spores, and other particles in the outdoor air can enter buildings through ventilation systems, doors, windows and people via resuspension. Additionally, outdoor activities or nearby sources such as construction sites can contribute to the presence of bioaerosols indoors. The sources and composition of bioaerosols can vary depending on the geographical location, climate, and human activities in a given environment (Després *et al.*, 2012).

Pollen release into the atmosphere usually follows a seasonal pattern, with higher concentrations occurring during specific periods depending on the plant species. Pollen dispersal, or pollen

transport, allows pollen grains to reach greater distances from their source plants. Pollen can be carried by air currents for long-distance transport (LDT). Longitudinal pollen transport episodes are typically sporadic and unpredictable, as Smith et al. (2008) noted. These episodes can potentially disrupt the pollen season's regular course, as highlighted by Sofiev *et al.* (2006). Strong winds can transport pollen grains high into the atmosphere. The size and shape of pollen grains play a role in their dispersal capability. Lightweight pollen grains with aerodynamic structures are more likely to be carried by wind currents. Airborne pollen grains are generally assumed to have a 50-100 km natural dispersal range. As a result, air masses can transport these pollen grains farther from their source region (Skjøth *et al.*, 2007).

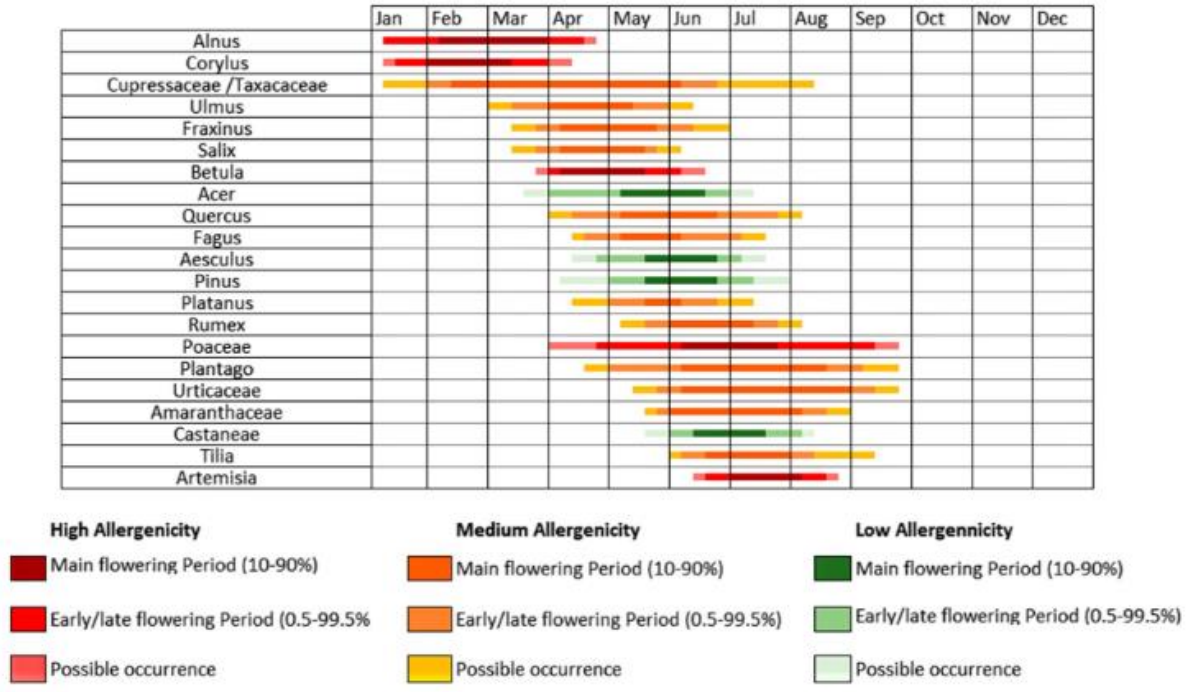

Figure 1.2. Pollen calendar for Dublin (Markey *et al.*, 2022).

The pollen calendar in Figure 1.2 provides information on the timing and abundance of different types of pollen in Dublin throughout the year. It references specific pollen types prevalent in the air based on long-term monitoring of airborne pollen concentrations. The data collected over several years allows for identifying recurring patterns and developing a calendar indicating the pollen types' peak seasons. The calendar is organised by months or seasons and provides

information on the predominant types of pollen during that period. Certain pollen types are significant due to their allergenic effects and prevalence in the atmosphere, as highlighted by Sofiev and Bergmann (2013). In the Irish environment, several of these allergenic pollen types are notable, including Alnus (alder), Corylus (hazel), and Betula (birch) pollen from the Betulaceae family, as well as Poaceae (grass) pollen. Annual observations reveal that while general seasonal trends in pollen patterns exist, variations can occur yearly, primarily due to meteorological changes. This means the Major Pollen Season (MPS) can differ significantly between years. To accommodate these variations, it is advised to include a minimum of 5-7 years of data when constructing a pollen calendar, as Galán *et al.* (2017) suggested. Incorporating multiple years of data helps to capture the interannual variability and provide a more comprehensive and accurate representation of the pollen season.

Bioaerosols can be removed from the atmosphere through two main processes: dry deposition, which involves diffusion or sedimentation, and wet deposition, which occurs through precipitation via nucleation or scavenging. This is primarily influenced by the aerodynamic diameter of the fungal spore particles was found to range between 1 and 30 mm, which was more significant than that for bacteria, which ranged from 0.2 to 0.8 mm. The diameter of a spherical particle with a unit density that has the same terminal velocity in the air as the particle in question is shown in Figure 1.3.

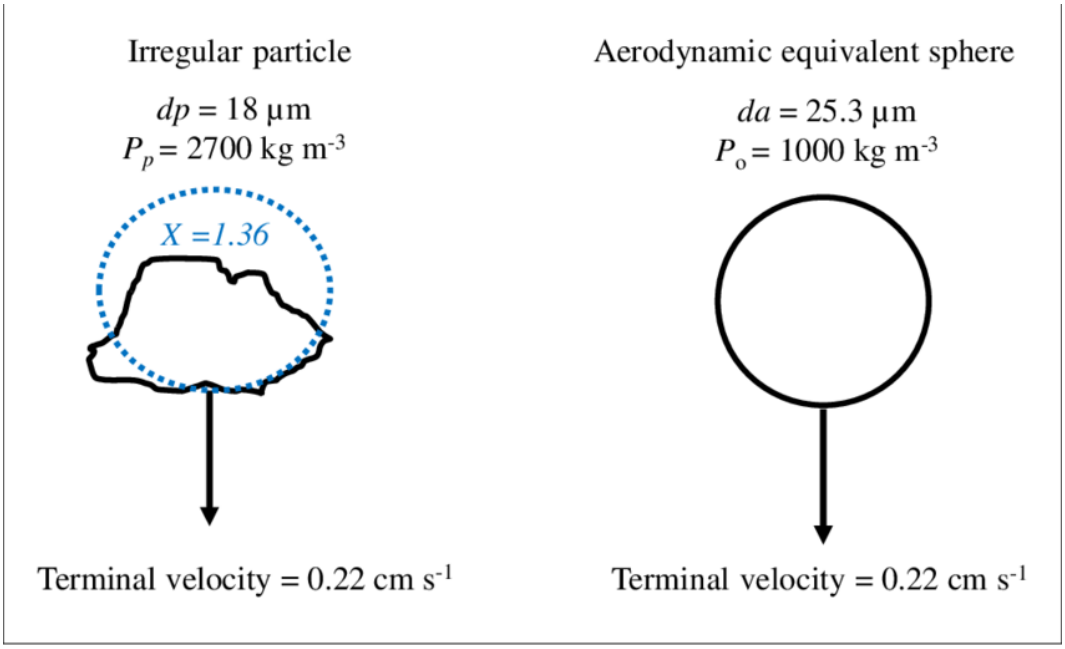

Figure 1.3. The aerodynamic equivalent diameter of a particle with an irregular shape compared to one with a spherical shape (*Aerosol Technology: Properties, Behavior, and Measurement of Airborne Particles, 2nd Edition | Wiley*).

However, biological particles, such as fungal spores, pollen, and seeds, often have complex structures with rough surfaces, internal pores, and asymmetric shapes, causing their physical and aerodynamic sizes to differ significantly. Some of these particles have adaptations that make them aerodynamically buoyant, facilitating long-range airborne transport. However, distances exceeding 200 km are only typically associated with LDT, as noted by Orlanski (1975) and Smith *et al.* (2013).

Particles in the air can be eliminated through two main processes: sedimentation, deposition onto surfaces like the ground or plants, and washout by precipitation. The average residence time of different biological particles in the atmosphere varies depending on their size and aerodynamic properties. The most effective way to remove particles with a size range from 0.1 to 2.5 µm is through the washout process caused by falling precipitation. Even a drizzle or a single instance of rain can efficiently eliminate a significant portion of these particles from the air in various conditions. This washout process demonstrates high efficiency in purging the atmosphere of these smaller particles (McDonald, 1962). When these particles settle, they can interact with terrestrial

or aquatic ecosystems, potentially initiating biological processes that lead to the release of other particles, such as through growth and reproduction (Després et al., 2012).

1.3 Chemical and Physical Properties of PBAPs

PBAPs range from ~ 1 nm to ~ 100 mm (Zhang *et al.*, 2021). The size distribution depends on the source and can vary widely. For example, fungal spores typically range from 2 to 50 μm in diameter, with most allergenic spores in the respirable size range of 3 to 10 μm (Patel *et al.*, 2018). Differentiating fungal spores via microscopy relies on crucial factors such as their size, shape, and colour. The size of fungal spores can range significantly from Poaceae μm in species like Penicillium/Aspergillus, making them virtually indistinguishable via optical microscopy, to larger conidia of Alternaria measuring between 20 - 63 μm (de Ana *et al.*, 2006). Alternaria shows that fungal spores can exist as single cells, while other fungal spores have one septum, like Didymella (Figure 1.4), or possess multiple septa.

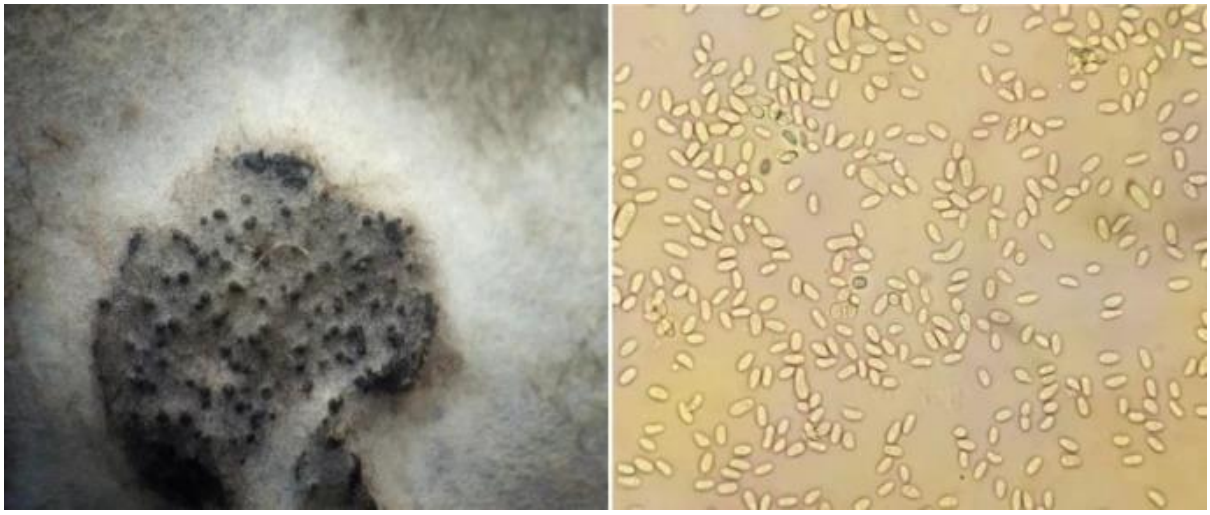

Figure 1.4. Morphological characteristics of Didymella (Latif *et al.*, 2021)

Airborne spores exhibit a variety of colours, including hyaline, i.e., meaning they are effectively translucent (e.g. Erysiphe or Didymella), yellow-brown (Cladosporium), gold-brownish (Ganoderma), or brown (Alternaria), depending on the specific spore under examination (Figure 1.5).

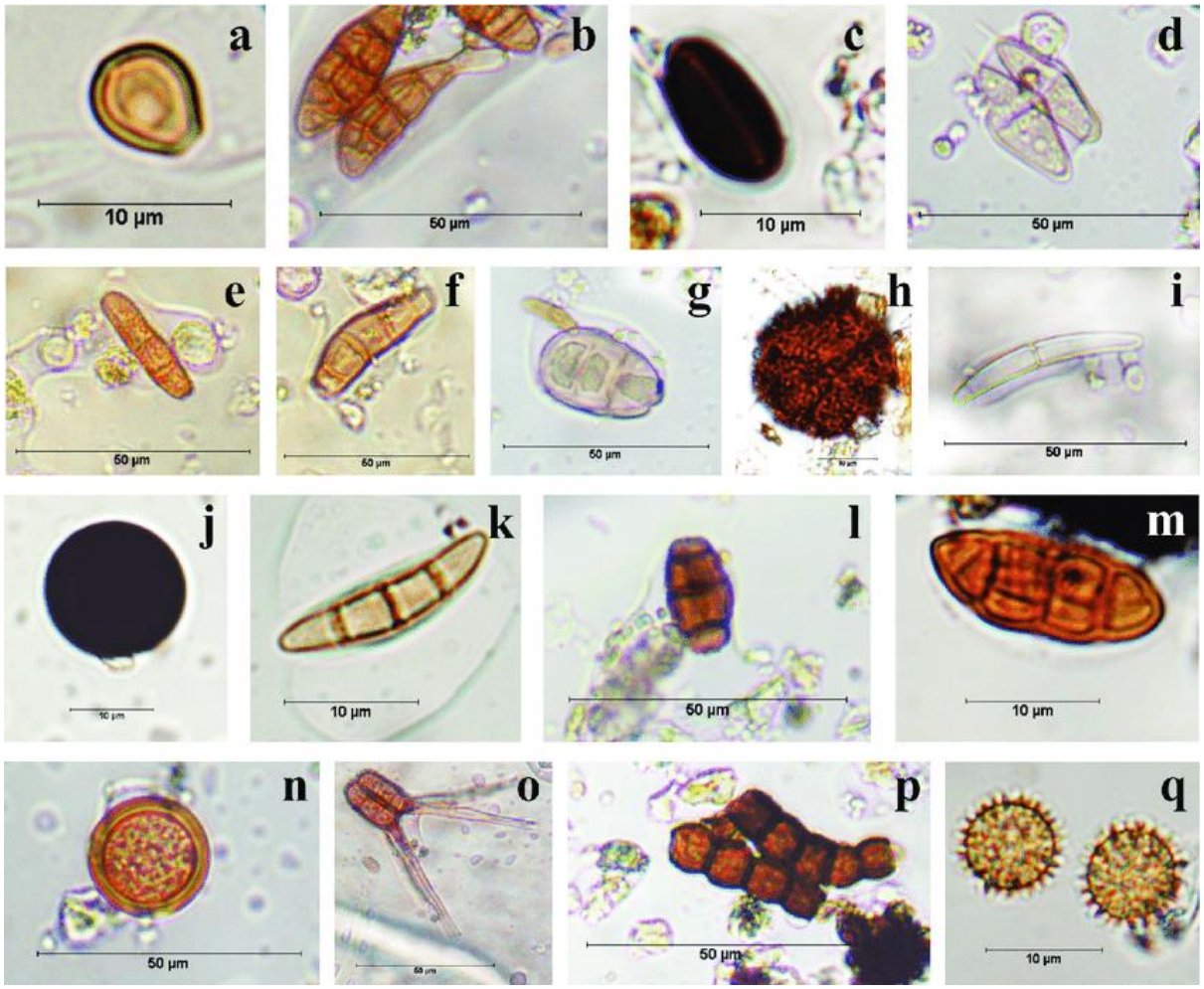

Figure 1.5. a. Agrocybe sp. b. Alternaria sp. c. Arthrinium sp. d. Beltrania sp. e. Cladosporium sp. f. Curvularia sp. g. Dreschslera sp. h. Epicoccum sp. i. Fusarium sp. j. Nigrospora sp. k. Leptosphaeria. l. Pithomyces sp. m. Pleospora sp. n. Puccinia sp. o. Tetraploa sp. p. Torula sp. q. Pisolithus sp. (Alzate et al., 2015).

Pollen grains are larger on the other hand, typically in the 10-100 µm range, and exhibit a wide range of sizes and come in diverse shapes. These grains possess a sturdy outer shell that safeguards the sperm cells during transportation. As PBAPs, pollen grains can be found in intact forms and fragmented pieces. When exposed to high humidity, pollen has the potential to rupture. These fragments of pollen grains are primarily composed of the same materials found in intact pollen grains, which consist of several components, including the exine (cellulose and pectins), intine

(sporopollenin), and cytoplasmic contents measuring between 30 nm and 5 µm (Taylor et al., 2002, 2004; Miguel et al., 2006). Pollen grains can exhibit various shapes, including spherical or nearly spherical forms, typically with smooth surfaces. Ellipsoidal grains, on the other hand, are elongated and often feature a furrow or groove encircling their circumference. Another shape observed is discoid, with flat and disk-shaped pollen grains displaying a raised or concave centre.

In contrast, irregular pollen grains possess lobed or irregular outlines and frequently exhibit extensions or protrusions, resulting in a distinctive appearance. Pollen grains' shape and surface characteristics are crucial for dispersal and pollination. Additionally, the specific shape of a pollen grain affects its aerodynamic properties and ability to adhere to pollinators.

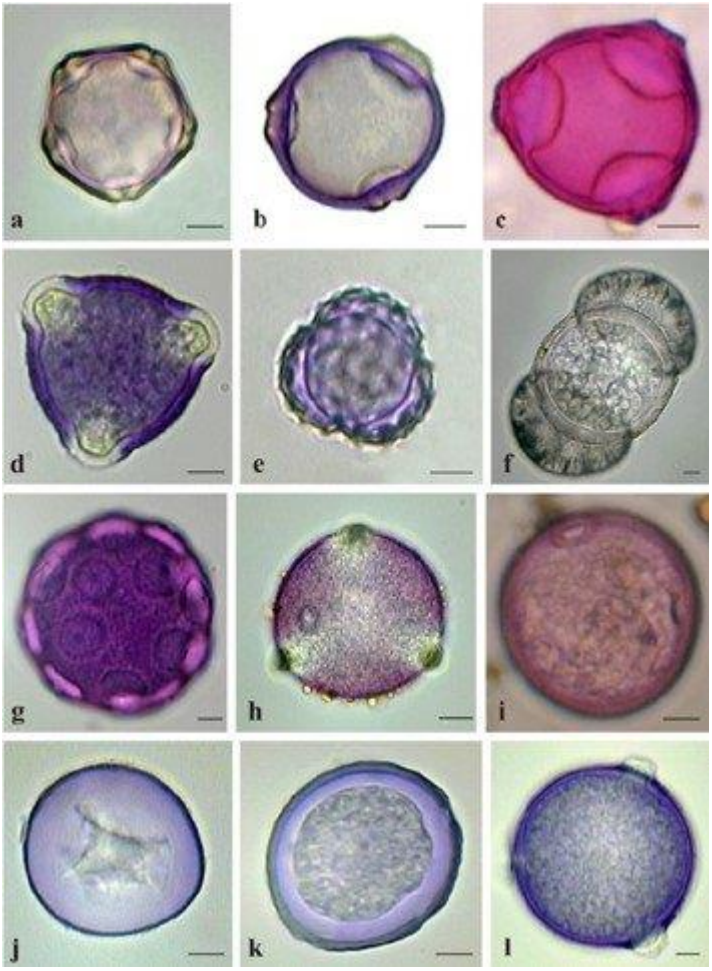

Figure 1.6. a. Alnus glutinosa, b. Betula pendula, c. Corylus avellana, d. Quercus robur, e. Ambrosia artemisiifolia, f. Pinus sylvestris, g. Juglans regia, h. Acer sp., i. Poaceae, j. Taxus baccata, k. Ulmus sp. and l. Fagus sylvatica (Boldeanu et al., 2021).

PBAPs can have hygroscopic properties, meaning they can absorb water vapour from the surrounding environment. The hygroscopicity depends on the composition and structure of the particles. Hygroscopicity refers to the ability of a particle to absorb water vapour from its surroundings as biological; pollen grains and fungal spores can exhibit hygroscopic properties. When exposed to high humidity, these particles can swell as they absorb water, changing their size and physical characteristics. The specific response of pollen grains and fungal spores to humidity can vary depending on their species, morphology, and chemical composition.

In some cases, the hygroscopic swelling of pollen grains and fungal spores can cause them to become viscous and adhesive when exposed to high humidity (Rathnayake *et al.,* 2017). This sticky behaviour can be advantageous for their dispersal and adhesion to surfaces, such as plant stigma for pollination or substrates for fungal growth. It can also influence their transport and deposition in the atmosphere.

The increased scattering cross-section for fungal fragments suggests that fragmented particles could directly impact the climate through radiative effects (Brock *et al.*, 2021). These processed particles would not be easily identified as spores if analysed using standard analytical methods or inspected based on their morphology. Detecting and distinguishing aged spores is challenging due to the diverse sources of biological particle emissions and the potential for fragmentation during atmospheric processing. Consequently, microscopy methods underestimate the contribution of biological particles to the overall atmospheric aerosol (Zang *et al.*, 2019).

1.4 Impacts of Bioaerosols

1.4.1 Health

Bioaerosols are significant in various ecological processes and can negatively impact human health and the environment. Global reports from the World Health Organization (WHO) in 2018 estimated that approximately 4.2 million people suffer from heart, respiratory, and lung disorders each year

due to exposure to ambient air pollutants, of which bioaerosol can make up a significant portion. Accurate monitoring and identification of bioaerosols are essential to understand their sources, transport mechanisms, and potential health impacts.

Pollen

Allergy sufferers experience allergic reactions when encountering certain substances known as allergens. While pollen itself is not an allergen, its proteins act as allergens. These proteins can trigger an exaggerated immune response in susceptible individuals, leading to the symptoms commonly associated with allergies. Allergies are hypersensitive immune responses elicited by allergens, typically innocuous substances that do not provoke a reaction in most individuals. Histamine and other chemicals cause the typical symptoms of an allergic reaction, which can include itching, runny nose, watery eyes, hives, swelling, and difficulty breathing. Allergy sufferers often manage their condition by avoiding known allergens such as pollen and fungal spores, taking medication to alleviate symptoms, and seeking medical help for severe reactions. Exposure to allergens, including major pollen allergens known to cause allergic reactions in susceptible individuals, such as Bet v 1 found in birch pollen and Amb a 1 found in ragweed pollen, which is known to trigger allergic reactions in sensitive individuals (Zbîrcea *et al.*, 2023).

As Bioaerosols encompass various biological particles suspended in the air, they can be inhaled, leading to an immune response in individuals sensitive to these particles. Recent years have seen a significant surge in research on PBAP due to mounting evidence linking certain biological particles to adverse health effects (Douwes *et al.*, 2003). High concentrations of fungal spores and pollen have been associated with various health problems in humans, plants, and animals. For instance, respiratory issues such as asthma, allergic rhinitis, chronic obstructive pulmonary disease (COPD), and farmer's lungs have been conclusively linked to aeroallergen interactions (D'Amato *et al.*, 2019) (Jensen-Jarolim *et al.*, 2015; Séguin *et al.*, 2010).

Industry-related activities, particularly those related to agriculture, have long been recognised as potentially hazardous due to exposure to harmful vapours, gases, and clouds of dust containing significant levels of bacterial and fungal components (Kirkhorn and Garry, 2000; Rylander and Jacobs, 1994). Various respiratory illnesses and infections, including Farmers' lung, hypersensitivity pneumonitis, aspergillosis, and COPD, have been linked to agricultural work (Weinhold, 2007; Bailey *et al.,* 2008; Kirkhorn and Garry, 2000; Ader *et al.,* 2005).

Pollen allergy has had a significant clinical impact throughout Europe, and a growing body of evidence indicates an increasing prevalence of respiratory allergic reactions triggered by pollen. The estimated prevalence of pollen allergy is as high as 40% (D'Amato *et al.*, 2007). Since respiratory allergies caused by airborne allergens do not adhere to national borders, the study of pollinosis cannot be confined within national, as is the case with many diseases that can be prevented by avoiding exposure to the causative agents. In Dublin, the primary pollen season spans approximately half the year, from spring to autumn.

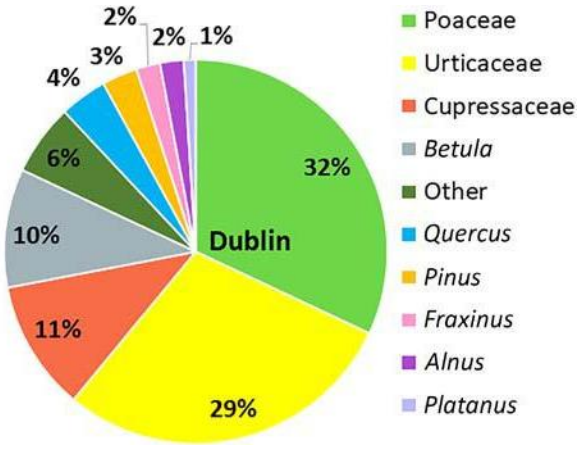

Figure 1.7. Pollen type prevalence in Dublin (POMMEL).

The pollen calendar (Figure 1.2) illustrates the primary pollen season when during this period, different types of plants release their pollen into the air, triggering allergic reactions in susceptible

individuals. The duration and intensity of the pollen season can vary depending on various factors, including geographical location, climate, and the types of plants present in a particular area. To determine the pollen calendar for prevalent pollen taxa in the Irish environment, mean daily pollen values were calculated for 21 specific pollen types (Figure 1.7), with the daily values for each month being divided into five sections, each containing six days. The mean value for each section is calculated for every pollen type. Early and late flowering periods are identified outside the main flowering period. The early flowering period is defined when the annual mean pollen concentration ranges from greater than 5% to less than 10%, while the late flowering period corresponds to an annual mean pollen concentration greater than 90% and less than 99.5%, as shown.

The rise in respiratory allergies aligns with the escalation of outdoor and indoor air pollution. While the precise role of outdoor pollutants in sensitising the airways to allergens is still not fully understood, it is widely acknowledged that outdoor pollution exacerbates respiratory symptoms in individuals with atopy. Both acute and chronic exposure to air pollution components such as sulphur dioxide, nitrogen dioxide, ozone, and respirable particulate matter (either in isolation or in various combinations) heighten airway responsiveness to aeroallergens in individuals with atopy.

Equally, pollutants can adhere to the surfaces of pollen grains, fungal spores, and plant-derived micro-particles, altering their morphology and allergenic potential. Additionally, air pollutants like diesel exhaust particulates can facilitate the immunoglobulin (Ig)E response, contributing to the manifestation of symptoms associated with pollinosis in individuals with atopy (D'Amato, 2000).

Fungal Spores

Fungal spores, such as Aspergillus fumigatus and Penicillium, have been associated with the illnesses mentioned above as causal factors and agents that exacerbate the conditions (Ader et al., 2005; Gregory and Lacey, 1963). Aspergillosis derives its name from the fungal spore that is

particularly detrimental to the lungs. Fungal contamination was closely associated with adverse health effects in occupants, with reported incidence rates of allergy, infection, and inflammation reaching approximately 30% (Idrose *et al.*, 2020; Kono *et al.,* 2020; Rowan *et al.,* 2020; Welsh *et al.,* 2021). The significant role of fungi in allergic diseases has been recognised for a long time (van Tilburg Bernardes et al., 2020). Inhalation of fungal bioaerosols could lead to allergic asthma and rhinitis (Fisk et al., 2010). In hospital environments, infectious fungal aerosols, such as Aspergillus fumigatus, pose a definite risk to patients (Kwon-Chung and Sugui, 2013). Homes with visible mould often experience sinusitis, characterised by inflammation of the sinuses (Khan and Karuppayil, 2012). Adverse health effects resulting from fungal exposure could occur in various settings, including flood-affected buildings, hospitals, and farms (Johanning *et al.,* 2014; Kwon-Chung and Sugui, 2013; Muise *et al.,* 2010; Tomio *et al.,* 2011). Fungal exposure primarily occurs through respiratory inhalation and skin contact with aerosolised fungal spores (Awad *et al.,* 2020). Fungi tend to colonise natural or synthetic materials when suitable nutrition is available and favourable environmental conditions. Sources of nutrients can include settled dust or the materials themselves. (Doherty *et al.,* 2011; Seo *et al.,* 2009). Fungal infestation can also occur on wallpapers attached to indoor walls. Insulation materials made of glass fibre and ceilings are prone to infestation by various fungi, including Aspergillus versicolor, Alternaria brassicicola, Cladosporium, Penicillium, and others.

Bacteria

Due to their small size, bacteria exhibit a relatively long atmospheric residence time, often lasting several days or more, compared to larger particles. This characteristic enables them to be transported over long distances, sometimes spanning thousands of kilometres. Measurements have indicated that average concentrations of bacteria in ambient air can exceed 10,000 cells per cubic meter over land (Bauer *et al.*, 2002).

Airborne bacteria can exist as individual cells, although they are more commonly found attached to other particles, such as soil or leaf fragments or in the form of agglomerates containing multiple bacterial cells (Shaffer and Lighthart, 1997). Consequently, while individual bacteria typically have sizes of 1 micrometre or less, the median aerodynamic diameter of particles containing bacteria may differ depending on their associations with other particles.

Numerous studies conducted in occupational settings have consistently demonstrated positive associations between exposure to endotoxin and various health effects. These effects include reversible conditions like asthma, chronic airway obstruction, respiratory symptoms (such as those associated with asthma, bronchitis, and byssinosis), and increased airway responsiveness. These findings have been observed across a wide range of occupational environments with different levels of exposure and varying compositions of bioaerosol exposures (Milton *et al.,* 1996; Douwes and Heederik, 1997).

For example, a study conducted in the potato processing industry revealed that acute airway obstruction became evident at levels of approximately 50 endotoxin units (EU)/m^3 (approximately 5 ng/m^3) (Zock *et al.,* 1998). Individuals with increased bronchial hyper-responsiveness and asthma are more susceptible to developing symptoms (Post *et al.*, 1998)

Moreover, several studies conducted in indoor environments have suggested a causal association between endotoxin and asthma exacerbation in children and adults (Michel *et al.,* 1996; Park et al., 2001). These findings collectively highlight the potential health risks associated with exposure to endotoxin and the importance of considering susceptible individuals when assessing the impact of such exposures.

1.4.2 PBAPs Interaction with Air Pollution

Air pollution from both natural and human activities imposes a significant environmental burden. Ensuring healthy living spaces and good air quality is a global priority, considering individuals inhale approximately 15,000 litres of air within 24 hours (WHO, 2006). Consequently, current efforts to monitor and reduce exposure to air pollutants present a significant challenge. Among the crucial indicators for assessing indoor and outdoor air quality are bioaerosols.

Bioaerosols and pollution have a complex and multifaceted relationship where certain types of pollution can influence bioaerosols' production, dispersion, and longevity in the environment. Pollutants such as sulphur dioxide, nitrogen oxides, and particulate matter (PM) can affect bioaerosols in several ways. For instance, high concentrations of these pollutants can inhibit the growth of certain fungi and bacteria, potentially reducing their contribution to the bioaerosol population.

Monitoring and controlling bioaerosol emissions from industrial sources and agricultural activities are also essential for reducing pollution levels, as pollution can significantly affect the distribution and abundance of fungal spores in the environment. Air pollution, exceptionally high levels of particulate matter and pollutants such as nitrogen dioxide and sulfur dioxide, can have several effects on fungal spores.

Pollution can also impact the ecological dynamics of fungi. Air quality, temperature, and humidity due to pollution can influence the growth and distribution of fungi, altering their abundance and diversity (Gajewska *et al.*, 2022). Certain fungal species may thrive under polluted conditions, while others may decline. For example, Aspergillus fumigatus can be found in environments with high levels of heavy metals, such as arsenic and cadmium. Studies have confirmed the potential of pathogenic fungal species, including Fusarium sp., Penicillium sp., and Aspergillus sp., in the

bioremediation of environmental contamination caused by heavy metals (HM) such as lead (Pb), chromium (Cr), nickel (Ni), and silver (Ag). These pathogenic fungi have demonstrated the ability to remove or mitigate HM pollutants from contaminated environments effectively. It exhibits a high tolerance to metal pollution and can accumulate and detoxify these metals within its cells (Gajewska *et al.*, 2022). In mitigating the impacts of pollution on fungal spores and human health, it is crucial to address the sources of pollution, improve air quality, and implement effective measures for indoor and outdoor air filtration. Monitoring and understanding the interactions between pollution and fungal spores can contribute to better environmental management and public health strategies.

Monitoring anemophilous fungi can provide valuable insights into environmental changes associated with pollution. These fungi, dispersed by air currents, can serve as indicators of atmospheric conditions affected by pollution. When subjected to disturbances, fungal spores can detach from colonies growing on indoor materials and enter the air, contributing to bioaerosol formation and air pollution (Bonetta *et al.,* 2010). A study investigated microbial concentrations in the air of public buildings using the conventional plate count method (Gots *et al.,* 2003). The study revealed that the average concentration of airborne fungi in commercial buildings exceeded 1500 CFU m^{-3}, while the average value in 820 residential buildings was 1252 CFU m^{-3} (Sessa *et al.*, 2002).

Indoor environments provide favourable conditions for the growth and reproduction of fungi. Common fungal species in indoor settings include Aspergillus, Alternaria, Cladosporium, Penicillium, Trichoderma, and others. Components of HVAC systems such as cooling coils, ventilation ducts, and filters serve as ideal substrates for fungal growth. When subjected to high-speed airflow, fungal spores detach from colonies and disperse indoors, leading to indoor air

pollution. Indoor pollution can stem from various sources, including abiotic agents such as dust, particulate matter, wall coverings, synthetic paints, adhesives, and polishes.

Moreover, these factors contribute to the phenomenon known as Sick Building Syndrome (SBS) (Chao *et al.,* 2002; Horner, 2003), emphasising the importance of addressing indoor air quality to safeguard human health. Health issues related to indoor environments have raised concerns in both occupational and residential settings, describing the increased prevalence of respiratory diseases among individuals inhabiting human-constructed homes or workplaces. Additionally, fungal spores are recognised for their pathogenic characteristics, causing diseases in crops and natural vegetation. The consequences of these fungal diseases negatively impact the economy and public health.

Anemophilous fungi, a subset of bioaerosols, can serve as bioindicators for air pollution, plant diseases, and allergic reactions, encompassing a broad range of clinical manifestations. Their concentration in urban areas varies due to the interplay between biological and environmental factors (Emygdio *et al.,* 2018). While advancements in monitoring air pollutants have been significant in recent decades, the progress in monitoring pollen and other airborne allergens has been slower (Mücke *et al.,* 2014). This is particularly relevant for studying the short-term health effects of air pollution, while long-term exposure is typically obtained through modelling techniques (Hertel *et al.,* 2013).

In health assessment studies on air pollution, urban background levels are generally considered a better exposure indicator than pollutant levels on busy streets (McNabola *et al.*, 2011). People spend most of their time indoors, and buildings are typically ventilated towards the backyards rather than the heavily trafficked streets. Additionally, only a limited amount of pollen enters buildings. Dose-response relationships have been established for air pollutants and various health outcomes using the urban background as an exposure proxy (evidenced in studies like Andersen *et al.,* 2009). It has been observed that background pollen concentrations correlate well with measurements taken

at the height of human breathing (Rantio-Lehtimäki *et al.,* 1991, Alcazar *et al.,* 1999, Peel *et al.,* 2013b). Moreover, background concentrations correlate well with average daytime personal exposure and short-term measurements of pollen grain doses, although substantial quantitative differences may exist. Therefore, outdoor background concentrations of pollen and chemical air pollutants can be considered reliable qualitative proxies for exposure.

1.4.3 Weather/ Climate

Weather conditions significantly affect the atmosphere's release, dispersal, and concentration of pollen and fungal spores. Various weather factors can directly or indirectly influence the behaviour of these bioaerosols. Temperature affects pollen and fungal spores' growth, development, and release. Warmer temperatures can accelerate plant growth and flowering, increasing pollen production (Twohy *et al.*, 2016). Similarly, fungi thrive in specific temperature ranges, and warmer conditions can promote their growth and sporulation. However, extreme temperatures, whether too hot or too cold, can inhibit the release of bioaerosols. Humidity plays a vital role in germinating and releasing fungal spores. High humidity provides favourable conditions for fungal growth and sporulation. Conversely, low humidity can inhibit spore release. However, excessive humidity can cause fungal spores to clump together, reducing their dispersal potential. Pollen grains can also be affected by humidity, as high humidity can cause them to rupture and release allergenic particles (Zang *et al.*, 2019). Wind is a crucial factor in the dispersal of both pollen and fungal spores. Strong winds can carry these bioaerosols over long distances, facilitating their spread. The pollen spectrum is intricately influenced by the interplay of land cover, wind direction, and trap placement. The types and quantities of airborne pollen can vary significantly based on the surrounding vegetation and land use. Wind direction determines the source and trajectory of bioaerosols, affecting localized pollen and spore concentrations. Additionally, gusty winds can increase pollen release by shaking plants or dislodging fungal spores from surfaces (Huang *et al.*, 2015).

Rainfall can have varying effects on pollen and fungal spores. Light rain can temporarily reduce airborne pollen and spore levels by causing them to settle. However, heavy rain can lead to the bursting of fungal fruiting bodies, resulting in a sudden release of spores into the air. Rain can also wash pollen from the air, temporarily alleviating symptoms for allergy sufferers. Following rainfall, humidity levels may rise, creating favourable conditions for fungal growth (Gabey *et al.*, 2011).

Climate can also significantly affect pollen and fungal spores' production, release, and distribution, affecting their abundance and allergenic potential. While weather and climate are linked, climate is increasingly important as climate change continues to be seen (Emberlin, 1994). Several parameters will be affected, such as climate patterns, especially long-term temperature trends, which can impact the timing and duration of pollen seasons. Warmer temperatures can lead to earlier flowering and prolonged pollen release, extending the allergy season for pollen-sensitive individuals (Norris-Hill, 1997). Climate change-induced temperature shifts may alter the phenology of plants, affecting pollen production and potentially exacerbating allergic reactions. Changes in precipitation patterns can influence fungal spores' growth, sporulation, and dispersal. Increased rainfall can promote fungal growth and enhance spore production (Bauer *et al.*, 2002). Changes in seasonal patterns, such as longer or shorter seasons, can affect the duration and severity of allergy symptoms. Climate factors influence air quality, which in turn can impact the dispersal and allergenicity of pollen and fungal spores (D'Amato, 2000). Poor air quality, including high levels of pollutants, can exacerbate allergic reactions and respiratory symptoms in individuals exposed to bioaerosols (Douwes *et al.*, 1999).

1.5 Bioaerosol Monitoring

1.5.1 Traditional

Hirst

The Hirst spore trap is the most widely used instrument for monitoring airborne pollen and fungal spores. It was named after the British mycologist John Hirst, who developed it in the 1950s while working at the UK's National Institute for Medical Research to develop a way to study the epidemiology of asthma and hay fever, conditions known to be triggered by airborne allergens. Hirst recognised that to understand these diseases, it would be necessary to monitor the presence of these allergens in the air over extended periods.

The Hirst spore trap works on the principle of impaction. It draws in the air volume per unit of time using a vacuum pump. The air is directed onto a sticky surface, typically a rotating drum covered with adhesive tape. Particles in the air, including pollen grains and fungal spores, impact the tape and stick to it. The drum is set to rotate at a fixed speed so that the tape moves at a constant rate, approximately 2 mm per hour. Examining the tape under a microscope makes it possible to identify and count the trapped particles. This quantitatively measures the concentration of different types of PBAPs in the air. Since the tape moves constantly, tracking changes in bioaerosol concentrations over time is also possible. The Hirst spore trap has several advantages contributing to its widespread use. It is relatively simple and inexpensive to build and operate. It can run continuously for extended periods. The need to manually analyse the tape under a microscope makes it labour-intensive and limits the speed at which data can be obtained.

Traditional monitoring and real-time monitoring are two approaches to data collection and analysis. Traditional monitoring involves collecting data at regular intervals, which can result in a time delay between data collection and analysis. Data is typically collected manually or using automated instruments that require periodic maintenance and calibration. Traditional monitoring methods may be accurate but are subject to environmental conditions, sample collection, and analysis variations. Data precision can vary depending on the quality of instruments and laboratory techniques. The time-consuming nature of manual counting is a major concern. The manual methods, although a major leap forward in pollen and spore monitoring at the time they were

developed, have several drawbacks (Maya-Manzano et al., 2023). The subjectivity and potential bias introduced by different individuals in the manual counting process can compromise data accuracy and reliability. Other uncertainties stem from fluctuations in the airflow. There is a need for rapid reporting of airborne pollen as well as for alleviating the workload of manual operation (Oteros et al., 2015). In recent years, fluorescence detection for real-time monitoring of ambient particles has gained popularity.

Passive Samplers

Passive samplers, often called "Passive deposition" or "passive impaction" samplers, are the simplest type of samplers in this category. They operate by allowing particles to deposit or impact onto their surfaces without active airflow. It should be noted that the capture of spores by these samplers is influenced by wind speed, with lower volumes of spores collected during periods of reduced wind speeds. Consequently, "Passive samplers" are valuable for recognising airborne fungal spores and are particularly recommended for qualitative analysis in remote areas where volumetric samplers are impractical (Martínez-Bracero *et al.*, 2019).

Rotorod Sampler

A Rotorod Sampler, often called a rotorod or whirling arm, is an air sampling device used in aerobiology and environmental studies to collect and quantify airborne particles, particularly spores and pollen. The device operates based on the principle of impaction. It has several small rods (usually 1-4) that rotate in the air, often coated with an adhesive substance. Airborne particles impact the rods and stick to them due to their inertia. This allows the sampler to collect a representative sample of particles from the surrounding air. Depending on the study, after a fixed exposure period, which could be minutes to hours, the rods are removed, and the particles adhered to them are counted and identified under a microscope. This enables quantifying the number and type of airborne particles in the volume of air sampled. The rotorod sampler is relatively

inexpensive, portable, and requires little power, making it a popular choice for many field studies. It can be used for indoor or outdoor air sampling and is particularly useful for bioaerosol studies, such as those looking at allergenic pollen and fungal spores. It is often used in allergen monitoring networks to provide information about pollen and spore levels to allergy sufferers and healthcare providers. However, the rotorod sampler also has some limitations. For instance, it may not accurately represent the particle size distribution in the air, especially for smaller particles. It also requires regular cleaning and servicing to maintain its performance. Additionally, the collected samples require manual identification and counting under a microscope, which can be labour-intensive and requires expertise in particle identification.

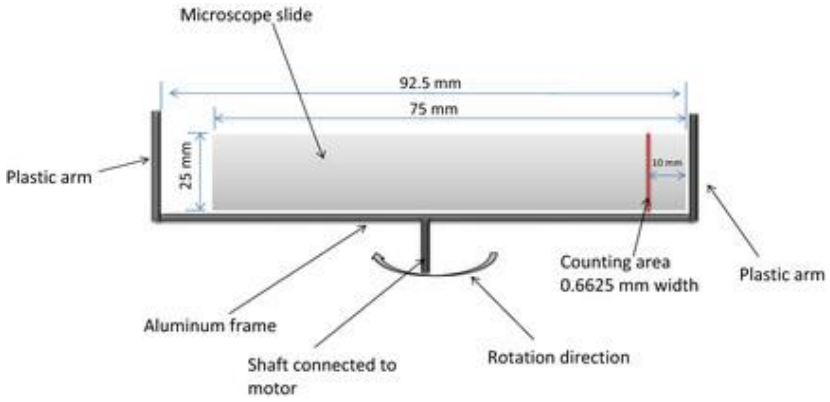

Figure 1.8. Schematic of sampling head of the Rotorod (Huang *et al.*, 2015).

Each of these instruments has its strengths and weaknesses. For example, microscopic methods can provide detailed information about the types of particles present, but they can be labour-intensive and may not capture microscopic particles effectively. Automated systems can provide real-time data but may not be as accurate or detailed as microscopic analyses. Molecular techniques can provide detailed and accurate information but can be expensive and require specialised knowledge and equipment.

Andersen Sampler

The Andersen sampler, also known as an Andersen Impactor or Andersen Cascade Impactor, is an air sampling device primarily used in microbiological and environmental studies to collect and quantify airborne particles, particularly viable microorganisms like bacteria and fungi.

The Andersen sampler operates on the impaction principle, like the Rotorod sampler. The air, containing suspended particles, is drawn into the sampler and passes through a series of stages with perforated plates. These plates, often six to eight in number, have progressively smaller hole sizes, creating a cascade. It is shown in the figure below.

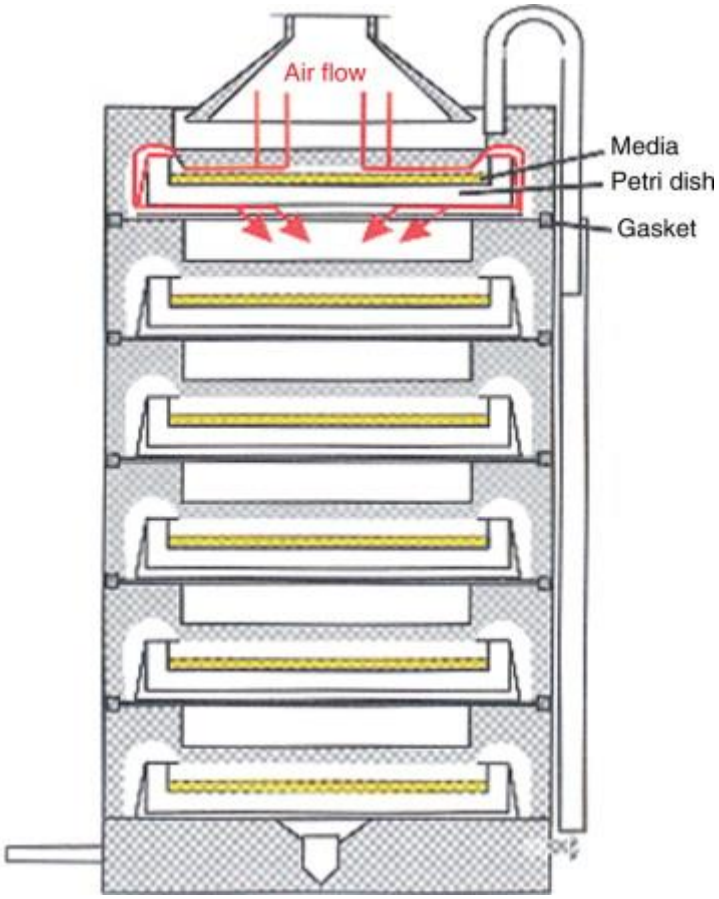

Figure 1.9. Andersen sampler Cascade Impactor Schematic. The diagram illustrates a 6-stage Andersen cascade impactor. Each stage is equipped with a Petri plate filled with nutrient agar. The stages are designed with progressively smaller nozzles, resulting in higher impaction velocities of particles onto the agar (Andersen, 1958).

As the air flows through each stage, particles of a specific size have enough inertia to impact and stick to the plates, which are usually loaded with a culture medium for microorganism growth. Smaller particles remain suspended and continue to the next stage with smaller hole sizes, where

they may be captured if they are large enough. The smallest particles can be captured in a final filter. By the end of the cascade, particles are sorted roughly by size, with larger particles in the earlier stages and smaller particles in the later stages. The plates can then be incubated to grow the captured microorganisms, enabling quantification and identification of viable airborne microorganisms.

Andersen samplers are widely used because they capture and segregate particles of different sizes and collect viable microorganisms. However, they also have limitations. They are typically more expensive and less portable than other types of samplers. The sample analysis process can also be labour-intensive, as each plate needs to be separately incubated and analysed. Furthermore, humidity and temperature can affect the sampler's performance, requiring careful calibration and maintenance.

Andersen sampling is the preferred method for gauging mesophilic bacteria and Aspergillus fumigatus concentrations at compost facilities, although using
filters coupled with lab culture is also an option. The samples obtained are then sent to the lab for further growth (Després *et al.,* 2012). The approach has two significant drawbacks: first, it only assesses the spores and bacteria that are viable on its specific medium, and second, it collects a small volume of air offsite for a brief period (Hryhorczuk *et al.,* 2001). Short collection spans of 2–10 minutes prevent plate overloading, as microorganisms are directly impacted onto the agar surface. This risk is exceptionally high in environments with high concentrations, such as compost sites. Therefore, Andersen sampling should never be carried out on-site at compost facilities. Instead, sampling takes place 100–250 meters upwind and downwind from the source in Ireland (Cartwright *et al.,* 2009, Eduarda and Heederik, 1998, Williams *et al.,* 2013).

1.5.2 Real-Time

Continuous real-time bioaerosol detection systems utilise several methodologies, including intrinsic autofluorescence, light scatter and particle polarity (Kwaśny *et al.*, 2023). These systems have begun to be commonly employed in atmospheric bioaerosol studies, biodefense, and biosecurity applications (Pöhlker *et al.*, 2012). These devices have been shown to distinguish between biological and non-biological particles, providing information on particle size and specific bioaerosol chemical characteristics. The availability of real-time information is expected to significantly reduce direct and indirect healthcare expenses related to allergies in Europe. These costs are estimated to range between €50-150 billion per year (Tummon *et al.*, 2021). The major real-time devices used within the literature are briefly discussed below to highlight their prevalence in the scientific literature.

WIBS

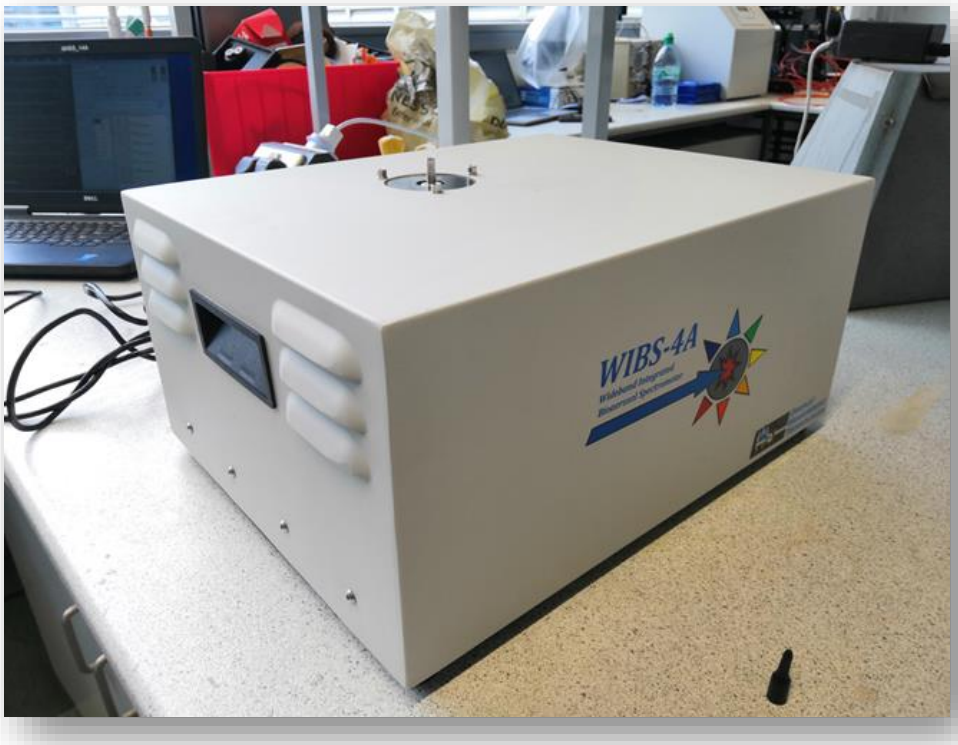

Figure 1.10. WIBS instrument (image taken by author).

The Wideband Integrated Bioaerosol Sensor (WIBS) is an advanced instrument designed to detect and characterise PBAPs in real-time. It employs optical techniques, including laser-induced fluorescence (LIF) and elastic scattering, to identify and classify individual particles based on their fluorescence and size characteristics. The WIBS-4+ draws air samples and directs the particles through a focused laser beam and two Xeon flash lamps. When the particles pass through the beam, they scatter light, and when excited by the Xeon flash lamps, they emit fluorescence signals if they contain fluorescent molecules. The scattered light is detected and analysed to determine the particle size, while the fluorescence signals are analysed for their intensity and wavelength characteristics. The WIBS-4+ can detect the fluorescent biological component of aerosol particles, such as tryptophan, riboflavin, or NADH, during measurement, which provides valuable information on the composition of the sampled air (Table 1.1). It can detect particles ranging from 0.5 to 20 μm, making it suitable for monitoring various PBAPs.

Table 1.1. Fluorophore Excitation and hysplit Wavelengths nm (Fennelly *et al.*, 2018).

Fluorophore	**Excitation Wavelengths (nm)**	**Emission Wavelengths (nm)**
Amino acids	260–295	280–360
NADH and NAD(P)H	290–295, 340–366	440–470
Flavins	450–488	520–560
Cellulose	250–350	350–500
Chitin	335	413
Lignin	240–320	360
Melanin	469–471	543–548
Sporopollenin	300–550	400–650
Chlorophyll	390–470	630–730
Flavonoids	365	440–610

Carotenoids	400–500	520–560
Alkaloids	360–380	410–600
Nucleic acids	270, 320	280–370 / 350–470
Terpenoids	250–395	400–725
Phenolic compounds	300–380	400–500

The WIBS has been utilised in a variety of environments to observe changes in bioaerosol concentrations, including rainforests (Gabey *et al.*, 2010), (Whitehead *et al.*, 2010), urban areas (Gabey *et al.*, 2011a), biowaste (Feeney *et al.*, 2018), green-waste (O'Connor *et al.,* 2015), coastal regions (Daly *et al.*, 2019), indoor settings (Li *et al.*, 2020), and clinical settings (Fennelly *et al.*, 2018). Real-time instruments like the WIBS have become increasingly popular due to several advantages, including high time resolution (in milliseconds), non-destructive sampling, and low consumption of consumables. These techniques also require less operator training compared to traditional methods. The popularity of fluorescent detection for particle monitoring in aerobiological studies continues to grow, and newer monitoring devices with improved functionality and efficiency have emerged. One such device is the WIBS-4+, an upgraded version of the WIBS-4 and is the focus of this study.

Swisens Poleno

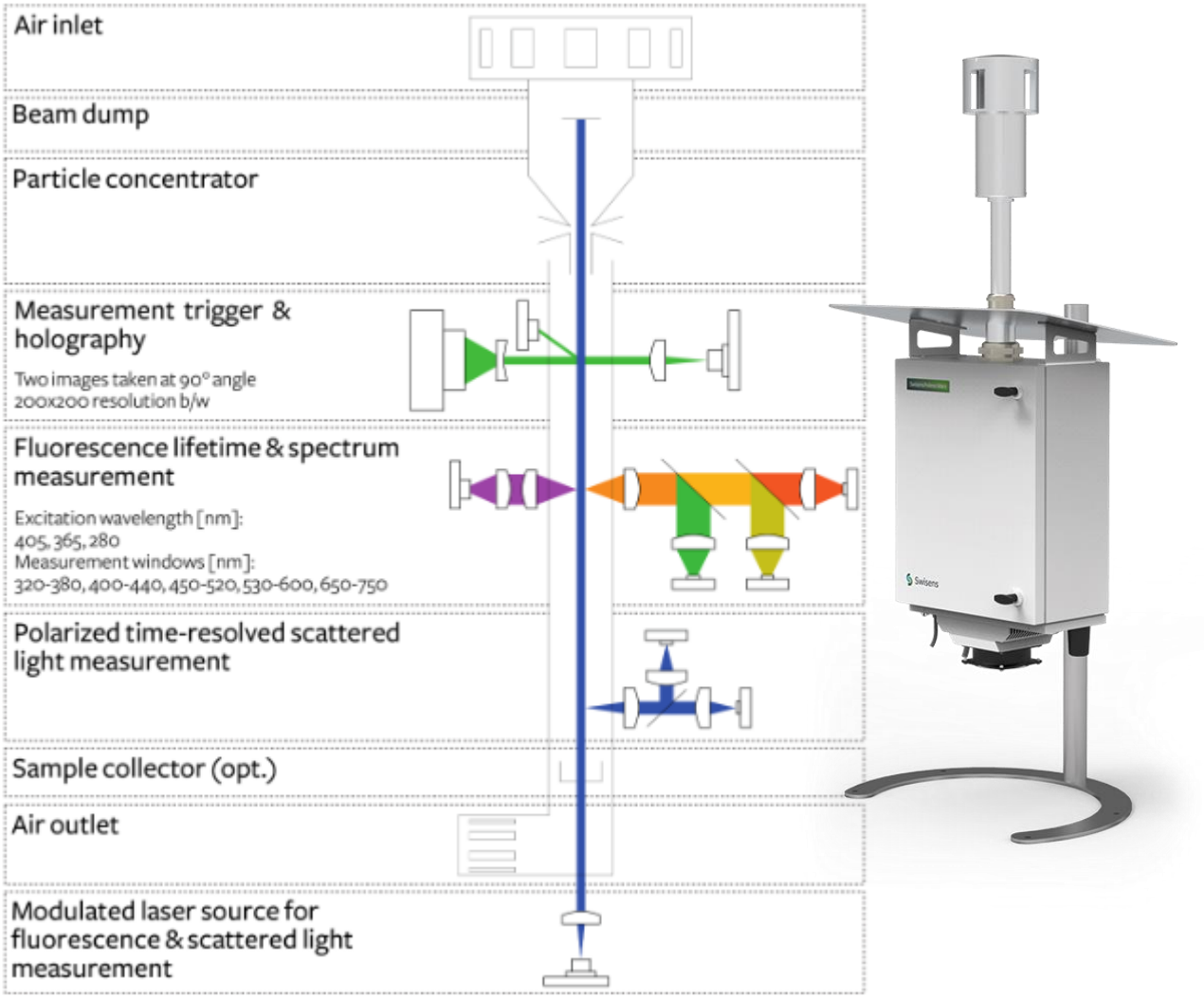

Figure 1.11. The measurement principle of the Swisens Poleno, provided by Swisens AG.

The Swisens Poleno is an airflow cytometer identifying pollen and other airborne particles. It combines digital holography and fluorescence techniques for accurate analysis (Sauvageat *et al.*, 2020). The instrument operates by drawing air through a pump at 40 L/min. A virtual impactor concentrates particles with aerodynamic diameters exceeding 10 µm. Two holography cameras, positioned at a 90° angle to each other, capture digital images of the particles at a resolution of 0.5 µm. These images reconstruct each particle's two in-focus images, enabling detailed analysis. Additionally, a light-emitting diode excites fluorescence at wavelengths of 280 nm and 365 nm.

The Poleno device, developed and manufactured by Swisens AG in Lucerne, Switzerland, uses advanced particle analysis technologies. Additionally, LEDs induce fluorescence at excitation wavelengths 280 nm, 365 nm, and 405nm. The resulting fluorescence is recorded in five different channels spanning 335–380 nm, 415–455 nm, 465–500 nm, 540–580 nm, and 660–690 nm. The quality of the captured images enables preliminary visual verification of particle classification, such as distinguishing between pollen and non-pollen particles and even identifying easily different pollen taxa in some instances. The analysis primarily relies on the captured images, which are processed using convolutional neural networks (CNN). This approach has enabled the identification of eight different pollen taxa, as demonstrated by (Sauvageat *et al.*, 2020).

Plair Rapid-E

Figure 1.12. The Rapid-E Intelligent Real-Time Bioaerosol Sensing, developed by Plair SA.

The Rapid-E device, developed and manufactured by Plair SA in Geneva, Switzerland, is an advanced instrument designed for air particle analysis. Operating at a sampling rate of 2.8 L/min, the Rapid-E utilises a 400 nm laser to capture a scattered light signal at 24 different angles ranging from 45° to 135°. Additionally, each particle undergoes two interactions with a single pulse from a 337 nm laser. The resulting fluorescence is recorded across 32 spectral channels, with a resolution

of 14.51 nm per pixel, covering a spectral range of 350 nm to 800 nm. The fluorescence acquisition is performed in eight sequential acquisitions, each with a retention time of 500 ns.

The instrument's rapid acquisition capability allows for the fluorescence lifetime estimation in four spectral bands: 350–400 nm, 420–460 nm, 511–572 nm, and 672–800 nm. The temporal resolution for fluorescence lifetime measurements is 2 ns (Kiselev et al., 2013; Crouzy et al., 2016; Šauliene et al., 2019; Chappuis et al., 2019). The Rapid-E was operated in a mode suitable for particles ranging from 0.5 μm to 100 μm in diameter for the specific experiment mentioned. In cases where excessive noise is detected on the detector, the instrument automatically adapts the thresholds, reducing sensitivity to small particles. The KH-3000, studied by (Kawashima *et al.*, 2007), and the BAA500, are also recognised for their performance in intercomparison campaigns (Maya-Manzano et al., 2023), which have recently contributed to the field of PBAP monitoring. The ongoing discussions about the KH-3000's performance and the acknowledgement of the BAA500 as a more accurate device providing valuable data into the advancements of real-time pollen monitoring. The inclusion of these devices in previous studies enhances the development of the state-of-the-art equipment used in real-time PBAP monitoring (Oteros et al., 2015; Suarez Suarez et al., 2023).

1.6 Modelling and Forecasting

Modelling bioaerosols involves developing mathematical or statistical models to simulate and predict airborne biological particles' behaviour, dispersion, and concentration. These models help understand the dynamics of bioaerosols, assess exposure risks, and evaluate the effectiveness of control strategies. Modelling bioaerosols helps assess the potential risks of exposure to airborne biological particles. By simulating the dispersion and concentration of bioaerosols, models can estimate the levels of exposure in different scenarios and locations. This information is valuable for evaluating the health risks to individuals and populations, particularly in occupational settings or areas with potential disease transmission. Modelling bioaerosols, especially in the context of

airborne diseases, can aid in predicting outbreaks and understanding disease transmission dynamics to simulate the spread of infections based on bioaerosol exposure and other relevant factors. Such models can inform public health interventions and assist in planning response measures.

Dispersion models simulate the movement and dispersion of bioaerosols in the atmosphere. These models incorporate factors such as meteorological conditions, emission sources, particle characteristics, and terrain features to predict the transport and spread of bioaerosols. Dispersion models can be used to estimate concentration levels, determine the potential exposure of populations, and support decision-making during public health emergencies or environmental assessments.

The Hybrid Single-Particle Lagrangian Integrated Trajectory (HYSPLIT) is a comprehensive method and software platform established by the National Oceanic and Atmospheric Administration (NOAA). It is designed to compute the path and spread of air pollutants, including PBAPs. Frequently used in atmospheric science and air quality studies, HYSPLIT assists in elucidating airborne particulates' movement and ultimate destiny providing a potential source of PBAPs.

The HYSPLIT model combines a Lagrangian technique, which follows individual air particles or parcels through time, accounting for large-scale air mass movement. This dual methodology offers a thorough examination of atmospheric dispersion patterns. Meteorological data, such as wind patterns, temperature, and pressure, are required for HYSPLIT. This information can be procured from weather stations, atmospheric models, or datasets re-analysed. HYSPLIT utilises these data points in tracking the motion of particles or air parcels over a series of time increments. Trajectories are determined considering wind velocity, direction, and vertical mixing. HYSPLIT accounts for various physical mechanisms influencing particle dispersion, including vertical blending,

atmospheric turbulence, and diffusion. These processes rely on empirical parameterisations and characteristics of the atmospheric boundary layer. HYSPLIT can be used reversely to speculate potential source locations of detected pollutants or PBAPs. Studying backward trajectories helps identify potential emission sources. Graphical outputs, such as trajectory maps, concentration contours, and dispersion models provided by HYSPLIT, facilitate a better understanding of transport routes, source-receptor relationships, and potential exposure zones.

HYSPLIT's broad applicability has seen its use in studying diverse atmospheric events, including pollutant dispersion from industrial sources, volcanic ash clouds, smoke from wildfires, and the transport of biological agents. It is flexible and user-friendly software making it an essential instrument for researchers, environmental bodies, and policymakers to evaluate air quality and comprehend atmospheric processes. Developing a pollen dispersion model utilising HYSPLIT has previous studies that have been conducted with this in mind (Monroy-Colín *et al.*, 2020). Daily 24-hour backward dispersion analysis was conducted to investigate the air mass transport patterns above Badajoz, and this analysis followed the methodology described in previous studies (de Weger *et al.*, 2016). The hourly analysis indicated that the highest peaks in air mass concentration for 2017 and 2018 were observed between 13:00 and 15:00. These air mass plumes were calculated using the HYSPLIT model, and this period corresponded to the anticipated arrival of air masses. Obtained from the Global Data Analysis System (GDAS) data with a 0.5 × 0.5 degrees resolution from the NOAA ARL FTP server. This study focused on analysing particles' position within the atmospheric layers from 0 to 4,000 meters above ground level (AGL). It was calculated with a starting time of 15:00 (3:00 PM) for two consecutive days preceding each episode to track the air masses' trajectory. This analysis was conducted during a mismatch between the major pollen season (MPS) and the phenological phenophases from 2016 to 2019.

For enhanced accuracy, three-dimensional trajectories were selected over other computational methods, such as isobaric and isentropic approaches, in the HYSPLIT model (Hernandez-Ceballos *et al.*, 2013). The trajectory represented the integration of the particle's position vector in both space and time. It was interpolated from the native horizontal coordinate system of the meteorological data to an internal terrain-following (r) vertical coordinate system during computation. The final position is determined based on the average velocity at the initial position and the first-guess position. Weather data for these models were obtained from the European Centre for Medium-Range Weather Forecast (ECMWF) with a time interval of 3 hours and a spatial resolution of 25x25 km^2. The data consisted of 75 hybrid vertical levels. This standardised approach ensures consistent results, facilitating a meaningful comparison between the two modelling approaches. The results presented insights into the sources of olive pollen observed in Córdoba, highlighting the influence of three primary source regions during specific periods.

Modelling PBAPs involves developing and implementing computational models to study and understand the dispersion and distribution of airborne pollen particles in the atmosphere. These models aim to simulate the behaviour and movement of bioaerosols, considering various factors such as wind patterns, topography, vegetation distribution, and meteorological conditions. Relevant data on pollen and fungal spore concentrations, meteorological conditions, land cover, and topography are required from various sources such as monitoring stations, weather stations, and satellite imagery. A suitable modelling approach is chosen based on the research objectives, available data, and computational resources such as Eulerian, Lagrangian, and numerical weather prediction models.

The model parameters are defined, which may include PBAP emission rates, deposition rates, particle size distribution, viability, and aerodynamic properties. The selected model equations and algorithms are programmed and implemented on a computational platform. This involves

discretising the domain into a grid, solving the governing equations, and incorporating the defined parameters. The model's performance is evaluated by comparing its predictions with observed data. This step helps assess the accuracy and reliability of the model and identify any discrepancies or areas for improvement. Sensitivity tests examine the model's response to changes in various input parameters. This analysis helps understand the relative importance of different factors affecting PBAPs and identify critical parameters significantly influencing the model's output.

Modelling techniques for pollen and fungal spore forecasting aim to predict and provide information about these bioaerosols' future concentrations and distribution (O'Connor *et al.*, 2014; Maya-Manzano *et al.*, 2021). Several approaches are employed to develop such models. Statistical models utilise observed data to establish relationships between bioaerosol concentrations and relevant influencing factors. These models can identify critical predictors, estimate exposure-response relationships, and predict bioaerosol concentrations based on environmental variables, meteorological data, or other covariates. Statistical models are often used with field measurements to assess exposure risks and predict bioaerosol levels in different scenarios. Observation-oriented models rely on our understanding of the environment in specific locations. For instance, by utilising average pollen concentrations from the same day in previous years, pollen calendars can be transformed into forecasting tools (Šikoparija *et al.,* 2018a). In these mathematical and statistical models, the dependent variables are phenological observations or airborne pollen concentrations, which can be predicted using one or more independent variables, such as meteorological data. However, a notable drawback of this approach is its site-specific nature, making it challenging to extrapolate the findings to other locations.

Conventional modelling approaches include regression, time-series analyses, and process-based phenological models. Linear regression is a statistical method that involves analysing the relationship between two quantitative variables, where one variable is the dependent variable (Y)

and the other is the independent variable (X), which is explained by a straight line. Multiple regression analysis extends this approach by incorporating multiple independent variables to predict the dependent variable (Y), allowing for linear or nonlinear relationships between the variables (Kinnear and Gray, 1999). In these regression analyses, the historical observations of the parameters are used to predict future values, such as pollen concentrations. The establishment of a regression model involves determining the slope (b) and correlation coefficient (r), which serve as indicators of the relationship and predictive value between the variables (Comtois, 1998). Overall, linear regression and multiple regression analyses provide a framework for predicting and understanding the relationship between dependent and independent variables, with historical observations serving as a basis for future predictions. Regression analysis remains a widely employed method for modelling various aspects related to airborne pollen. It is utilised to analyse daily average pollen concentrations (Janati et al., 2017) as well as different characteristics of the pollen season. These characteristics include the start date of the season (Zhang *et al.,* 2015; Novara *et al.,* 2016), peak day (Myszkowska, 2013), duration (Zhang and Huang, 2015), and intensity (Oteros *et al.,* 2013a; Bonini *et al.,* 2015). The POMMEL project published “Spatial and temporal variations in the distribution of birch trees and airborne Betula pollen in Ireland" by (Maya-Manzano et al., 2021) had the inclusion of x, y, and z coordinates with altitude data adding a layer of detail to the analysis, providing a more comprehensive understanding of the dynamics of birch pollen distribution. The use of advanced spatial analysis techniques and the incorporation of altitude data with 3D coordinates provided a more nuanced view of the environmental factors influencing pollen dispersal.

Time-series analysis is a valuable technique utilised in aerobiology to gain insights from observed data and examine the underlying relationships. This approach involves studying more extended datasets to forecast potential future trends and patterns. By analysing the temporal structure of the data, time-series analysis provides valuable information about the dynamics and behaviour of

aerobiological phenomena over time. The primary objective of time-series analyses is to decompose datasets into distinct patterns to isolate the disturbances caused by normal seasonal behaviour, such as weather parameters. However, apart from the random components that are difficult to define, residual noise may be present due to inter-annual variability or unknown factors. By decomposing the data, the underlying trend becomes more apparent and interpretable, allowing us to prevent other parameters from masking the actual pattern. This decomposition process enables a clearer understanding of the general trend and helps to disentangle it from other influences, ensuring a more accurate interpretation of the data.

The term "model building" is often overused, primarily focusing on establishing and testing the slope and correlation coefficients within the regression context. However, a relatively recent technique called Machine Learning (or Deep Learning) has gained significant traction in various fields of data mining. Machine Learning has successfully integrated and applied in diverse disciplines, including self-driving vehicles and image recognition (Zhang *et al.,* 2018). This analytical solution is viewed as a promising tool across different domains.

Anticipated advances in commercial production and expertise are expected to reduce the cost of automatic real-time monitoring devices soon. This cost reduction would enable faster sampling and analytical processing, leading to extended forecast horizons and improved predictions. Moreover, high temporal resolution measurements facilitated by such devices would enhance our understanding of atmospheric processes (Šikoparija *et al.,* 2018b; Chappuis *et al.,* 2020). In this discussion, we will explore the two primary approaches for modelling and forecasting airborne pollen, as Scheifinger *et al.,* (2013) outlined: observation-oriented and source-based models. Various machine learning techniques are utilised in pollen forecasting, with Artificial Neural Networks (ANNs), Support Vector Machines (SVMs), and Random Forests (RFs) being extensively discussed methods. Additionally, lesser-known machine learning techniques have been

studied for this purpose, including the Least Absolute Shrinkage and Selection Operator (LASSO) (Liu *et al.,* 2017), Cubist algorithms, and Multivariate Adaptive Regression Splines (MARS) (Nowosad *et al.,* 2018). These alternative techniques offer additional options for modelling and predicting pollen concentrations, contributing to the diversity of approaches in pollen forecasting.

Modelling bioaerosols provides a quantitative and predictive framework for understanding their behaviour, assessing exposure risks, guiding control strategies, predicting disease spread, and filling data gaps. It supports research, risk assessment, and decision-making processes related to bioaerosols in diverse fields, including public health, environmental science, occupational safety, and epidemiology.

References

.

Adams, R.I. *et al.* (2016) 'Ten questions concerning the microbiomes of buildings', *Building and Environment*, 109, pp. 224–234. Available at: https://doi.org/10.1016/j.buildenv.2016.09.001.

Aerosol Technology: Properties, Behavior, and Measurement of Airborne Particles, 2nd Edition | Wiley (no date) *Wiley.com*. Available at: https://www.wiley.com/en-ie/Aerosol+Technology%3A+Properties%2C+Behavior%2C+and+Measurement+of+Airborne+Particles%2C+2nd+Edition-p-9781118591970 (Accessed: 7 July 2023).

Alzate, F. *et al.* (2015) 'Atmospheric pollen and spore content in the urban area of the city of Medellin, Colombia', *Hoehnea*, 42, pp. 09–19. Available at: https://doi.org/10.1590/2236-8906-52/2013.

de Ana, S.G. *et al.* (2006) 'Seasonal distribution of Alternaria, Aspergillus, Cladosporium and Penicillium species isolated in homes of fungal allergic patients', *Journal of Investigational Allergology & Clinical Immunology*, 16(6), pp. 357–363.

Andersen, A.A. (1958) 'NEW SAMPLER FOR THE COLLECTION, SIZING, AND ENUMERATION OF VIABLE AIRBORNE PARTICLES, 12', *Journal of Bacteriology*, 76(5), pp. 471–484.

Bauer, H. *et al.* (2002) 'The contribution of bacteria and fungal spores to the organic carbon content of cloud water, precipitation and aerosols', *Atmos. Res*, 64, pp. 109–119. Available at: https://doi.org/10.1016/S0169-8095(02)00084-4.

Beck, J.M., Young, V.B. and Huffnagle, G.B. (2012) 'The microbiome of the lung', *Translational Research: The Journal of Laboratory and Clinical Medicine*, 160(4), pp. 258–266. Available at: https://doi.org/10.1016/j.trsl.2012.02.005.

Belizario, J.A., Lopes, L.G. and Pires, R.H. (2021) 'Fungi in the indoor air of critical hospital areas: a review', *Aerobiologia*, 37(3), pp. 379–394. Available at: https://doi.org/10.1007/s10453-021-09706-7.

Brock, C.A. *et al.* (2021) 'Ambient aerosol properties in the remote atmosphere from global-scale in situ measurements', *Atmospheric Chemistry and Physics*, 21(19), pp. 15023–15063. Available at: https://doi.org/10.5194/acp-21-15023-2021.

Burrows, S.M. *et al.* (2009) 'Bacteria in the global atmosphere – Part 2: Modeling of emissions and transport between different ecosystems', *Atmospheric Chemistry and Physics*, 9(23), pp. 9281–9297. Available at: https://doi.org/10.5194/acp-9-9281-2009.

Cascade Impactor - an overview | ScienceDirect Topics (no date). Available at: https://www.sciencedirect.com/topics/chemistry/cascade-impactor (Accessed: 28 June 2023).

Cheek, E. *et al.* (2021) 'Portable air purification: Review of impacts on indoor air quality and health', *Science of The Total Environment*, 766, p. 142585. Available at: https://doi.org/10.1016/j.scitotenv.2020.142585.

Chen, Q. and Hildemann, L.M. (2009) 'The effects of human activities on exposure to particulate matter and bioaerosols in residential homes', *Environmental Science & Technology*, 43(13), pp. 4641–4646. Available at: https://doi.org/10.1021/es802296j.

Cho, E.-M. *et al.* (2019) 'Distribution and Influencing Factors of Airborne Bacteria in Public Facilities Used by Pollution-Sensitive Population: A Meta-Analysis', *International Journal of Environmental Research and Public Health*, 16(9), p. 1483. Available at: https://doi.org/10.3390/ijerph16091483.

Crawford, I. *et al.* (2015) 'Evaluation of hierarchical agglomerative cluster analysis methods for discrimination of primary biological aerosol', *Atmos. Meas. Tech*, 8, pp. 4979–4991. Available at: https://doi.org/10.5194/amt-8-4979-2015.

D'Amato, G. (2000) 'Urban air pollution and plant-derived respiratory allergy', *Clinical and Experimental Allergy*, 30(5), pp. 628–636.

D'Amato, G. *et al.* (2007) 'Allergenic pollen and pollen allergy in Europe', *Allergy*, 62(9), pp. 976–990. Available at: https://doi.org/10.1111/j.1398-9995.2007.01393.x.

Després, VivianeR. *et al.* (2012) 'Primary biological aerosol particles in the atmosphere: a review', *Tellus Series B Chemical and Physical Meteorology B*, 64, p. 15598. Available at: https://doi.org/10.3402/tellusb.v64i0.15598.

Dixon, J.M., Taniguchi, M. and Lindsey, J.S. (2005) 'PhotochemCAD 2: a refined program with accompanying spectral databases for photochemical calculations', *Photochemistry and Photobiology*, 81(1), pp. 212–213. Available at: https://doi.org/10.1562/2004-11-06-TSN-361.

Douwes, J. *et al.* (1999) 'Fungal extracellular polysaccharides in house dust as a marker for exposure to fungi: relations with culturable fungi, reported home dampness, and respiratory symptoms', *The Journal of Allergy and Clinical Immunology*, 103(3 Pt 1), pp. 494–500. Available at: https://doi.org/10.1016/s0091-6749(99)70476-8.

DOUWES, J. *et al.* (2003) 'Bioaerosol Health Effects and Exposure Assessment: Progress and Prospects', *The Annals of Occupational Hygiene*, 47(3), pp. 187–200. Available at: https://doi.org/10.1093/annhyg/meg032.

D'Ovidio, M. *et al.* (2021) 'Pollen and Fungal Spores Evaluation in Relation to Occupants and Microclimate in Indoor Workplaces', *Sustainability*, 13, p. 3154. Available at: https://doi.org/10.3390/su13063154.

Elbert, W. *et al.* (2007) 'Contribution of fungi to primary biogenic aerosols in the atmosphere: Wet and dry discharged spores, carbohydrates, and inorganic ions', *Atmospheric Chemistry and Physics*, 7(17), pp. 4569–4588. Available at: https://doi.org/10.5194/acp-7-4569-2007.

Emberlin, J. (1994) 'The Effects of Patterns in Climate and Pollen Abundance on Allergy', *Allergy*, 49, pp. 15-20,. Available at: https://doi.org/10.1111/j.1398-9995.1994.tb04233.x.

Ewa Brągoszewska, Magdalena Bogacka, and Krzysztof Pikoń (2020) 'Effectiveness and Eco-Costs of Air Cleaners in Terms of Improving Fungal Air Pollution in Dwellings Located in Southern Poland—A Preliminary Study'. Available at: https://www.mdpi.com/2073-4433/11/11/1255 (Accessed: 10 July 2023).

Feeney, P. *et al.* (2018) 'A comparison of on-line and off-line bioaerosol measurements at a biowaste site', *Waste Management*, 76, pp. 323–338. Available at: https://doi.org/10.1016/j.wasman.2018.02.035.

Fennelly, M.J. *et al.* (2018) 'Review: The Use of Real-Time Fluorescence Instrumentation to Monitor Ambient Primary Biological Aerosol Particles (PBAP)', *Atmosphere*, 9(1), p. 1. Available at: https://doi.org/10.3390/atmos9010001.

Fernández-Rodríguez, S., Tormo-Molina, R., Lemonis, N., Clot, B., O'Connor, D.J., *et al.* (2018) 'Comparison of fungal spores concentrations measured with wideband integrated bioaerosol sensor and Hirst methodology', *Atmos. Environ*, 175, pp. 1–14. Available at: https://doi.org/10.1016/j.atmosenv.2017.11.038.

Fernández-Rodríguez, S., Tormo-Molina, R., Lemonis, N., Clot, B., O'Connor, D. J., *et al.* (2018) 'Comparison of fungal spores concentrations measured with wideband integrated bioaerosol sensor and Hirst methodology', *Atmospheric Environment*, 175(May 2017), pp. 1–14. Available at: https://doi.org/10.1016/j.atmosenv.2017.11.038.

Flint, K.M. and Thomson, S. V. (2000) 'Seasonal infection of the weed dyer's woad by a Puccinia sp. rust used for biocontrol, and effects of temperature on basidiospore production', *Plant Disease*, 84(7), pp. 753–759. Available at: https://doi.org/10.1094/PDIS.2000.84.7.753.

Franchitti, E. *et al.* (2020) 'Methods for Bioaerosol Characterization: Limits and Perspectives for Human Health Risk Assessment in Organic Waste Treatment', *Atmosphere*, 11(5), p. 452. Available at: https://doi.org/10.3390/atmos11050452.

Gabey, A.M. *et al.* (2010) 'Measurements and comparison of primary biological aerosol above and below a tropical forest canopy using a dual channel fluorescence spectrometer', *Atmos. Chem. Phys*, 10, pp. 4453–4466. Available at: https://doi.org/10.5194/acp-10-4453-2010.

Gabey, A.M. *et al.* (2011) 'The fluorescence properties of aerosol larger than 0.8 μ in urban and tropical rainforest locations', *Atmos. Chem. Phys*, 11, pp. 5491–5504. Available at: https://doi.org/10.5194/acp-11-5491-2011.

Gabey, A. M. *et al.* (2011) 'The fluorescence properties of aerosol larger than 0.8 μ in urban and tropical rainforest locations', *Atmospheric Chemistry and Physics*, 11(11), pp. 5491–5504. Available at: https://doi.org/10.5194/acp-11-5491-2011.

Gajewska, J. *et al.* (2022) 'Fungal and oomycete pathogens and heavy metals: an inglorious couple in the environment', *IMA Fungus*, 13(1), p. 6. Available at: https://doi.org/10.1186/s43008-022-00092-4.

Galán, C. *et al.* (2007) 'Spanish Aerobiology Network (REA): Management and Quality Manual; Servicio de Publicaciones Universidad de Córdoba'. Edited by Ed.

Gollakota, A.R.K. *et al.* (2021) 'Bioaerosols: Characterization, pathways, sampling strategies, and challenges to geo-environment and health', *Gondwana Research*, 99, pp. 178–203. Available at: https://doi.org/10.1016/j.gr.2021.07.003.

Gravesen, S. (1979) 'Fungi as a cause of allergic disease', *Allergy*, 34, pp. 135–154.

Griffin, D.W., Westphal, D.L. and Gray, M.A. (2006) 'Airborne microorganisms in the African desert dust corridor over the mid-Atlantic ridge, Ocean Drilling Program, Leg 209', *Aerobiologia*, 22(3), pp. 211–226. Available at: https://doi.org/10.1007/s10453-006-9033-z.

Gubanova, D.P. *et al.* (2021) 'Time Variations in the Composition of Atmospheric Aerosol in Moscow in Spring 2020', *Izvestiya, Atmospheric and Oceanic Physics*, 57(3), pp. 297–309. Available at: https://doi.org/10.1134/S0001433821030051.

Guercio, V. *et al.* (2021) 'Exposure to indoor and outdoor air pollution from solid fuel combustion and respiratory outcomes in children in developed countries: a systematic review and meta-analysis', *Science of The Total Environment*, 755, p. 142187. Available at: https://doi.org/10.1016/j.scitotenv.2020.142187.

Hand, J.L. *et al.* (2014) 'Journal of Geophysical Research : Atmospheres Aerosols across the United States', *Journal of Geophysical Research : Atmospheres*, 119, pp. 832-849,. Available at: https://doi.org/10.1002/2014JD022495.Received.

Hart, M.L., Wentworth, J.E. and Bailey, J.P. (1994) 'The effects of trap height and weather variables on recorded pollen concentration at leicester', *Grana*, 33(2), pp. 100–103. Available at: https://doi.org/10.1080/00173139409427840.

Healy, D.A. *et al.* (2012) 'A laboratory assessment of the Waveband Integrated Bioaerosol Sensor (WIBS-4) using individual samples of pollen and fungal spore material', *Atmospheric Environment*, 60, pp. 534–543. Available at: https://doi.org/10.1016/j.atmosenv.2012.06.052.

Healy, D.A. *et al.* (2014a) 'Ambient measurements of biological aerosol particles near Killarney, Ireland: a comparison between real-time fluorescence and microscopy techniques', *Atmospheric Chemistry and Physics*, 14(15), pp. 8055–8069. Available at: https://doi.org/10.5194/acp-14-8055-2014.

Healy, D.A. *et al.* (2014b) 'Ambient measurements of biological aerosol particles near Killarney, Ireland: A comparison between real-time fluorescence and microscopy techniques', *Atmospheric Chemistry and Physics*, 14(15), pp. 8055–8069. Available at: https://doi.org/10.5194/acp-14-8055-2014.

Hernandez, M. *et al.* (2016) 'Chamber Catalogues of Optical and Fluorescent Signatures Distinguish Bioaerosol Classes', *Atmospheric Measurement Techniques*, 9, pp. 3283-3292,. Available at: https://doi.org/10.5194/amt-9-3283-2016.

Hernandez, Mark *et al.* (2016) 'Chamber catalogues of optical and fluorescent signatures distinguish bioaerosol classes', *Atmospheric Measurement Techniques*, 9(7), pp. 3283–3292. Available at: https://doi.org/10.5194/amt-9-3283-2016.

Hernández Trejo, F. *et al.* (2012) 'Airborne ascospores in Mérida (SW Spain) and the effect of rain and other meteorological parameters on their concentration', *Aerobiologia*, 28(1), pp. 13–26. Available at: https://doi.org/10.1007/s10453-011-9207-1.

Hernandez-Ceballos, M.A. *et al.* (2013) 'Analysis of atmospheric dispersion of olive pollen in southern Spain using SILAM and HYSPLIT models', *Aerobiologia*, 30(3), p. 239.

Hirst, J.M. (1952) 'An Automatic Volumetric Spore Trap', *Annals of Applied Biology*, 39(2), pp. 257–265. Available at: https://doi.org/10.1111/j.1744-7348.1952.tb00904.x.

Hollins, P.D. *et al.* (2004a) 'Relationships between airborne fungal spore concentration of Cladosporium and the summer climate at two sites in Britain', *International Journal of Biometeorology*, 48(3), pp. 137–141. Available at: https://doi.org/10.1007/s00484-003-0188-9.

Hollins, P.D. *et al.* (2004b) 'Relationships between airborne fungal spore concentration of Cladosporium and the summer climate at two sites in Britain', *International Journal of Biometeorology*, 48(3), pp. 137–141. Available at: https://doi.org/10.1007/s00484-003-0188-9.

Horner, H.T. (2009) 'Fluorescing World of Plant Secreting Cells. By Victoria V. Roshchina.', *The Quarterly Review of Biology*, 84(1), pp. 110–111. Available at: https://doi.org/10.1086/598302.

Huang, H. *et al.* (2015) 'Wind-mediated horseweed (Conyza canadensis) gene flow: Pollen emission, dispersion, and deposition', *Ecology and evolution*, 5, pp. 2646–58. Available at: https://doi.org/10.1002/ece3.1540.

Huffman, J.A. *et al.* (2013) 'High concentrations of biological aerosol particles and ice nuclei during and after rain', *Atmospheric Chemistry and Physics*, 13(13), pp. 6151–6164. Available at: https://doi.org/10.5194/acp-13-6151-2013.

Jesús Aira, M. *et al.* (2012) 'Cladosporium airborne spore incidence in the environmental quality of the Iberian Peninsula', *Grana*, 51(4), pp. 293–304. Available at: https://doi.org/10.1080/00173134.2012.717636.

Jordan, B.M.M. (1990) 'cepae , leaf blotch pathogens of leek and onion . 11 . Infection of host plants'.

Kawashima, S. *et al.* (2007) 'An algorithm and a device for counting airborne pollen automatically using laser optics', *Atmospheric Environment*, 41, pp. 7987–7993. Available at: https://doi.org/10.1016/j.atmosenv.2007.09.019.

Kellogg, C.A. *et al.* (2004) 'Characterization of aerosolized bacteria and fungi from desert dust events in Mali, West Africa', *Aerobiologia*. Available at: https://doi.org/10.1023/B:AERO.0000032947.88335.bb.

Kruglyakova, E., Mirskaya, E. and Agranovski, I.E. (2022) 'Bioaerosol Release from Concentrated Microbial Suspensions in Bubbling Processes', *Atmosphere*, 13(12), p. 2029. Available at: https://doi.org/10.3390/atmos13122029.

Kwaśny, M. *et al.* (2023) 'Fluorescence Methods for the Detection of Bioaerosols in Their Civil and Military Applications', *Sensors*, 23(6), p. 3339. Available at: https://doi.org/10.3390/s23063339.

de La Guardia, C.D. *et al.* (1998) 'An aerobiological study of Urticaceae pollen in the city of Granada (S. Spain): Correlation with meteorological parameters', *Grana*, 37(5), pp. 298–304. Available at: https://doi.org/10.1080/00173139809362682.

Latif, R. *et al.* (2021) 'First report et al. of Didymella americana causing leaf blight on Lily [Lilium hybrida (Longiflorum x Asiatic)] in India', *Indian Phytopathology*, 74(3), pp. 855–857. Available at: https://doi.org/10.1007/s42360-021-00386-4.

Li, D.W. and Kendrick, B. (1995) ‘A year-round study on functional relationships of airborne fungi with meteorological factors’, *International Journal of Biometeorology*, 39(2), pp. 74–80. Available at: https://doi.org/10.1007/BF01212584.

Li, J. *et al.* (2020) ‘Size-resolved dynamics of indoor and outdoor fluorescent biological aerosol particles in a bedroom: A one-month case study in Singapore’, *Indoor Air*, 30(5), pp. 942–954. Available at: https://doi.org/10.1111/ina.12678.

Lieberherr, G. *et al.* (2021) ‘Assessment of real-time bioaerosol particle counters using reference chamber experiments’, *Atmospheric Measurement Techniques*, 14(12), pp. 7693–7706. Available at: https://doi.org/10.5194/amt-14-7693-2021.

Lim, S.H. *et al.* (1998) ‘Outdoor airborne fungal spores in Singapore’, *Grana*, 37(4), pp. 246–252. Available at: https://doi.org/10.1080/00173139809362674.

Luo, Y. *et al.* (2021) ‘The effects of indoor air pollution from solid fuel use on cognitive function among middle-aged and older population in China’, *Science of The Total Environment*, 754, p. 142460. Available at: https://doi.org/10.1016/j.scitotenv.2020.142460.

Madhwal, S. *et al.* (2020) ‘Ambient bioaerosol distribution and associated health risks at a high traffic density junction at Dehradun city, India’, *Environmental Monitoring and Assessment*, 192(3), p. 196. Available at: https://doi.org/10.1007/s10661-020-8158-9.

Mandal, J. and Brandl, H. (2011) ‘Bioaerosols in Indoor Environment - A Review with Special Reference to Residential and Occupational Locations’, *The Open Environmental & Biological Monitoring Journal*, 4(1). Available at: https://benthamopen.com/ABSTRACT/TOEBMJ-4-83 (Accessed: 10 July 2023).

Markey, E. *et al.* (2022) ‘A Modified Spectroscopic Approach for the Real-Time Detection of Pollen and Fungal Spores at a Semi-Urban Site Using the WIBS-4+, Part I’, *Sensors*, 22(22), p. 8747. Available at: https://doi.org/10.3390/s22228747.

Martinez-Bracero, M. *et al.* (2022) ‘Airborne Fungal Spore Review, New Advances and Automatisation’, *Atmosphere*, 13(2), p. 308. Available at: https://doi.org/10.3390/atmos13020308.

Maya-Manzano, J.M. *et al.* (2021) ‘Spatial and temporal variations in the distribution of birch trees and airborne Betula pollen in Ireland’, *Agricultural and Forest Meteorology*, 298–299, p. 108298. Available at: https://doi.org/10.1016/j.agrformet.2020.108298.

MCCARTNEY, H.A. and LACEY, M.E. (1990) ‘The production and release of ascospores of Pyrenopeziza brassicae on oilseed rape’, *Plant Pathology*, 39(1), pp. 17–32. Available at: https://doi.org/10.1111/j.1365-3059.1990.tb02471.x.

McNabola, A. *et al.* (2011) ‘Analysis of the relationship between urban background air pollution concentrations and the personal exposure of office workers in Dublin, Ireland, using baseline separation techniques’, *Atmospheric Pollution Research*, 2(1), pp. 80–88. Available at: https://doi.org/10.5094/APR.2011.010.

Monroy-Colín, A. *et al.* (2020) ‘HYSPLIT as an environmental impact assessment tool to study the data discrepancies between Olea europaea airborne pollen records and its phenology in SW Spain’, *Urban Forestry & Urban Greening*, 53, p. 126715. Available at: https://doi.org/10.1016/j.ufug.2020.126715.

Moulin, C. *et al.* (1997) ‘Control of atmospheric export of dust from North Africa by the North Atlantic Oscillation’, *Nature*, 387(6634), pp. 691–694. Available at: https://doi.org/10.1038/42679.

Nazaroff, W.W. (2016) ‘Teaching indoor environmental quality’, *Indoor Air*, 26(4), pp. 515–516. Available at: https://doi.org/10.1111/ina.12309.

Nevalainen, A., Täubel, M. and Hyvärinen, A. (2015) ‘Indoor fungi: companions and contaminants’, *Indoor Air*, 25(2), pp. 125–156. Available at: https://doi.org/10.1111/ina.12182.

Norris-Hill, J. (1997) 'The Influence of Ambient Temperature on the Abundance of Poaceae Pollen', *Aerobiologia (Bologna*, 13, pp. 91-97,. Available at: https://doi.org/10.1007/BF02694424.

O'Connor, D.J. *et al.* (2014) 'Using the WIBS-4 (Waveband Integrated Bioaerosol Sensor) Technique for the On-Line Detection of Pollen Grains', *Aerosol Science and Technology*, 48(4), pp. 341–349. Available at: https://doi.org/10.1080/02786826.2013.872768.

O'Connor, D.J., Daly, S.M. and Sodeau, J.R. (2015) 'On-line monitoring of airborne bioaerosols released from a composting/green waste site', *Waste Management*, 42, pp. 23–30. Available at: https://doi.org/10.1016/j.wasman.2015.04.015.

O'Gorman, C.M. and Fuller, H.T. (2008) 'Prevalence of culturable airborne spores of selected allergenic and pathogenic fungi in outdoor air', *Atmos. Environ*, 42, pp. 4355–4368. Available at: https://doi.org/10.1016/j.atmosenv.2008.01.009.

Pace, L. *et al.* (2019) 'Temporal variations in the diversity of airborne fungal spores in a Mediterranean high altitude site', *Atmospheric Environment*, 210, pp. 166–170. Available at: https://doi.org/10.1016/j.atmosenv.2019.04.059.

Pan, Y. Le *et al.* (2021) 'Atmospheric aging processes of bioaerosols under laboratory-controlled conditions: A review', *Journal of Aerosol Science*, 155(January), p. 105767. Available at: https://doi.org/10.1016/j.jaerosci.2021.105767.

Patel, T.Y. *et al.* (2018) 'Variation in airborne fungal spore concentrations among five monitoring locations in a desert urban environment', *Environmental Monitoring and Assessment*, 190(11), p. 634. Available at: https://doi.org/10.1007/s10661-018-7008-5.

Pearson, C. *et al.* (2015) 'Exposures and health outcomes in relation to bioaerosol emissions from composting facilities: a systematic review of occupational and community studies', *Journal of Toxicology and Environmental Health. Part B, Critical Reviews*, 18(1), pp. 43–69. Available at: https://doi.org/10.1080/10937404.2015.1009961.

Pérez-Badia, R. *et al.* (2013) 'Dynamics and Behaviour of Airborne Quercus Pollen in Central Iberian Peninsula', *Aerobiologia (Bologna*, 29, pp. 419-428,. Available at: https://doi.org/10.1007/s10453-013-9294-2.

Perring, A.E. *et al.* (2015) 'Airborne observations of regional variation in fluorescent aerosol across the United States', *Journal of Geophysical Research: Atmospheres*, 120(3), pp. 1153–1170. Available at: https://doi.org/10.1002/2014JD022495.

Pfaar, O. *et al.* (2017) 'Defining pollen exposure times for clinical trials of allergen immunotherapy for pollen-induced rhinoconjunctivitis - an EAACI position paper', *Allergy*, 72(5), pp. 713–722. Available at: https://doi.org/10.1111/all.13092.

Pöhlker, C., Huffman, J.A. and Pöschl, U. (2012) 'Autofluorescence of atmospheric bioaerosols – fluorescent biomolecules and potential interferences', *Atmospheric Measurement Techniques*, 5(1), pp. 37–71. Available at: https://doi.org/10.5194/amt-5-37-2012.

Post, W., Heederik, D. and Houba, R. (1998) 'Decline in lung function related to exposure and selection processes among workers in the grain processing and animal feed industry', *Occupational and Environmental Medicine*, 55(5), pp. 349–355. Available at: https://doi.org/10.1136/oem.55.5.349.

R Core Team (2017) 'R: A Language and Environment for Statistical Computing'. Foundation for Statistical Computing; Vienna, Austria, 2017.

Robinson, N.H. *et al.* (2013) 'Cluster analysis of WIBS single-particle bioaerosol data', *Atmos. Meas. Tech*, 6, pp. 337–347. Available at: https://doi.org/10.5194/amt-6-337-2013.

Rodríguez de la Cruz, D., Sánchez-Reyes, E. and Sánchez-Sánchez, J. (2015) 'A contribution to the knowledge of Cupressaceae airborne pollen in the middle west of Spain', *Aerobiologia*, 31(4), pp. 435–444. Available at: https://doi.org/10.1007/s10453-015-9376-4.

Ruiz-Gil, T. *et al.* (2020) 'Airborne bacterial communities of outdoor environments and their associated influencing factors', *Environment International*, 145, p. 106156. Available at: https://doi.org/10.1016/j.envint.2020.106156.

Ruske, S. *et al.* (2018) 'Machine learning for improved data analysis of biological aerosol using the WIBS', *Atmospheric Measurement Techniques*, 11(11), pp. 6203–6230. Available at: https://doi.org/10.5194/amt-11-6203-2018.

Sarda Estève, R. *et al.* (2018) 'Temporal Variability and Geographical Origins of Airborne Pollen Grains Concentrations from 2015 to 2018 at Saclay, France', *Remote Sensing*, 10(12), p. 1932. Available at: https://doi.org/10.3390/rs10121932.

Sarda-Estève, R. *et al.* (2018) 'Temporal Variability and Geographical Origins of Airborne Pollen Grains Concentrations from 2015 to 2018 at Saclay, France', *Remote Sensing*, 10. Available at: https://doi.org/10.3390/rs10121932.

Sarda-Estève, R. *et al.* (2019) 'Variability and Geographical Origin of Five Years Airborne Fungal Spore Concentrations'. Available at: https://doi.org/10.3390/rs11141671.

Sarda-Estève, Roland *et al.* (2019) 'Variability and Geographical Origin of Five Years Airborne Fungal Spore Concentrations Measured at Saclay, France from 2014 to 2018', *Remote Sensing*, 11(14), p. 1671. Available at: https://doi.org/10.3390/rs11141671.

Sarda-Estève, R. *et al.* (2020) 'Atmospheric Biodetection Part I: Study of Airborne Bacterial Concentrations from January 2018 to May 2020 at Saclay, France', *International Journal of Environmental Research and Public Health*, 17(17), p. E6292. Available at: https://doi.org/10.3390/ijerph17176292.

Sauvageat, E. *et al.* (2020) 'Real-time pollen monitoring using digital holography', *Atmospheric Measurement Techniques*, 13(3), pp. 1539–1550. Available at: https://doi.org/10.5194/amt-13-1539-2020.

Savage, N.J. *et al.* (2017) 'Systematic characterization and fluorescence threshold strategies for the wideband integrated bioaerosol sensor (WIBS) using size-resolved biological and interfering particles', *Atmos. Meas. Tech*, 10, pp. 4279–4302. Available at: https://doi.org/10.5194/amt-10-4279-2017.

Savage, Nicole J. *et al.* (2017) 'Systematic characterization and fluorescence threshold strategies for the wideband integrated bioaerosol sensor (WIBS) using size-resolved biological and interfering particles', *Atmospheric Measurement Techniques*, 10(11), pp. 4279–4302. Available at: https://doi.org/10.5194/amt-10-4279-2017.

Savage, N.J. and Huffman, J.A. (2018) 'Evaluation of a hierarchical agglomerative clustering method applied to WIBS laboratory data for improved discrimination of biological particles by comparing data preparation techniques', *Atmos. Meas. Tech*, 11, pp. 4929–4942. Available at: https://doi.org/10.5194/amt-11-4929-2018.

Sessa, R. *et al.* (2002) 'Microbiological indoor air quality in healthy buildings', *The New Microbiologica*, 25(1), pp. 51–56.

Shaffer, B.T. and Lighthart, B. (1997) 'Survey of Culturable Airborne Bacteria at Four Diverse Locations in Oregon: Urban, Rural, Forest, and Coastal', *Microbial Ecology*, 34(3), pp. 167–177. Available at: https://doi.org/10.1007/s002489900046.

Shoute, L.C.T. *et al.* (2018) 'Immuno-impedimetric Biosensor for Onsite Monitoring of Ascospores and Forecasting of Sclerotinia Stem Rot of Canola', *Scientific Reports*, 8(1), pp. 1–9. Available at: https://doi.org/10.1038/s41598-018-30167-5.

Siqueira, V.M. *et al.* (2011) 'Filamentous Fungi in Drinking Water, Particularly in Relation to Biofilm Formation', *International Journal of Environmental Research and Public Health*, 8(2), pp. 456–469. Available at: https://doi.org/10.3390/ijerph8020456.

Skjøth, C.A. *et al.* (2007) 'The long-range transport of birch (Betula) pollen from Poland and Germany causes significant pre-season concentrations in Denmark', *Clin. Exp. Allergy*, 37, pp. 1204–1212. Available at: https://doi.org/10.1111/j.1365-2222.2007.02771.x.

Skjøth, C.A. *et al.* (2021) 'Air Pollution Affecting Pollen Concentrations through Radiative Feedback in the Atmosphere', *Atmosphere*, 12(11), p. 1376. Available at: https://doi.org/10.3390/atmos12111376.

Spiers, A.G. (1985) 'Factors affecting basidiospore release by Chondrostereum purpureum in New Zealand', *European Journal of Forest Pathology*, 15(2), pp. 111–126. Available at: https://doi.org/10.1111/j.1439-0329.1985.tb00874.x.

Stanley, S., W.R.K.,. P, (2009) 'WIBS-4 Bioaerosol Sensor: User Manual'.

Swanson, B.E. and Huffman, J.A. (2018) 'Development and characterization of an inexpensive single-particle fluorescence spectrometer for bioaerosol monitoring', *Opt. Express*, 26, p. 3646. Available at: https://doi.org/10.1364/oe.26.003646.

Targonski, P.V., Persky, V.W. and Ramekrishnan, V. (1995) 'Effect of environmental molds on risk of death from asthma during the pollen season', *Journal of Allergy and Clinical Immunology*, 95(5), pp. 955–961. Available at: https://doi.org/10.1016/S0091-6749(95)70095-1.

Toprak, E. and Schnaiter, M. (2013) 'Fluorescent biological aerosol particles measured with the Waveband Integrated Bioaerosol Sensor WIBS-4: laboratory tests combined with a one year field study', *Atmospheric Chemistry and Physics*, 13(1), pp. 225–243. Available at: https://doi.org/10.5194/acp-13-225-2013.

Tournas, V.H. (2005) 'Spoilage of vegetable crops by bacteria and fungi and related health hazards', *Critical Reviews in Microbiology*, 31(1), pp. 33–44. Available at: https://doi.org/10.1080/10408410590886024.

Trapero-Casas, A., Navas-Cortés, J.A. and Jiménez-Díaz, R.M. (1996) 'Airborne ascospores of Didymella rabiei as a major primary inoculum for Ascochyta blight epidemics in chickpea crops in southern Spain', *European Journal of Plant Pathology*, 102(3), pp. 237–245. Available at: https://doi.org/10.1007/BF01877962.

Troutt, C. and Levetin, E. (2001) 'Correlation of spring spore concentrations and meteorological conditions in Tulsa, Oklahoma', *International Journal of Biometeorology*, 45(2), pp. 64–74. Available at: https://doi.org/10.1007/s004840100087.

Tummon, F., Adamov, S., *et al.* (2021) 'A first evaluation of multiple automatic pollen monitors run in parallel', *Aerobiologia* [Preprint]. Available at: https://doi.org/10.1007/s10453-021-09729-0.

Tummon, F., Arboledas, L.A., *et al.* (2021) 'The need for Pan-European automatic pollen and fungal spore monitoring: A stakeholder workshop position paper', *Clinical and Translational Allergy*, 11(3), p. e12015. Available at: https://doi.org/10.1002/clt2.12015.

Twohy, C.H. *et al.* (2016) 'Abundance of fluorescent biological aerosol particles at temperatures conducive to the formation of mixed-phase and cirrus clouds', *Atmos. Chem. Phys*, 16, pp. 8205–8225. Available at: https://doi.org/10.5194/acp-16-8205-2016.

Vélez-Pereira, A.M. *et al.* (2019) 'Logistic regression models for predicting daily airborne Alternaria and Cladosporium concentration levels in Catalonia (NE Spain', *Int. J. Biometeorol*, 63, pp. 1541–1553.

Vélez-Pereira, A.M. *et al.* (2021) 'Spatial distribution of fungi from the analysis of aerobiological data with a gamma function', *Aerobiologia*, 37(3), pp. 461–477. Available at: https://doi.org/10.1007/s10453-021-09696-6.

de Weger, L.A. *et al.* (2016) 'The long distance transport of airborne Ambrosia pollen to the UK and the Netherlands from Central and south Europe', *International Journal of Biometeorology*, 60(12), pp. 1829–1839. Available at: https://doi.org/10.1007/s00484-016-1170-7.

World Health Organization. Occupational and Environmental Health Team (2006) *WHO Air quality guidelines for particulate matter, ozone, nitrogen dioxide and sulfur dioxide : global update 2005 : summary of risk*

assessment. WHO/SDE/PHE/OEH/06.02. World Health Organization. Available at: https://apps.who.int/iris/handle/10665/69477 (Accessed: 29 September 2021).

Xie, W. *et al.* (2020) 'The source and transport of bioaerosols in the air: A review', *Frontiers of Environmental Science & Engineering*, 15(3), p. 44. Available at: https://doi.org/10.1007/s11783-020-1336-8.

Yue, S. *et al.* (2016) 'Springtime precipitation effects on the abundance of fluorescent biological aerosol particles and HULIS in Beijing', *Scientific Reports*, 6(June), pp. 1–10. Available at: https://doi.org/10.1038/srep29618.

Zang, L. *et al.* (2019) 'Roles of Relative Humidity in Aerosol Pollution Aggravation over Central China during Wintertime', *International Journal of Environmental Research and Public Health*, 16(22), p. 4422. Available at: https://doi.org/10.3390/ijerph16224422.

Zbîrcea, L.-E. *et al.* (2023) 'Relationship between IgE Levels Specific for Ragweed Pollen Extract, Amb a 1 and Cross-Reactive Allergen Molecules', *International Journal of Molecular Sciences*, 24(4), p. 4040. Available at: https://doi.org/10.3390/ijms24044040.

Zhang, M. *et al.* (2021) 'Sensitivities to biological aerosol particle properties and ageing processes: potential implications for aerosol–cloud interactions and optical properties', *Atmospheric Chemistry and Physics*, 21(5), pp. 3699–3724. Available at: https://doi.org/10.5194/acp-21-3699-2021.

Chapter 2 – Methodology

Pollen and fungal spore monitoring involves methods and techniques to track and analyse airborne PBAPs in the environment. This type of monitoring is essential for several reasons, including understanding PBAP seasonality, assessing allergenic risks, and studying the impact of climate change on pollen distribution.

Traditional monitoring is suitable for applications where real-time data is not critical, such as historical trend analysis, long-term research, and compliance monitoring.
Real-time monitoring using the WIBS provides data continuously, without significant delays between data generation and analysis. Data is collected using automated sensors and instruments, reducing the need for manual intervention, and improving data consistency. Real-time monitoring systems can provide highly accurate data due to constant monitoring and sensor calibration. Real-time data can be more precise and less prone to variations. The comparison between traditional and real-time monitoring will be explored in this chapter.

2.1 Sampling site

The sampling campaign was conducted at the CEA monitoring station situated in Saclay, France (48.7247°N, 2.1488°E), approximately 30 km from Paris in the French suburbs of the Île-de-France. The sampling site was surrounded by crops, forests, and small villages (Figure 2.1). Saclay's CEA hosted the Wideband Integrated Bioaerosol Sensor (WIBS) and a Hirst-Lanzoni bioaerosol impactor from 21st April to 15 June 2017. All sampling inlets were normalised and located 15 m above the ground. It should be noted that there was a five-day interruption in the operation of the WIBS instrument from 5th May to 10th May due to a power loss. The primary urban centre of Paris impacts the site, and as a result, the site has been characterised as semi-

urban, situated amid the surrounding countryside, and located south of the urban megacity of Paris.

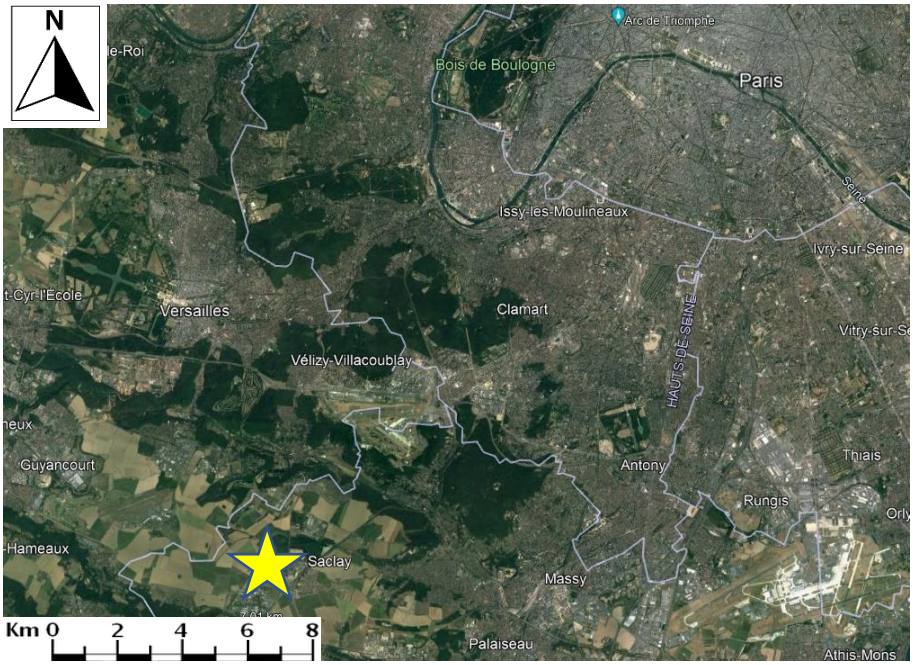

Figure 2.1. Site of sampling at CEA in Saclay (48.7247◦ N, 2.1488◦ E) (Source Google Earth).

2.2 Instrumentation

2.2.1 Hirst-type bioaerosol instrumentation

The Burkard Pollen and Fungal Spore Impaction Instrument, commonly known as the Burkard Sampler or Hirst-type sampler, is a widely used device in aerobiology for collecting and quantifying airborne pollen grains and fungal spores. It was developed in the 1950s and has since become a standard tool in pollen and spore monitoring studies. The instrument is designed to capture particles from the air onto adhesive-coated slides or tapes, allowing for subsequent analysis and identification. The Hirst spore trap consists of a rotating drum (as seen in Figure 2.2). The sampling head pictured is situated upon a swivel which ensures that the sampling is constantly facing the wind.

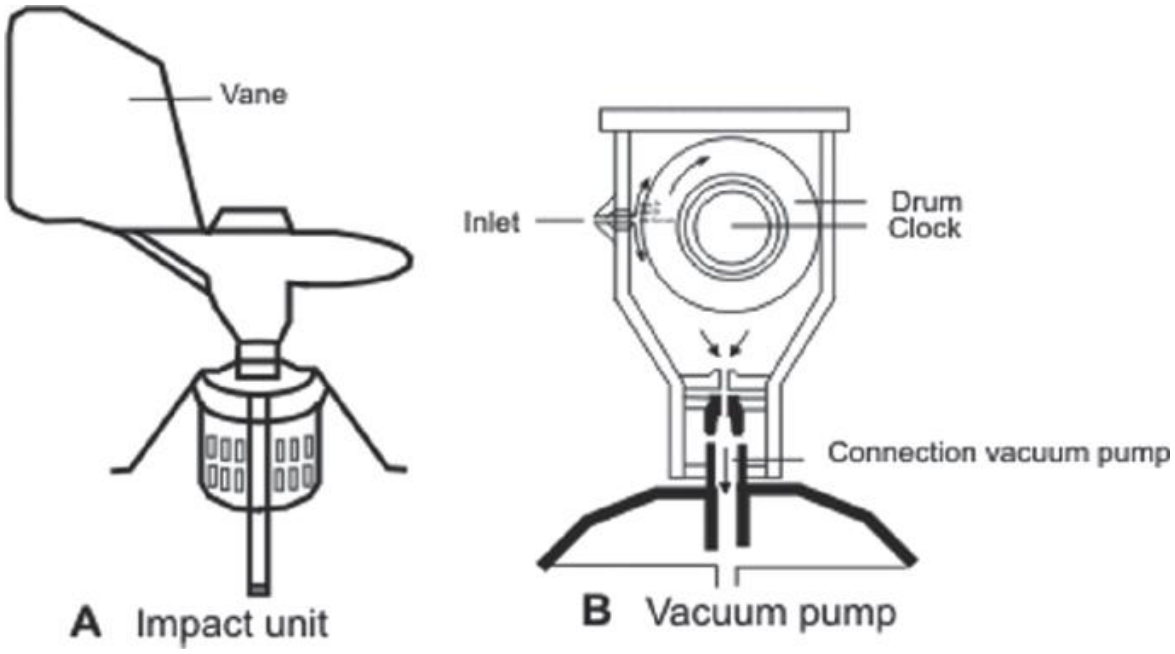

Figure 2.2. Hirst volumetric sampler and impact unit schematic diagram (Hirst, 1952; Galán, González, et al., 2007).

The Hirst sampler samples ambient air using a vacuum pump located in the heart of the sampling head. This pump sucks air through a 2mm by 14mm orifice at 10 litres per min. Like other impaction methods, this sample flow is impacted onto a suitable substrate which in the case of this work is a silicon tape. This substrate is attached to the circumference of the drum. In the figure below we can see a drum being prepared before being placed into the sampler head. A clockwork mechanism drives the drum at a rate of 2 mm per hour when the trap is set for a 7-day sampling period in a clockwise direction. Thus, every 2mm of the substrate will correspond to an hour of sampling and 48mm will be representative of a full day of data.

Figure 2.3. Image of a drum being prepared for placement within spore watch sampling head (Lacey and West, 2006).

It should be noted that the height at which the trap is positioned is critical. This determines the bioaerosol harvest. High elevation will yield a high proportion of tree pollen. When the trap is too close to the ground, bioaerosols from local sources predominate. The trapping surface must be correctly coated to ensure the adherence of pollen grains and fungal spores.

2.2.1.1 Preparation of the sampling drum

The double-sided sticky tape was cut into a 0.5 x 2.5cm piece and placed at the central mark B on the spore watch internal drum as seen in Figure 4. The trapping tape (silicon tape) was then secured to the circumference of the drum. This can be seen below in Figure 2.4.

The trapping substrate was cut square ensuring that the edge was straight and was then placed halfway across the double-sided tape and pressed to secure Figure 2.4 (C). The tape was wound tightly around the drum until the tape was adhered to the remaining exposed half of the sticky tape Figure 2.4 (D). The excess tape was then cut flush using a razor, making certain that there was no gap or overlap in the tape surrounding the drum Figure 2.4 (E and F).

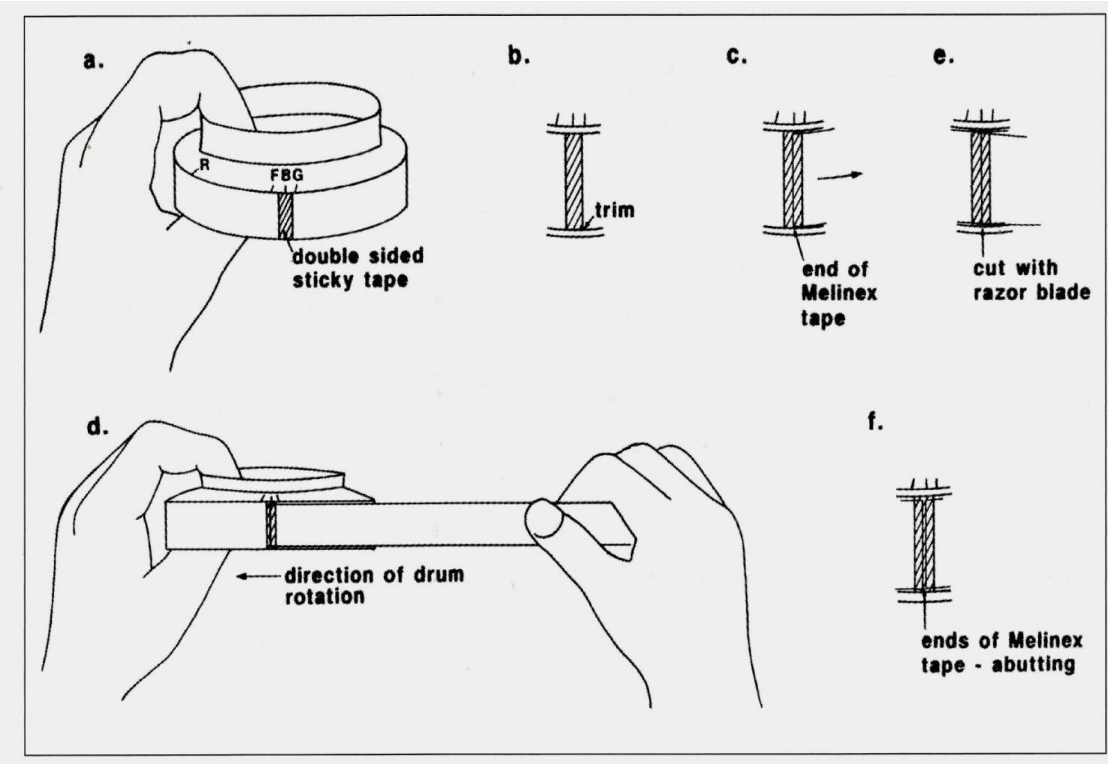

Figure 2.4. Images of the various stages of preparation of the spore watch drum for sampling (Lacey and West, 2006).

The drum was then placed inside the sampling head at the given sampling site and set for a seven-day sampling period. Upon completion of the sampling period the drum was removed and treated in the following manner.

- A razor was used to cut the double-sided sticky tape in half between the two ends of the silicon tape.

- The silicon tape and sticky tape were then lifted off the drum and transferred to a cutting block. The tape was placed from left to right on the cutting block. This was done ensuring that the end positioned on the left corresponded with the beginning of the sampling period.

- The sticky tape was pressed down on both ends securing the tape. The cutting template incorporated cutting groves every 48mm which indicates 24-hour periods of sampling on the tape. The silicon tape was cut into 48mm segments, each segment representing 24 hours of sampling. The silicon tape connected to the sticky tape was then removed.

- Self-adhesive 11 x 22mm labels were prepared with the date, time and campaign identification number for each of the segments prepared in the section above. These labels were adhered to a microscope slide.

- Each 24-hour silicon tape segment was transferred to its corresponding microscope slide. This was done by placing a thin 4cm long layer of distilled water upon the slide and cautiously lowering the corresponding 24-hour sampling segment onto it.

- Great care was taken to ensure that the silicon tape was placed left to right similar in fashion to the way that the segments had been positioned while they were being divided. This was done so that no errors in the time series could occur.

- Excess water was removed with tissue paper. Forceps were used to position the tape such

that the sides of the tape were parallel. This was done to remove an error that could occur while using the transverse counting method.

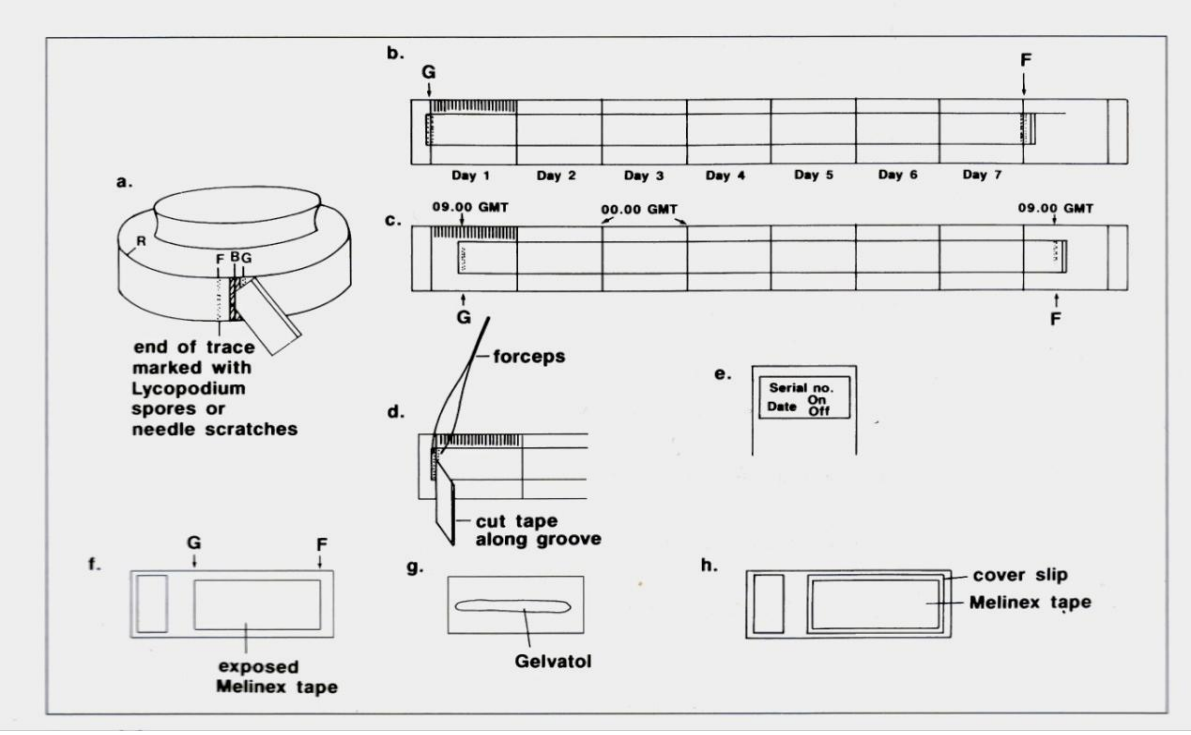

Figure 2.5. Images of the different stages in mounting the melinex tape (Lacey and West, 2006).

- The slide was then protected by placing a 50 x 22 mm coverslip upon it. This was done by preparing a permanent mountant to fix the coverslip to the slide.

- The mountant was made by placing 2g of phenol into 100 ml of distilled water. 35g of gelvatol was then added and the mixture was allowed to stand overnight. 50mls of glycerol was added and the mixture was then heated gradually whilst gently being stirred.

- A few crystals of basic fuchsin were added to the mountant to stain any pollen grains present and to allow for easier determination of fungal spores during optical analysis.

- The mountant was placed onto the coverslip and placed onto a slide. The slide was then

inverted, and gravity ensured the spread of the mountant (Figure G + H).

After a sample had been prepared, the slides were kept in a specifically designed slide box to guard against damage and loss. The slides were then analyzed optically using an optical microscope. Pollen and spore identification as well as the concentrations of pollens and spores were determined.

2.2.1.2 Bioaerosol counting procedure

The counting technique used by the European Aerobiology Network (EAN) (Galán *et al.*, 2007) involves four continuous horizontal sweeps across the entire slide utilizing a 400x magnification. This subsampling represents approximately 12-13% of the total surface, a percentage that can vary based on the size of the microscopic field at that magnification, which differs according to the microscope model.

Each identified pollen and fungal spore species was counted during these sweeps, which offers data regarding the pollen and fungal spore concentrations throughout the day. To understand the intra-diurnal variation, a use a custom-made ruler was used. This ruler was an acetate piece, cut to match the size of the daily-sample slide and transversely divided into twenty-four 2 mm intervals corresponding to the tape's hourly rotation. The divisions were marked in permanent blue ink with a super fine marker, as it provides the best light refraction. This ruler was carefully aligned over the slide, ensuring that the first blue line was flush with the beginning of the tape section to be analysed, and it was secured in place with adhesive tape.

The counts of pollen or spores for each hour were recorded following this workflow shown in Figure 2.6. The initial hour ranges from 12:00 p.m. to 1:00 p.m. on a specified day, and the final hour spans from 11:00 a.m. to 11:59 a.m. the next day. The quantity of pollen or fungal spore per

hour was documented in an Excel form, along with the date and location of sampling. The counted PBAPs are multiplied by a factor considering the volume of the sampled air and the size of the utilised microscope's field of vision.

Based on previous study findings, it was suggested that conducting fungal spore analysis on approximately 5% of the slide, which corresponds to two transects in this study, is sufficient (Galán *et al.,* 2021). This recommendation was based on the results obtained from this sample size which showed no significant differences compared to using five transects.

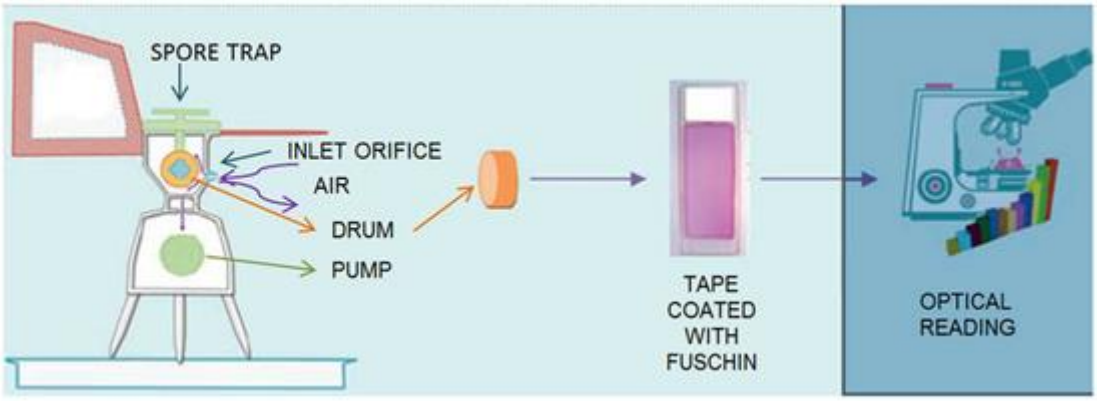

Figure 2.6. The analytical procedure of pollen grains collection and counting (Sarda Estève et al., 2018).

2.2.1.3 Calculating the correction factor

The diameter of the field of vision was determined to be 0.45 mm from the microscope field of vision. The air sampling rate equals 600 litres/hour, 14,400 litres/day, or 14.4 m^3/day. The area of one horizontal sweep was calculated as 48 mm x 0.45 mm, resulting in 21.6 mm^2. Consequently, the surface analysed in one horizontal sweep was 21.6 mm^2. Considering two sweeps, the total surface analysed amounted to 21.6 mm^2 x 2 which equals 43.2 mm^2. The overall surface sampled was calculated by multiplying the length of 48 mm by the width of 14 mm, resulting in 672 mm^2.

$$CF = (T_s/S_s)x(1/V_d)$$

Equation 2.1. Correction factor formula in which CF = correction factor applied to convert the counted particles into particles by (m^3), Ts = Total surface (mm^2), Ss = scanned surface (mm^2), Vd = volume daily (mm^3).

Thus, the particle content per cubic meter of air can be expressed as N x 0.54 from Equation 2.1

Figure 2.7. A one-day sample slide, including applying an identification label for optical counting and positioning the acetate ruler on top of the slide to obtain a daily sample (images taken by the author).

2.2.2 WIBS instrumentation

2.3.2.1 Background overview

WIBS is the most recent of several comparatively low-cost bioaerosol sensors developed by the University of Hertfordshire. Over the past decade in particular, many prototype online fluorescent bioaerosol detection instruments have been developed (Martinez-Bracero *et al.*, 2022) as the need to curtail the potentially harmful effect of deliberate exposure of bioaerosols to the public.

These newer instruments have attempted to use UV-excited intrinsic fluorescence of biological particles as a means of almost instantaneous discrimination within an ambient atmosphere. However, these instruments have tended towards the use of expensive solid-state lasers, which coupled with their need for excessive amounts of power make the use of these instruments in a continuous routine monitoring sense quite difficult. They also often do not incorporate an optimal excitation wavelength for key bio-fluorophores such as tryptophan (peak absorption at ~280nm).

The WIBS instruments have used a contrary method in the attempt to use intrinsic fluorescence of bio-particles through the usage of UV xenon sources rather than lasers. These miniature xenon flash tubes (refined versions of those used in disposable cameras), provide the UV flux necessary to excite intrinsic fluorescence from individual airborne particles detected by a low-power trigger laser beam. These xenon sources are not only far less expensive than UV lasers but also, since the xenon emission spectrum is continuous between ~200 and 900nm, allow the selection (by using optical band-pass filters) of precise UV excitation wavebands.

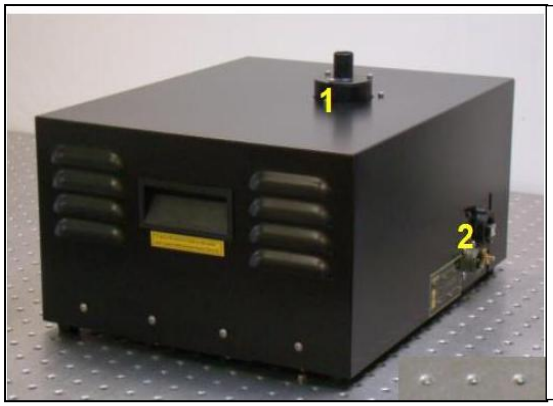

1. Aerosol inlet
2. USB and power connectors
3. Oversize particle trap
4. Pump
5. Main optical chamber
6. Xenon sources
7. Fluorescence detection channels
8. Quadrant PMT, particle 'shape' detector
9. Power distribution board
10. Analogue acquisition and digitization board.

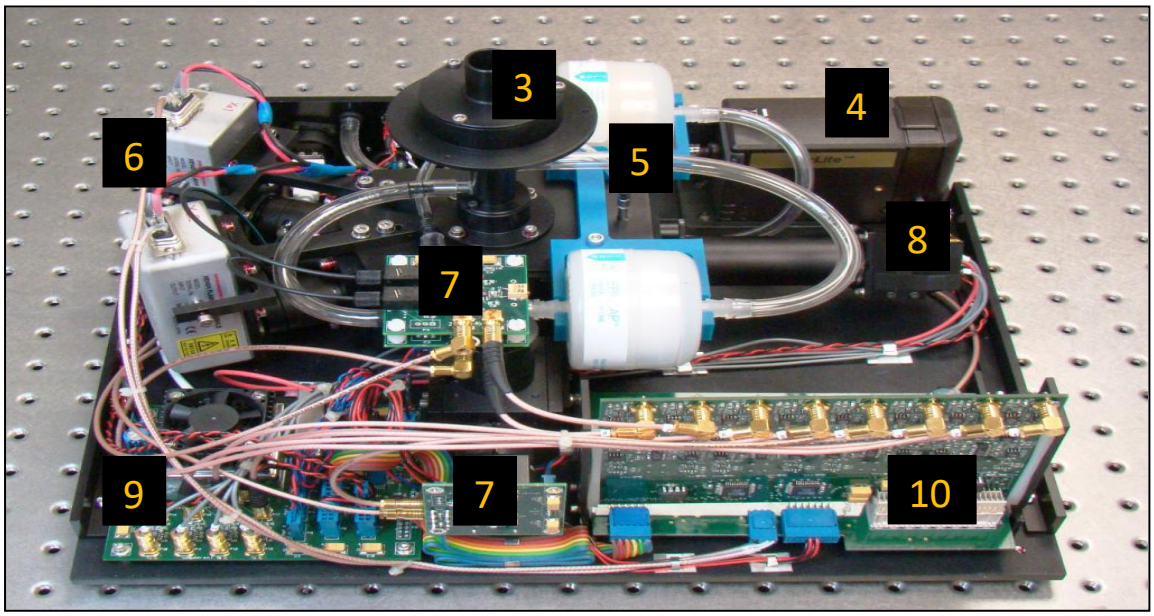

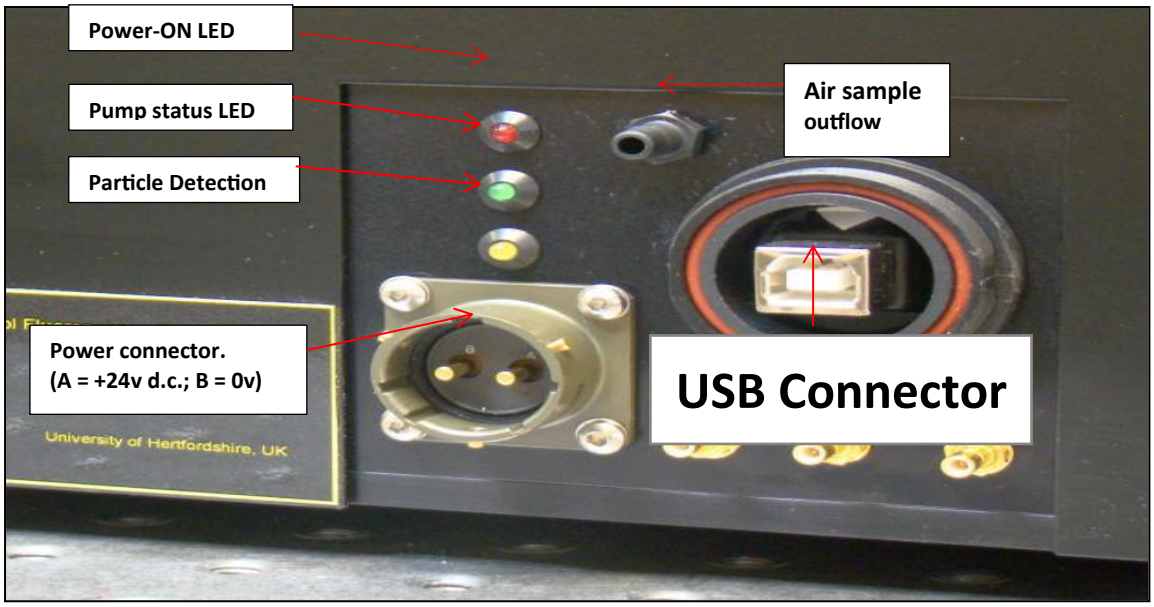

Figure 2.8. Internal and external parts of the WIBS instrument (Stanley, 2009).

2.3.2.2 Overview of WIBS4 principal components

The WIBS4 instrument is a single particle online fluorescence spectrometer which incorporates (1) continuous-wave diode lasers (635nm) used to size and characterize the shape of particles and (2) a pair of xenon flash used to evaluate the fluorescent properties of the particle under investigation. These components can be seen in the internal configurations' schematics and images of the WIBS internal configuration in both Figures 2.8 and 2.9.

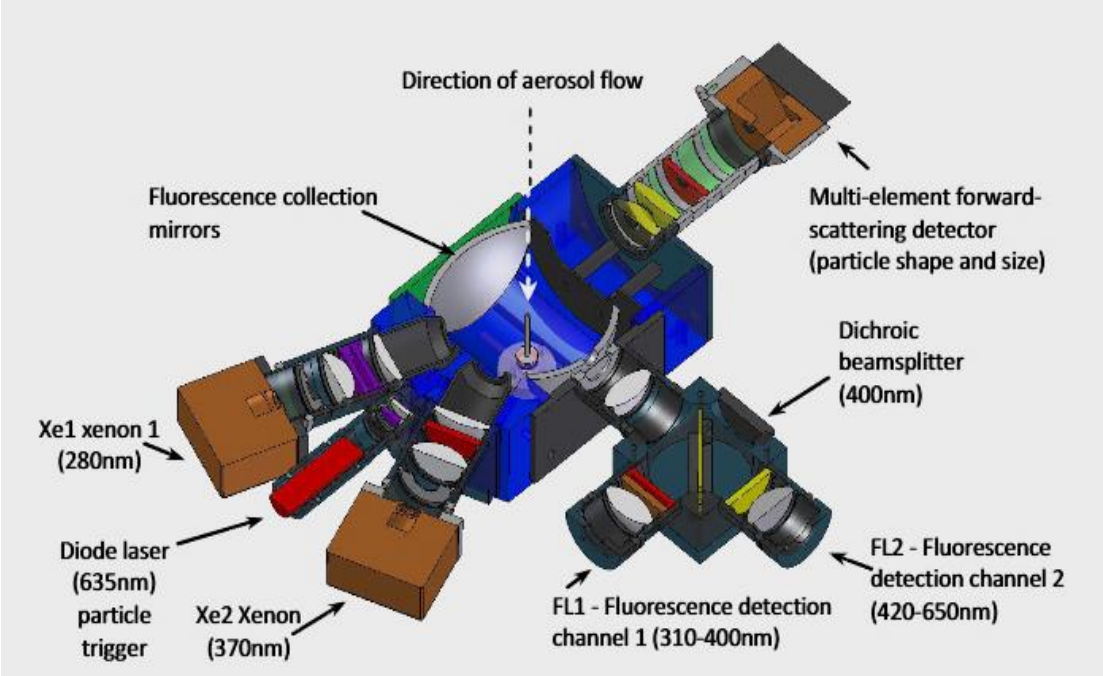

Figure 2.9. Schematic of the central optical chamber of the WIBS (Stanley, 2009).

Hence significant information on the size, shape and fluorescence of individual particles can be gleaned. The principle that underpins WIB4 is similar to that used with other fluorescent techniques. Intrinsic particle fluorescence is a well-known method to help discriminate biological particles from non-biological particles. When bioaerosols are excited by UV radiation tuned to the principal biological fluorophores contained within the organisms, the fluorescent light that they emit can be used to provide a differentiated signal from non-fluorescing particles or particles that emit at different spectral wavelengths of light.

In the WIBS4+ the UV radiation used to excite these bio-fluorophores is attained through the use of xenon flash lamps (see Figures 2.8 and 2.9 above). These Xenon lamps allow for the irradiation of up to 125 particles per second due to the need for the xenon lamps to recharge. The two xenon lamps are set to emit UV pulses at ~280 nm and ~370 nm, which are optimal for the excitation of the bio-fluorophores tryptophan and NADH (nicotinamide adenine dinucleotide) respectively (Dixon, Taniguchi and Lindsey, 2005; Horner, 2009, Pöhlker, Huffman and Pöschl, 2012).

Samples are introduced into the WIB4 using a pump that sucks ambient air in at ~2.4 l/min through an inlet tube. This Aerosol is drawn from the ambient atmosphere via a laminar-flow delivery system which renders suspended particles in essentially single file. The 635nm sizing laser and xenon lamps then evaluate the particle. The optical arrangement of the xenon flash lamps, and laser scatter detectors is such that they are all in the same plane, orthogonal to the sample flow. This enables the filtered light from the triggered xenon flash lamps to be tightly focused onto individual particles, increasing the fluorescence emitted per particle.

The xenon lamps emitting at 370nm and 280nm excite single particles, which may subsequently fluoresce. The 2D fluorescence is captured in one, none or multiple channels namely the FL1, FL2, and FL3, where photomultiplier tubes are used to capture the emission signatures. Traditionally the fluorescence detection channels were named FL1, FL2, and FL3 as outlined above however in more recent times the channels have utilized a naming convention adopted by (Perring *et al.*, 2015). Where the channels were renamed A, B and C. This allowed particles that exhibited fluoresce in multiple channels to be denoted with a label indicating such emission profiles. For instance, a particle with fluoresce from both the FL1 and FL2 channels would be labelled AB (Figure 2.10). If a particle exhibited fluoresce in all three channels it would be designated ABC. Thus, using this naming convention 7 fluorescent categories were formed. Older work in the area is only utilised.

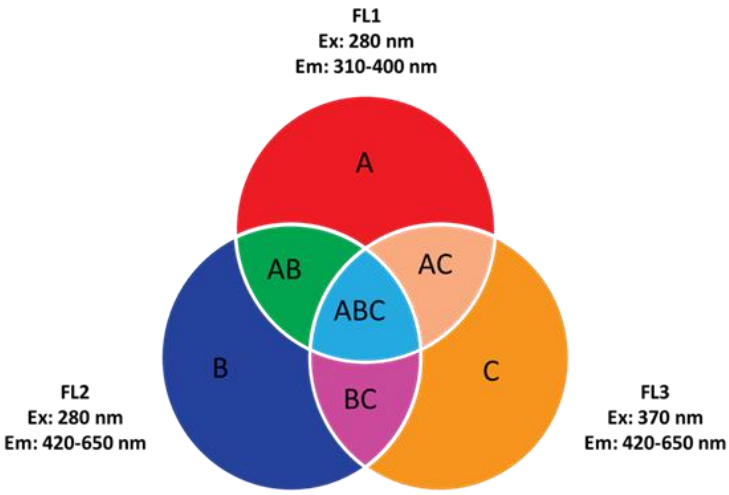

Figure 2.10. Particle type classification, as initially presented by Perring et al. (2015).

In this visual. representation, sizable circles correspond to individual fluorescence channels, denoted as FL1, FL2, and FL3. The coloured regions within these circles signify distinct particle categories, each of which displays fluorescence in either one, two, or all three of the channels.

Table 2.1. The WIBS channel annotation matrix associated channels with their respective excitation wavelengths and emission wavebands.

Channel	**Excitation (nm)**	**Emission (nm)**
FL1 or A	280	310-400
FL2 or B	280	420-650
FL3 or C	370	420-650
AB	280	310-400
		420-650
AC	280	310-400
	370	420-650
BC	280	420-650
	370	
ABC	280	310-400
		420-650
	370	420-650

Generally, fluorescence signatures correspond to bio-fluorophores which are significant components of biological entities such as pollen, fungal spores, bacteria, and viruses and hence can be used to estimate their concentration in the ambient environment. Complimentary to the WIBS4 ability to evaluate these biological fluorophores it also incorporates a continuous-wave diode laser. Particles are detected and sized by measurement of light scattered from the continuous-wave diode laser (635nm). The continuous-wave diode laser offers the potential to discriminate individual airborne particles by size, down to ~0.5μm in diameter (Stanley, 2009).

2.3.2.3 Aerosol Sampling System: Airflow

As stated above the WIBS instrument operates by drawing 2.4L/min of air through the system. The air flow entering the WIBS4 instrument however must first pass through an Oversize Particle Trap (OPT). The OPT is to ensure that very large particles do not block the delivery nozzle (which has a 1.2mm exit diameter), as this could prevent the sampling of aerosol and also place a strain on the pump by causing a pressure build-up (Stanley, 2009).

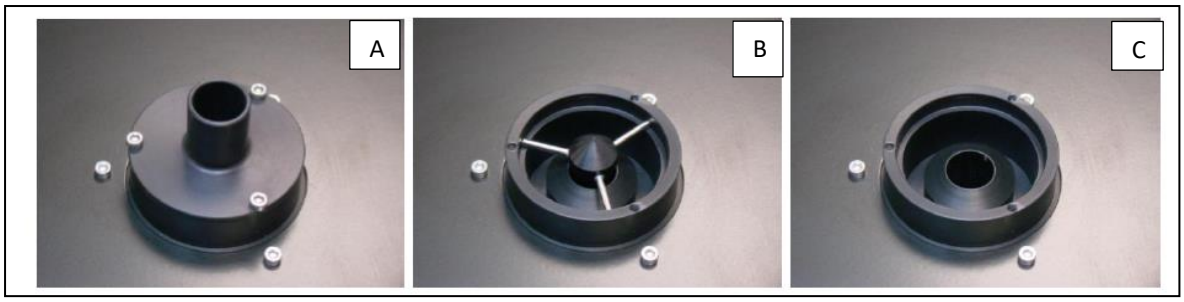

Figure 2.11. (A) The inlet of the WIBS4. (B) Oversize Particle Trap (OPT) within the inlet. (C) Inlet with OPT removed (Stanley, 2009).

The OPT incorporates a simple airflow deflector around which the airflow is forced. Silicone tubing is used to hold the OPT attachment to the WIBS inlet assembly (see Figure 2.12). This feature was incorporated to prevent any damage that could occur to the WIBS assembly and internal chamber by accidental striking of the OPT attachment.

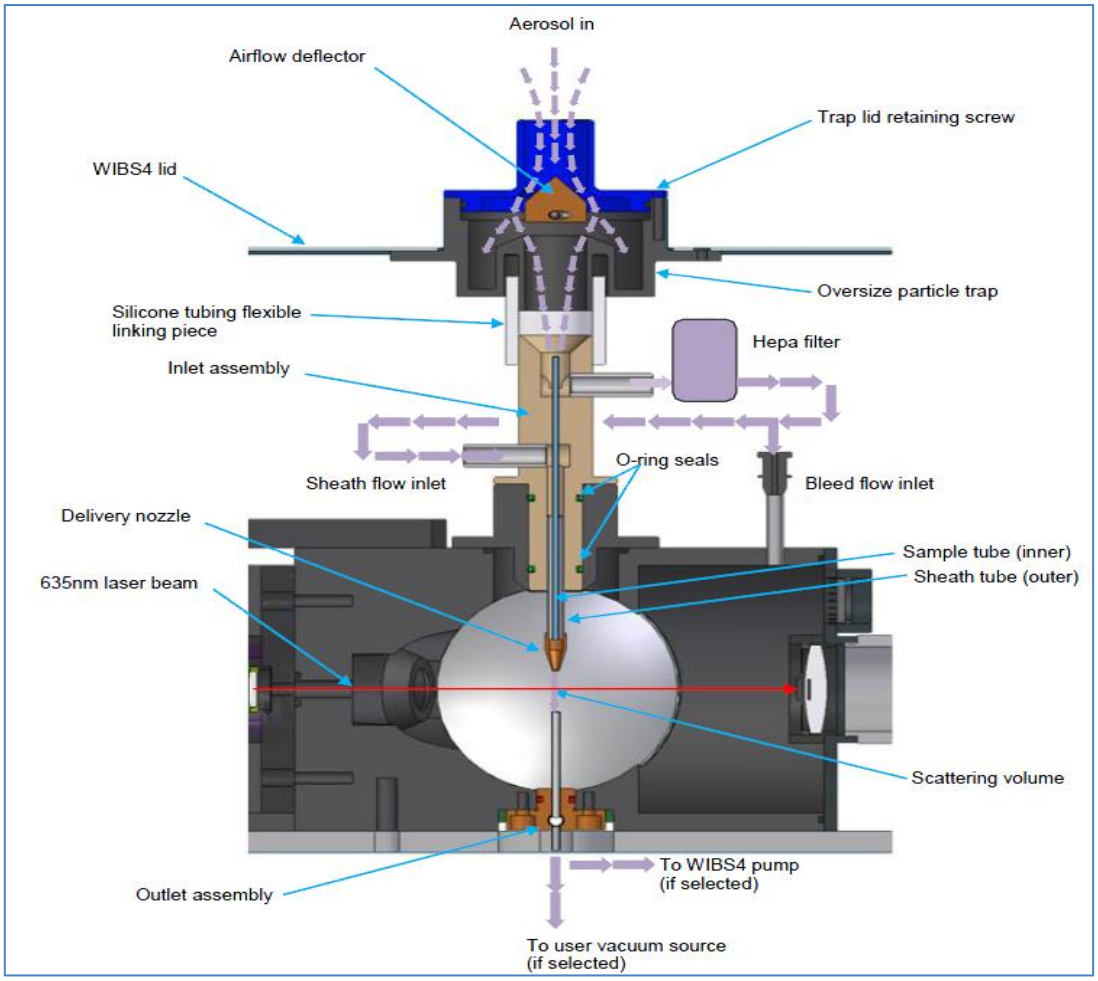

Figure 2.12. Sectional view of WIBS4 chamber showing aerosol flow (Stanley, 2009)

While 2.4L/min of aerosol is directly inhaled by the instrument, approximately 90% of the flow is focused through a HEPA filter before being returned to surround the remaining sample flow (0.23L/min) with a sheath of clean air and provide the low 'bleed flow' of clean air into the chamber. The sheath flow has the effect of constraining the sample flow as the two flows pass through the tapered delivery nozzle, as illustrated in Figure 2.13 below.

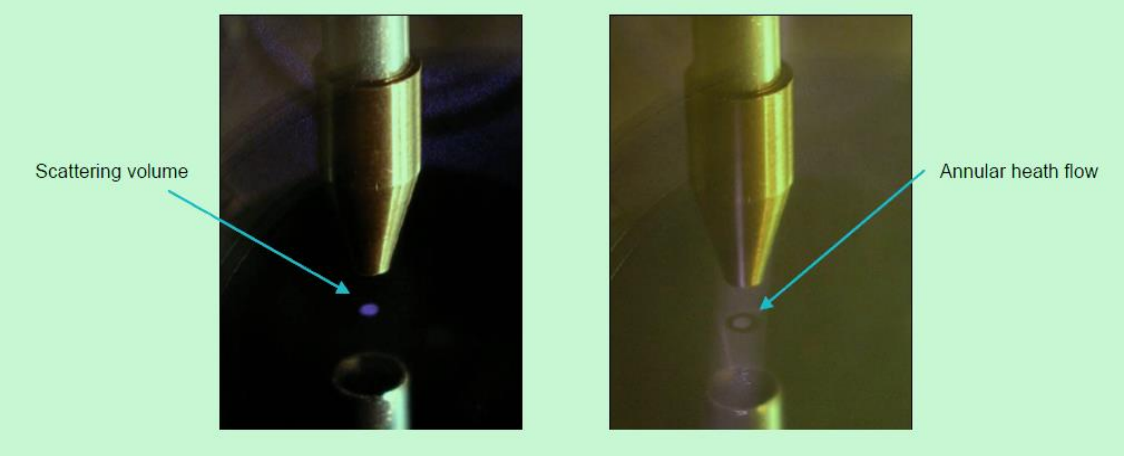

Figure 2.13. Smoke visualisation of scattering volume and its surrounding clean sheath flow (Stanley, 2009).

The scattering volume, defined by the intersection between the laser beam and the sample airflow column, is approximately 0.7mm in diameter and 130µm deep. The flow velocity at this point is typically ~18 m/s. The full aerosol flow (sample + sheath + bleed) is drawn out of the chamber by the WIBS4 sampling pump (Airlite 3 lpm diaphragm pump, SKC Inc., PA 15330 USA) via a HEPA filter (Stanley, 2009).

2.3.2.4 Data capture and timings

The figure below the alignment of each component of the optical chamber of the WIBS as a particle passes through the scattering volume.

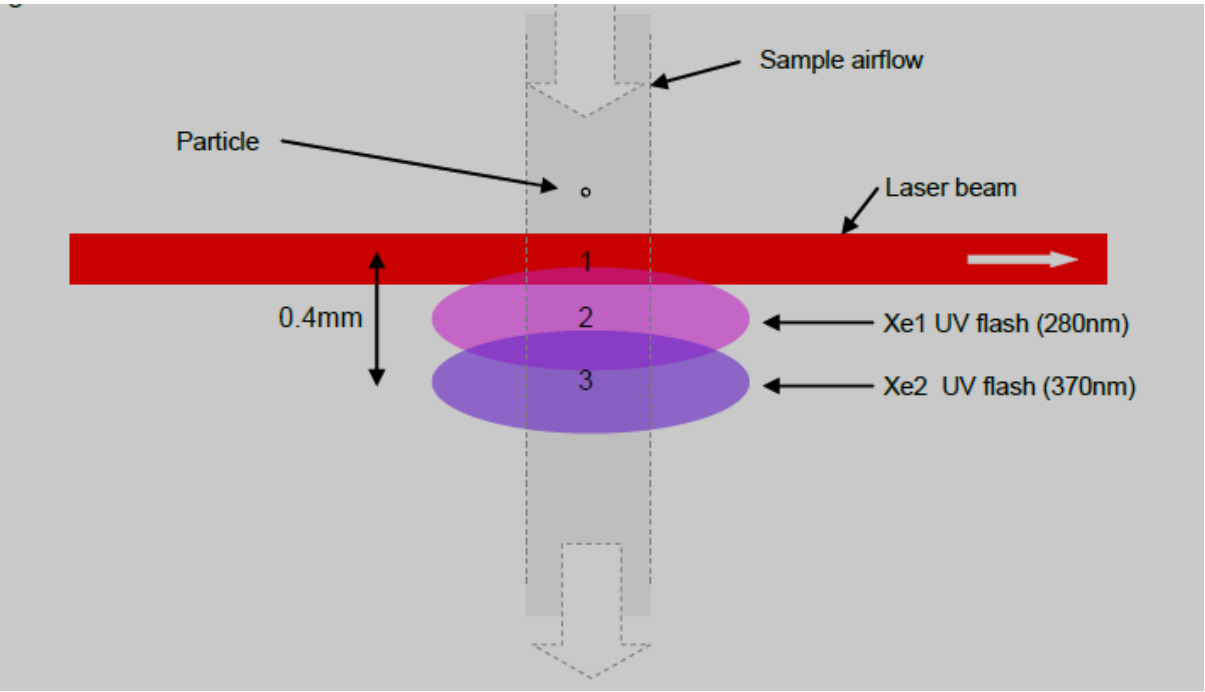

Figure 2.14. illustrates the spatial geometry of the laser and xenon UV pulses as the particle passes through the scattering volume. (Stanley, 2009).

As we can see the overall length of the scattering volume is 0.4mm. When the particle enters the laser beam indicated by the red colour and the number one in the figure above it scatters light forwards to the Quad-PMT detector and sideways to the FL2 detector. This scattering in turn gives rise to signal lines as shown in the oscilloscope trace (figure position 1). The particle continues in the air flow through the optical chamber until at position 2 it is illuminated by the 280nm xenon UV flash lamp 1 (Xe1). The resulting fluorescence gives rise to signals in the FL1 and FL2 detection channels as shown again in the oscilloscope trace (Figure 2.14). The particle then moves on to position 3, where it is irradiated by the 370nm xenon UV flash lamp 2 (Xe2). Again, the resulting fluorescence gives rise to pulses on the FL1 and FL2 channels once more shown in Figure 2.15 (Stanley, 2009).

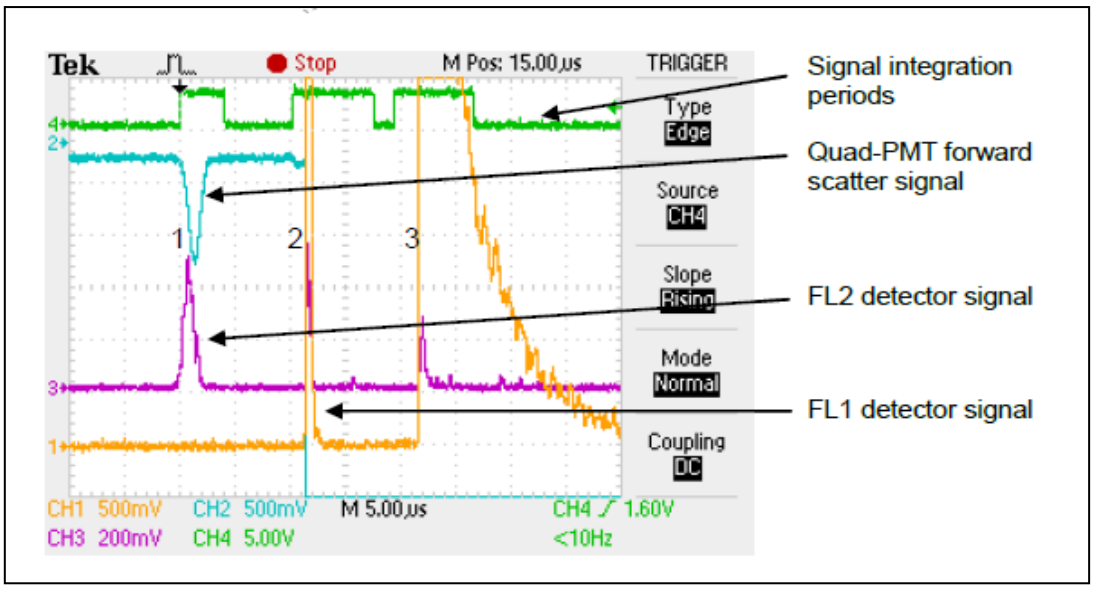

Figure 2.15. Schematic diagram showing the passage of a particle through the laser beam and then into the space below the laser beam where it is illuminated sequentially by the two xenon UV flashes. The accompanying oscilloscope plot shows the analogue signals resulting from this particle transit (Stanley, 2009).

However, it should be noted that the values from the FL1 detector upon excitation by the 370nm xenon UV flash lamp 2 (Xe2) are not valid as the detection range lies within the excitation wavelength. This is illustrated in the figure of the oscilloscope of the fluorescence from a particle passing through the WIBS instrument. The FL1 detection signal is saturated due to the firing of the Xe2 lamp.

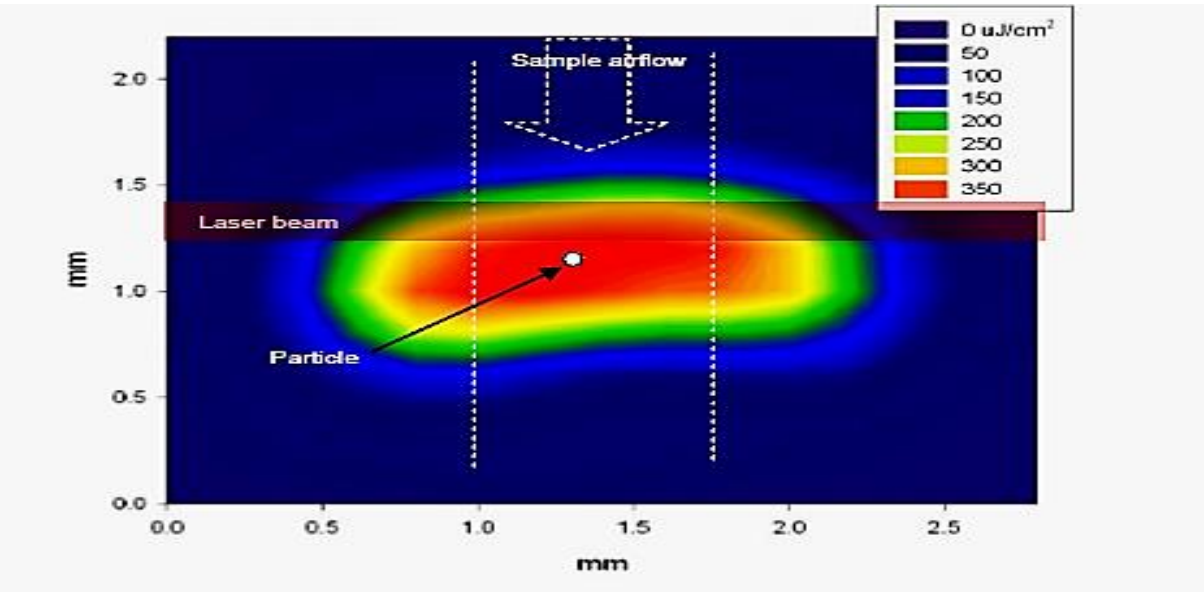

Figure 2.16. Energy density profile of typical xenon UV flash. Dotted lines indicate the relative position of the sample airflow column (Kaye et al., 2005)

Figure 2.16 above shows the standard energy density of each UV flash. This is important because the particle under investigation could be anywhere within the cross-section. Thus, a uniform UV flux across the scattering volume ensures little variation in the excitation of the particles of interest. Typically, a particle should be irradiated by a UV fluence of ~300μJ/cm^2 no matter its position in the cross-section.

2.3.2.5 Particle Size Determination

Particle size determination in the WIBS instrument is based on the forward and side scattering of light for a given particle. In theoretical terms, the WIBS uses Mie theory to determine the size of particles. Mie theory does this by using a particle size calibration based on a theoretical curve that assumes the particles are spherical and of a known refractive index. In the case of the WIBS, the known refractive index is that of the polystyrene latex spheres (PSL) which have a refractive index of 1.58.

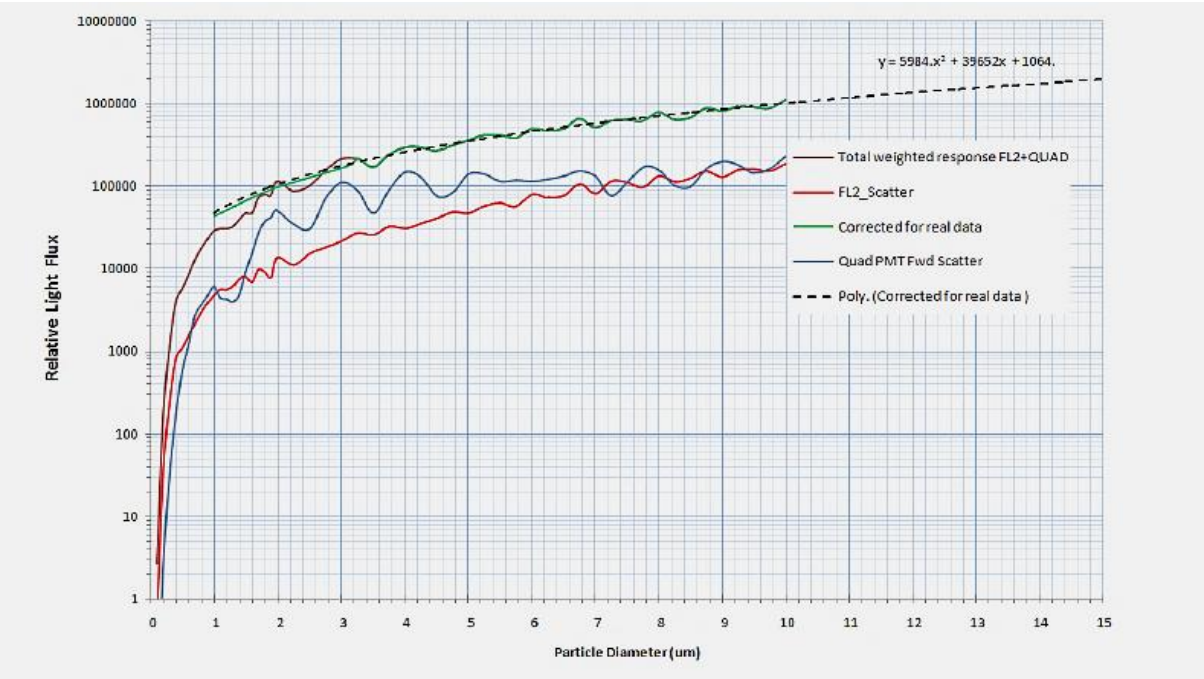

Figure 2.17. Graph showing calibration curve (dashed line) used in WIBS4 for particle size estimation (Stanley, 2009).

While both the forward and side scatter of a particle are evaluated in the WIBS, a weighted combination of the two is used in the overall determination of particle size. As can be seen from Figure 17 forward scattered light from a particle to the Quadrant PMT detector is more intense than the side scatter to the FL2 detector. Thus, forward scatter provides a more reliable signal for particle detection, especially those in smaller size ranges. However, one unfortunate aspect of the forward scatter is that it suffers from marked Mie oscillations in the response curve, visible in Figure 2.15. This in turn adds uncertainties in the size response as scatter values could represent many differing sizes. Thus, the side-scatter signals are used in conjunction with the forward scatter to estimate particle size (see dashed line in Figure 2.15), normalised to real data recorded from polystyrene latex (PSL) particles of accurately known sizes to overcome this uncertainty.

2.3.2.6 Particle Shape Estimation

Evaluation of the shape of a particle is yet another exciting ability incorporated into the WIBS instrument. Using the forward scattered light of a particle in a similar approach to that used in the sizing of particles, the forward PMT is used to evaluate the particle scattering asymmetry.

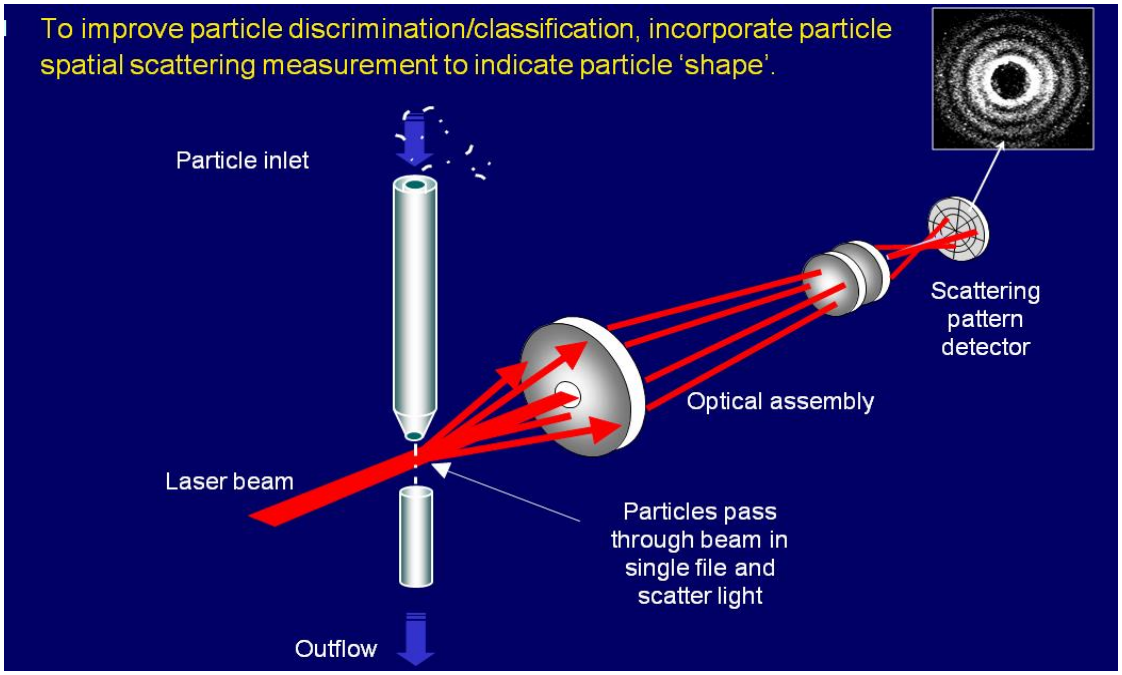

Figure 2.18. Example of the formation of a scattering pattern used to determine particle shape (Stanley, 2009).

A schematic of how the WIBS instrument evaluates a particle and a scattering pattern of water particles is shown in Figure 2.18. The sheath flow in the WIBS pushes the particle into the path of the sizing laser; the forward scattering is then focused upon a scatter pattern detector. This in turn forms a scatter image for individual particles. As seen in Figure 2.19 below there is a large variance in the sort of scattering patterns produced by several different types of particles. These images however are captured by ICCD camera and would take far too long to be produced in a real-time monitoring environment.

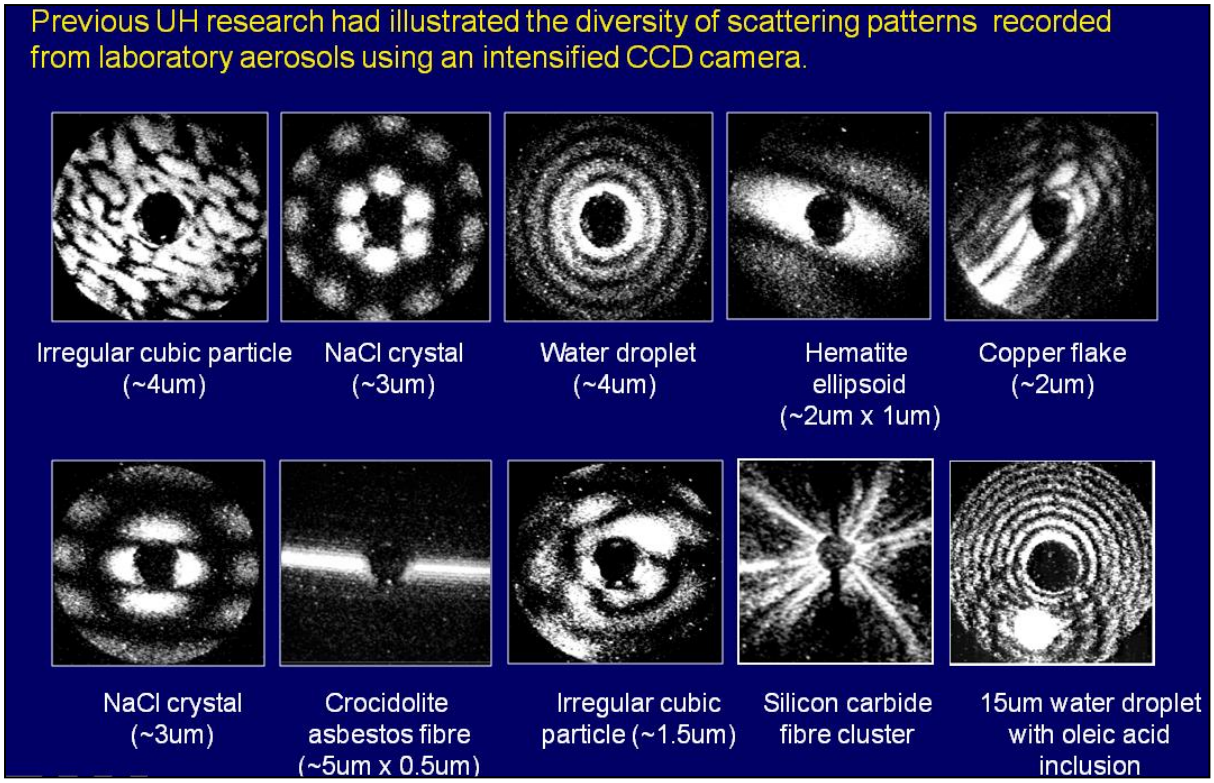

Figure 2.19. Variety of different particles and sizes and their light-scattering patterns (Stanley, 2009).

This is achieved by splitting up the forward PMT into a four-quadrant detector. This detector in turn evaluates the scattered light in each quadrant and equates this to a numerical value. Equation. 2.2 then combines these values to ascertain the shape of a particle known as the "Asymmetry Factor", or more concisely AF.

$$AF = \frac{k(\sum_{i=1}^{n}((\bar{E} - Ei)^2)^{1/2}}{\bar{E}}$$

Equation 2.2. Description of Asymmetry Factor calculation (Gabey *et al.*, 2010).

In the above equation, k is an instrument-defined constant, $\bar{E}$ is the mean intensity measured over the entire PMT and E_i is the intensity measured by the *i*th quadrant. Theatrically spherical particles such as water droplets should distribute equal light intensities of light in all four sections of the PMT. Thus, a low AF value should be seen. Increasing AF values indicate increasing irregular shapes with higher AF values seen for rod-like particles.

2.3 Data analysis

2.3.1 Geographical Origin Data

Regarding the geographical origins of airborne pollen and fungal spores, a source receptor approach was adopted using the ZeFir-v3.7 package (Petit *et al.,* 2017). This approach employed a two-dimensional non-parametric wind regression (NWR) variant, developed by Henry et al. (2009), which pairs wind speed and direction with ambient concentrations.

$$\mathbf{E}(\theta|\upsilon) = \frac{\sum_{i=1}^{N} \mathbf{K_1}\left(\frac{\theta - \mathbf{W_1}}{\sigma}\right) \cdot \mathbf{K_2}\left(\frac{\upsilon - \mathbf{T_1}}{\mathbf{h}}\right) \cdot \mathbf{C_i}}{\sum_{i=1}^{N} \mathbf{K_1}\left(\frac{\theta - \mathbf{W_1}}{\sigma}\right) \cdot \mathbf{K_2}\left(\frac{\upsilon - \mathbf{T_1}}{\mathbf{h}}\right)}$$

Equation 2.3. Description of the NWR calculation (Sarda Estève *et al.*, 2018). The formula above provides the method for computing NWR where E represents the projected concentration given a specific wind direction, denoted as θ, and speed, denoted as υ. Wi, Yi, and Ci are the wind direction, wind speed, and concentration data gathered at time ti, respectively. K_1 and K_2 serve as two Kernel functions, while σ and h are the parameters controlling the smoothness of these functions.

The formula shown in Equation 2.3 performs a weighted mean of the concentration, where the weights are established through the Kernel functions, and the σ and h parameters define their width. In the traditional application of NWR, the values of σ and h are kept constant, as depicted in the dataset's daily temporal resolution, rendering the NWR method ill-suited for this study given the atmospheric variability. It is presumed that the wind data associated with concentrations

are statistically representative, but the daily averages of wind direction and speed may not fully capture the range of wind conditions that could occur within a single day.

Consequently, if wind conditions fluctuate over time, reducing the corresponding concentration weight is appropriate to account for atmospheric stability more accurately. For this reason, a variant of NWR, known as the Sustained Wind Incidence Method (SWIM), developed in a previous study was used (Rodríguez *et al.*, 2015). While the core principle remains intact, an additional scalar weight is applied to concentrations, which is influenced primarily by the standard deviation of the wind direction.

$$S_i = \frac{C_i \cdot T_i}{\max(C_i \cdot T_i)} \cdot \frac{\bar{\delta}}{\delta_i}$$

Equation 2.4. Description of SWIM calculation (Sarda Estève *et al.*, 2018).

In Equation 2.4, δ denotes the standard deviation of the wind direction. This approach effectively reduces the weight of daily concentration values corresponding to high atmospheric variability within the same day.

Co-located measurements were used for the analysis with the SWIM-2 method, which employs constant smoothing parameters and a weighing scalar dependent on wind fluxes and wind direction standard deviation, utilised for local-scale wind analysis. The method was applied to highlight the localisation around Saclay and determine spatial domains by assessing their frequency of occurrence in eight directional and four wind speed bins. The methodology has been used in previous long-term monitoring studies from Saclay to determine the geographical origins of pollen, fungal spores, and bacteria (Sarda Estève *et al.*, 2018).

2.3.2 Meteorological Data

At the sampling site, meteorological and pollution data were collected. The meteorological parameters available for analysis included temperature (Temp) measured in degrees Celsius, precipitation (Rain) measured in millimetres, pressure (Pres) measured in hectopascals (hPa), relative humidity (RH) measured as a percentage, wind speed (Wind_s) measured in meters per second (m/s), and wind direction (Wind_d) measured in degrees.

The normal distribution of the data collected from the WIBS, Hirst, and meteorological/pollution measurements was assessed using the Shapiro-Wilk test. The test results indicated that most daily data did not follow a normal distribution. A Spearman correlation test was chosen to calculate the degree and correlation between selected variables. This test used the nortest and corrplot packages within the R statistical software (R Core Team, 2017).

2.3.3 Clustering analysis procedure

The K-means clustering analysis was conducted in RStudio, with raw data values scaled before the analysis. The excitation/emission wavelength criteria for these classifications can be found in Table 1.1.

The FL1, FL2, FL3 (A, B, C) intensity, size, and asymmetry factor were used in the K-means algorithm to distinguish between various PBAP fractions. The ideal number of clusters was ascertained by computing the Calinski-Harabasz index through the fpc package (Hennig, 2020) within R.

Cluster analysis, such as those conducted by (Crawford *et al.*, 2015) and (Ruske *et al.*, 2018), has demonstrated the ability to distinguish between FAPs beyond simple particle classification and filtering. K-means clustering was utilised to uncover more pragmatic approaches to identifying

bioaerosol fractions from the WIBS data. Although hierarchical clustering and gradient boosting have outperformed K-means in previous studies, they require advanced computational resources and lengthy processing times due to the high-resolution datasets produced by the WIBS (Robinson *et al.*, 2013; Crawford *et al.*, 2015; Savage and Huffman, 2018). In contrast, K-means clustering requires less processing power and time, making it a desirable alternative for the real-time deployment of the WIBS. Previous studies have overlooked the use of K-means clustering for WIBS data analysis owing to its ability to generate groups of similar sizes. However, recent research has demonstrated its potential in distinguishing between several pollen taxa using data from another fluorescence-based bioaerosol sensor (Swanson and Huffman, 2018, Robinson *et al.*, 2013).

References

Adams, R.I. *et al.* (2016) 'Ten questions concerning the microbiomes of buildings', *Building and Environment*, 109, pp. 224–234. Available at: https://doi.org/10.1016/j.buildenv.2016.09.001.

Aerosol Technology: Properties, Behavior, and Measurement of Airborne Particles, 2nd Edition | Wiley (no date) *Wiley.com*. Available at: https://www.wiley.com/en-ie/Aerosol+Technology%3A+Properties%2C+Behavior%2C+and+Measurement+of+Airborne+Particles%2C+2nd+Edition-p-9781118591970 (Accessed: 7 July 2023).

Alzate, F. *et al.* (2015) 'Atmospheric pollen and spore content in the urban area of the city of Medellin, Colombia', *Hoehnea*, 42, pp. 09–19. Available at: https://doi.org/10.1590/2236-8906-52/2013.

de Ana, S.G. *et al.* (2006) 'Seasonal distribution of Alternaria, Aspergillus, Cladosporium and Penicillium species isolated in homes of fungal allergic patients', *Journal of Investigational Allergology & Clinical Immunology*, 16(6), pp. 357–363.

Andersen, A.A. (1958) 'NEW SAMPLER FOR THE COLLECTION, SIZING, AND ENUMERATION OF VIABLE AIRBORNE PARTICLES, 12', *Journal of Bacteriology*, 76(5), pp. 471–484.

Bauer, H. *et al.* (2002) 'The contribution of bacteria and fungal spores to the organic carbon content of cloud water, precipitation and aerosols', *Atmos. Res*, 64, pp. 109–119. Available at: https://doi.org/10.1016/S0169-8095(02)00084-4.

Beck, J.M., Young, V.B. and Huffnagle, G.B. (2012) 'The microbiome of the lung', *Translational Research: The Journal of Laboratory and Clinical Medicine*, 160(4), pp. 258–266. Available at: https://doi.org/10.1016/j.trsl.2012.02.005.

Belizario, J.A., Lopes, L.G. and Pires, R.H. (2021) 'Fungi in the indoor air of critical hospital areas: a review', *Aerobiologia*, 37(3), pp. 379–394. Available at: https://doi.org/10.1007/s10453-021-09706-7.

Brock, C.A. *et al.* (2021) 'Ambient aerosol properties in the remote atmosphere from global-scale in situ measurements', *Atmospheric Chemistry and Physics*, 21(19), pp. 15023–15063. Available at: https://doi.org/10.5194/acp-21-15023-2021.

Burrows, S.M. *et al.* (2009) 'Bacteria in the global atmosphere – Part 2: Modeling of emissions and transport between different ecosystems', *Atmospheric Chemistry and Physics*, 9(23), pp. 9281–9297. Available at: https://doi.org/10.5194/acp-9-9281-2009.

Cascade Impactor - an overview | ScienceDirect Topics (no date). Available at: https://www.sciencedirect.com/topics/chemistry/cascade-impactor (Accessed: 28 June 2023).

Cheek, E. *et al.* (2021) 'Portable air purification: Review of impacts on indoor air quality and health', *Science of The Total Environment*, 766, p. 142585. Available at: https://doi.org/10.1016/j.scitotenv.2020.142585.

Chen, Q. and Hildemann, L.M. (2009) 'The effects of human activities on exposure to particulate matter and bioaerosols in residential homes', *Environmental Science & Technology*, 43(13), pp. 4641–4646. Available at: https://doi.org/10.1021/es802296j.

Cho, E.-M. *et al.* (2019) 'Distribution and Influencing Factors of Airborne Bacteria in Public Facilities Used by Pollution-Sensitive Population: A Meta-Analysis', *International Journal of Environmental Research and Public Health*, 16(9), p. 1483. Available at: https://doi.org/10.3390/ijerph16091483.

Crawford, I. *et al.* (2015) 'Evaluation of hierarchical agglomerative cluster analysis methods for discrimination of primary biological aerosol', *Atmos. Meas. Tech*, 8, pp. 4979–4991. Available at: https://doi.org/10.5194/amt-8-4979-2015.

D'Amato, G. (2000) 'Urban air pollution and plant-derived respiratory allergy', *Clinical and Experimental Allergy*, 30(5), pp. 628–636.

D'Amato, G. *et al.* (2007) 'Allergenic pollen and pollen allergy in Europe', *Allergy*, 62(9), pp. 976–990. Available at: https://doi.org/10.1111/j.1398-9995.2007.01393.x.

Després, VivianeR. *et al.* (2012) 'Primary biological aerosol particles in the atmosphere: a review', *Tellus Series B Chemical and Physical Meteorology B*, 64, p. 15598. Available at: https://doi.org/10.3402/tellusb.v64i0.15598.

Dixon, J.M., Taniguchi, M. and Lindsey, J.S. (2005) 'PhotochemCAD 2: a refined program with accompanying spectral databases for photochemical calculations', *Photochemistry and Photobiology*, 81(1), pp. 212–213. Available at: https://doi.org/10.1562/2004-11-06-TSN-361.

Douwes, J. *et al.* (1999) 'Fungal extracellular polysaccharides in house dust as a marker for exposure to fungi: relations with culturable fungi, reported home dampness, and respiratory symptoms', *The Journal of Allergy and Clinical Immunology*, 103(3 Pt 1), pp. 494–500. Available at: https://doi.org/10.1016/s0091-6749(99)70476-8.

DOUWES, J. *et al.* (2003) 'Bioaerosol Health Effects and Exposure Assessment: Progress and Prospects', *The Annals of Occupational Hygiene*, 47(3), pp. 187–200. Available at: https://doi.org/10.1093/annhyg/meg032.

D'Ovidio, M. *et al.* (2021) 'Pollen and Fungal Spores Evaluation in Relation to Occupants and Microclimate in Indoor Workplaces', *Sustainability*, 13, p. 3154. Available at: https://doi.org/10.3390/su13063154.

Elbert, W. *et al.* (2007) 'Contribution of fungi to primary biogenic aerosols in the atmosphere: Wet and dry discharged spores, carbohydrates, and inorganic ions', *Atmospheric Chemistry and Physics*, 7(17), pp. 4569–4588. Available at: https://doi.org/10.5194/acp-7-4569-2007.

Emberlin, J. (1994) 'The Effects of Patterns in Climate and Pollen Abundance on Allergy', *Allergy*, 49, pp. 15-20,. Available at: https://doi.org/10.1111/j.1398-9995.1994.tb04233.x.

Ewa Brągoszewska, Magdalena Bogacka, and Krzysztof Pikoń (2020) 'Effectiveness and Eco-Costs of Air Cleaners in Terms of Improving Fungal Air Pollution in Dwellings Located in Southern Poland—A Preliminary Study'. Available at: https://www.mdpi.com/2073-4433/11/11/1255 (Accessed: 10 July 2023).

Feeney, P. *et al.* (2018) 'A comparison of on-line and off-line bioaerosol measurements at a biowaste site', *Waste Management*, 76, pp. 323–338. Available at: https://doi.org/10.1016/j.wasman.2018.02.035.

Fennelly, M.J. *et al.* (2018) 'Review: The Use of Real-Time Fluorescence Instrumentation to Monitor Ambient Primary Biological Aerosol Particles (PBAP)', *Atmosphere*, 9(1), p. 1. Available at: https://doi.org/10.3390/atmos9010001.

Fernández-Rodríguez, S., Tormo-Molina, R., Lemonis, N., Clot, B., O'Connor, D.J., *et al.* (2018) 'Comparison of fungal spores concentrations measured with wideband integrated bioaerosol sensor and Hirst methodology', *Atmos. Environ*, 175, pp. 1–14. Available at: https://doi.org/10.1016/j.atmosenv.2017.11.038.

Fernández-Rodríguez, S., Tormo-Molina, R., Lemonis, N., Clot, B., O'Connor, D. J., *et al.* (2018) 'Comparison of fungal spores concentrations measured with wideband integrated bioaerosol sensor and Hirst methodology', *Atmospheric Environment*, 175(May 2017), pp. 1–14. Available at: https://doi.org/10.1016/j.atmosenv.2017.11.038.

Flint, K.M. and Thomson, S. V. (2000) 'Seasonal infection of the weed dyer's woad by a Puccinia sp. rust used for biocontrol, and effects of temperature on basidiospore production', *Plant Disease*, 84(7), pp. 753–759. Available at: https://doi.org/10.1094/PDIS.2000.84.7.753.

Franchitti, E. *et al.* (2020) 'Methods for Bioaerosol Characterization: Limits and Perspectives for Human Health Risk Assessment in Organic Waste Treatment', *Atmosphere*, 11(5), p. 452. Available at: https://doi.org/10.3390/atmos11050452.

Gabey, A.M. *et al.* (2010) 'Measurements and comparison of primary biological aerosol above and below a tropical forest canopy using a dual channel fluorescence spectrometer', *Atmos. Chem. Phys*, 10, pp. 4453–4466. Available at: https://doi.org/10.5194/acp-10-4453-2010.

Gabey, A.M. *et al.* (2011) 'The fluorescence properties of aerosol larger than 0.8 μ in urban and tropical rainforest locations', *Atmos. Chem. Phys*, 11, pp. 5491–5504. Available at: https://doi.org/10.5194/acp-11-5491-2011.

Gabey, A. M. *et al.* (2011) 'The fluorescence properties of aerosol larger than 0.8 μ in urban and tropical rainforest locations', *Atmospheric Chemistry and Physics*, 11(11), pp. 5491–5504. Available at: https://doi.org/10.5194/acp-11-5491-2011.

Gajewska, J. *et al.* (2022) 'Fungal and oomycete pathogens and heavy metals: an inglorious couple in the environment', *IMA Fungus*, 13(1), p. 6. Available at: https://doi.org/10.1186/s43008-022-00092-4.

Galán, C. *et al.* (2007) 'Spanish Aerobiology Network (REA): Management and Quality Manual; Servicio de Publicaciones Universidad de Córdoba'. Edited by Ed.

Gollakota, A.R.K. *et al.* (2021) 'Bioaerosols: Characterization, pathways, sampling strategies, and challenges to geo-environment and health', *Gondwana Research*, 99, pp. 178–203. Available at: https://doi.org/10.1016/j.gr.2021.07.003.

Gravesen, S. (1979) 'Fungi as a cause of allergic disease', *Allergy*, 34, pp. 135–154.

Griffin, D.W., Westphal, D.L. and Gray, M.A. (2006) 'Airborne microorganisms in the African desert dust corridor over the mid-Atlantic ridge, Ocean Drilling Program, Leg 209', *Aerobiologia*, 22(3), pp. 211–226. Available at: https://doi.org/10.1007/s10453-006-9033-z.

Gubanova, D.P. *et al.* (2021) 'Time Variations in the Composition of Atmospheric Aerosol in Moscow in Spring 2020', *Izvestiya, Atmospheric and Oceanic Physics*, 57(3), pp. 297–309. Available at: https://doi.org/10.1134/S0001433821030051.

Guercio, V. *et al.* (2021) 'Exposure to indoor and outdoor air pollution from solid fuel combustion and respiratory outcomes in children in developed countries: a systematic review and meta-analysis', *Science of The Total Environment*, 755, p. 142187. Available at: https://doi.org/10.1016/j.scitotenv.2020.142187.

Hand, J.L. *et al.* (2014) 'Journal of Geophysical Research : Atmospheres Aerosols across the United States', *Journal of Geophysical Research : Atmospheres*, 119, pp. 832-849,. Available at: https://doi.org/10.1002/2014JD022495.Received.

Hart, M.L., Wentworth, J.E. and Bailey, J.P. (1994) 'The effects of trap height and weather variables on recorded pollen concentration at leicester', *Grana*, 33(2), pp. 100–103. Available at: https://doi.org/10.1080/00173139409427840.

Healy, D.A. *et al.* (2012) 'A laboratory assessment of the Waveband Integrated Bioaerosol Sensor (WIBS-4) using individual samples of pollen and fungal spore material', *Atmospheric Environment*, 60, pp. 534–543. Available at: https://doi.org/10.1016/j.atmosenv.2012.06.052.

Healy, D.A. *et al.* (2014a) 'Ambient measurements of biological aerosol particles near Killarney, Ireland: a comparison between real-time fluorescence and microscopy techniques', *Atmospheric Chemistry and Physics*, 14(15), pp. 8055–8069. Available at: https://doi.org/10.5194/acp-14-8055-2014.

Healy, D.A. *et al.* (2014b) 'Ambient measurements of biological aerosol particles near Killarney, Ireland: A comparison between real-time fluorescence and microscopy techniques', *Atmospheric Chemistry and Physics*, 14(15), pp. 8055–8069. Available at: https://doi.org/10.5194/acp-14-8055-2014.

Hernandez, M. *et al.* (2016) 'Chamber Catalogues of Optical and Fluorescent Signatures Distinguish Bioaerosol Classes', *Atmospheric Measurement Techniques*, 9, pp. 3283-3292,. Available at: https://doi.org/10.5194/amt-9-3283-2016.

Hernandez, Mark *et al.* (2016) 'Chamber catalogues of optical and fluorescent signatures distinguish bioaerosol classes', *Atmospheric Measurement Techniques*, 9(7), pp. 3283–3292. Available at: https://doi.org/10.5194/amt-9-3283-2016.

Hernández Trejo, F. *et al.* (2012) 'Airborne ascospores in Mérida (SW Spain) and the effect of rain and other meteorological parameters on their concentration', *Aerobiologia*, 28(1), pp. 13–26. Available at: https://doi.org/10.1007/s10453-011-9207-1.

Hernandez-Ceballos, M.A. *et al.* (2013) 'Analysis of atmospheric dispersion of olive pollen in southern Spain using SILAM and HYSPLIT models', *Aerobiologia*, 30(3), p. 239.

Hirst, J.M. (1952) 'An Automatic Volumetric Spore Trap', *Annals of Applied Biology*, 39(2), pp. 257–265. Available at: https://doi.org/10.1111/j.1744-7348.1952.tb00904.x.

Hollins, P.D. *et al.* (2004a) 'Relationships between airborne fungal spore concentration of Cladosporium and the summer climate at two sites in Britain', *International Journal of Biometeorology*, 48(3), pp. 137–141. Available at: https://doi.org/10.1007/s00484-003-0188-9.

Hollins, P.D. *et al.* (2004b) 'Relationships between airborne fungal spore concentration of Cladosporium and the summer climate at two sites in Britain', *International Journal of Biometeorology*, 48(3), pp. 137–141. Available at: https://doi.org/10.1007/s00484-003-0188-9.

Horner, H.T. (2009) 'Fluorescing World of Plant Secreting Cells. By Victoria V. Roshchina.', *The Quarterly Review of Biology*, 84(1), pp. 110–111. Available at: https://doi.org/10.1086/598302.

Huang, H. *et al.* (2015) 'Wind-mediated horseweed (Conyza canadensis) gene flow: Pollen emission, dispersion, and deposition', *Ecology and evolution*, 5, pp. 2646–58. Available at: https://doi.org/10.1002/ece3.1540.

Huffman, J.A. *et al.* (2013) 'High concentrations of biological aerosol particles and ice nuclei during and after rain', *Atmospheric Chemistry and Physics*, 13(13), pp. 6151–6164. Available at: https://doi.org/10.5194/acp-13-6151-2013.

Jesús Aira, M. *et al.* (2012) 'Cladosporium airborne spore incidence in the environmental quality of the Iberian Peninsula', *Grana*, 51(4), pp. 293–304. Available at: https://doi.org/10.1080/00173134.2012.717636.

Jordan, B.M.M. (1990) 'cepae , leaf blotch pathogens of leek and onion . 11 . Infection of host plants'.

Kawashima, S. *et al.* (2007) 'An algorithm and a device for counting airborne pollen automatically using laser optics', *Atmospheric Environment*, 41, pp. 7987–7993. Available at: https://doi.org/10.1016/j.atmosenv.2007.09.019.

Kellogg, C.A. *et al.* (2004) 'Characterization of aerosolized bacteria and fungi from desert dust events in Mali, West Africa', *Aerobiologia*. Available at: https://doi.org/10.1023/B:AERO.0000032947.88335.bb.

Kruglyakova, E., Mirskaya, E. and Agranovski, I.E. (2022) 'Bioaerosol Release from Concentrated Microbial Suspensions in Bubbling Processes', *Atmosphere*, 13(12), p. 2029. Available at: https://doi.org/10.3390/atmos13122029.

Kwaśny, M. *et al.* (2023) 'Fluorescence Methods for the Detection of Bioaerosols in Their Civil and Military Applications', *Sensors*, 23(6), p. 3339. Available at: https://doi.org/10.3390/s23063339.

de La Guardia, C.D. *et al.* (1998) 'An aerobiological study of Urticaceae pollen in the city of Granada (S. Spain): Correlation with meteorological parameters', *Grana*, 37(5), pp. 298–304. Available at: https://doi.org/10.1080/00173139809362682.

Latif, R. *et al.* (2021) 'First report et al. of Didymella americana causing leaf blight on Lily [Lilium hybrida (Longiflorum x Asiatic)] in India', *Indian Phytopathology*, 74(3), pp. 855–857. Available at: https://doi.org/10.1007/s42360-021-00386-4.

Li, D.W. and Kendrick, B. (1995) 'A year-round study on functional relationships of airborne fungi with meteorological factors', *International Journal of Biometeorology*, 39(2), pp. 74–80. Available at: https://doi.org/10.1007/BF01212584.

Li, J. *et al.* (2020) 'Size-resolved dynamics of indoor and outdoor fluorescent biological aerosol particles in a bedroom: A one-month case study in Singapore', *Indoor Air*, 30(5), pp. 942–954. Available at: https://doi.org/10.1111/ina.12678.

Lieberherr, G. *et al.* (2021) 'Assessment of real-time bioaerosol particle counters using reference chamber experiments', *Atmospheric Measurement Techniques*, 14(12), pp. 7693–7706. Available at: https://doi.org/10.5194/amt-14-7693-2021.

Lim, S.H. *et al.* (1998) 'Outdoor airborne fungal spores in Singapore', *Grana*, 37(4), pp. 246–252. Available at: https://doi.org/10.1080/00173139809362674.

Luo, Y. *et al.* (2021) 'The effects of indoor air pollution from solid fuel use on cognitive function among middle-aged and older population in China', *Science of The Total Environment*, 754, p. 142460. Available at: https://doi.org/10.1016/j.scitotenv.2020.142460.

Madhwal, S. *et al.* (2020) 'Ambient bioaerosol distribution and associated health risks at a high traffic density junction at Dehradun city, India', *Environmental Monitoring and Assessment*, 192(3), p. 196. Available at: https://doi.org/10.1007/s10661-020-8158-9.

Mandal, J. and Brandl, H. (2011) 'Bioaerosols in Indoor Environment - A Review with Special Reference to Residential and Occupational Locations', *The Open Environmental & Biological Monitoring Journal*, 4(1). Available at: https://benthamopen.com/ABSTRACT/TOEBMJ-4-83 (Accessed: 10 July 2023).

Markey, E. *et al.* (2022) 'A Modified Spectroscopic Approach for the Real-Time Detection of Pollen and Fungal Spores at a Semi-Urban Site Using the WIBS-4+, Part I', *Sensors*, 22(22), p. 8747. Available at: https://doi.org/10.3390/s22228747.

Martinez-Bracero, M. *et al.* (2022) 'Airborne Fungal Spore Review, New Advances and Automatisation', *Atmosphere*, 13(2), p. 308. Available at: https://doi.org/10.3390/atmos13020308.

Maya-Manzano, J.M. *et al.* (2021) 'Spatial and temporal variations in the distribution of birch trees and airborne Betula pollen in Ireland', *Agricultural and Forest Meteorology*, 298–299, p. 108298. Available at: https://doi.org/10.1016/j.agrformet.2020.108298.

MCCARTNEY, H.A. and LACEY, M.E. (1990) 'The production and release of ascospores of Pyrenopeziza brassicae on oilseed rape', *Plant Pathology*, 39(1), pp. 17–32. Available at: https://doi.org/10.1111/j.1365-3059.1990.tb02471.x.

McNabola, A. *et al.* (2011) 'Analysis of the relationship between urban background air pollution concentrations and the personal exposure of office workers in Dublin, Ireland, using baseline separation techniques', *Atmospheric Pollution Research*, 2(1), pp. 80–88. Available at: https://doi.org/10.5094/APR.2011.010.

Monroy-Colín, A. *et al.* (2020) 'HYSPLIT as an environmental impact assessment tool to study the data discrepancies between Olea europaea airborne pollen records and its phenology in SW Spain', *Urban Forestry & Urban Greening*, 53, p. 126715. Available at: https://doi.org/10.1016/j.ufug.2020.126715.

Moulin, C. *et al.* (1997) 'Control of atmospheric export of dust from North Africa by the North Atlantic Oscillation', *Nature*, 387(6634), pp. 691–694. Available at: https://doi.org/10.1038/42679.

Nazaroff, W.W. (2016) 'Teaching indoor environmental quality', *Indoor Air*, 26(4), pp. 515–516. Available at: https://doi.org/10.1111/ina.12309.

Nevalainen, A., Täubel, M. and Hyvärinen, A. (2015) 'Indoor fungi: companions and contaminants', *Indoor Air*, 25(2), pp. 125–156. Available at: https://doi.org/10.1111/ina.12182.

Norris-Hill, J. (1997) 'The Influence of Ambient Temperature on the Abundance of Poaceae Pollen', *Aerobiologia (Bologna*, 13, pp. 91-97,. Available at: https://doi.org/10.1007/BF02694424.

O'Connor, D.J. *et al.* (2014) 'Using the WIBS-4 (Waveband Integrated Bioaerosol Sensor) Technique for the On-Line Detection of Pollen Grains', *Aerosol Science and Technology*, 48(4), pp. 341–349. Available at: https://doi.org/10.1080/02786826.2013.872768.

O'Connor, D.J., Daly, S.M. and Sodeau, J.R. (2015) 'On-line monitoring of airborne bioaerosols released from a composting/green waste site', *Waste Management*, 42, pp. 23–30. Available at: https://doi.org/10.1016/j.wasman.2015.04.015.

O'Gorman, C.M. and Fuller, H.T. (2008) 'Prevalence of culturable airborne spores of selected allergenic and pathogenic fungi in outdoor air', *Atmos. Environ*, 42, pp. 4355–4368. Available at: https://doi.org/10.1016/j.atmosenv.2008.01.009.

Pace, L. *et al.* (2019) 'Temporal variations in the diversity of airborne fungal spores in a Mediterranean high altitude site', *Atmospheric Environment*, 210, pp. 166–170. Available at: https://doi.org/10.1016/j.atmosenv.2019.04.059.

Pan, Y. Le *et al.* (2021) 'Atmospheric aging processes of bioaerosols under laboratory-controlled conditions: A review', *Journal of Aerosol Science*, 155(January), p. 105767. Available at: https://doi.org/10.1016/j.jaerosci.2021.105767.

Patel, T.Y. *et al.* (2018) 'Variation in airborne fungal spore concentrations among five monitoring locations in a desert urban environment', *Environmental Monitoring and Assessment*, 190(11), p. 634. Available at: https://doi.org/10.1007/s10661-018-7008-5.

Pearson, C. *et al.* (2015) 'Exposures and health outcomes in relation to bioaerosol emissions from composting facilities: a systematic review of occupational and community studies', *Journal of Toxicology and Environmental Health. Part B, Critical Reviews*, 18(1), pp. 43–69. Available at: https://doi.org/10.1080/10937404.2015.1009961.

Pérez-Badia, R. *et al.* (2013) 'Dynamics and Behaviour of Airborne Quercus Pollen in Central Iberian Peninsula', *Aerobiologia (Bologna*, 29, pp. 419-428,. Available at: https://doi.org/10.1007/s10453-013-9294-2.

Perring, A.E. *et al.* (2015) 'Airborne observations of regional variation in fluorescent aerosol across the United States', *Journal of Geophysical Research: Atmospheres*, 120(3), pp. 1153–1170. Available at: https://doi.org/10.1002/2014JD022495.

Pfaar, O. *et al.* (2017) 'Defining pollen exposure times for clinical trials of allergen immunotherapy for pollen-induced rhinoconjunctivitis - an EAACI position paper', *Allergy*, 72(5), pp. 713–722. Available at: https://doi.org/10.1111/all.13092.

Pöhlker, C., Huffman, J.A. and Pöschl, U. (2012) 'Autofluorescence of atmospheric bioaerosols – fluorescent biomolecules and potential interferences', *Atmospheric Measurement Techniques*, 5(1), pp. 37–71. Available at: https://doi.org/10.5194/amt-5-37-2012.

Post, W., Heederik, D. and Houba, R. (1998) 'Decline in lung function related to exposure and selection processes among workers in the grain processing and animal feed industry', *Occupational and Environmental Medicine*, 55(5), pp. 349–355. Available at: https://doi.org/10.1136/oem.55.5.349.

R Core Team (2017) 'R: A Language and Environment for Statistical Computing'. Foundation for Statistical Computing; Vienna, Austria, 2017.

Robinson, N.H. *et al.* (2013) 'Cluster analysis of WIBS single-particle bioaerosol data', *Atmos. Meas. Tech*, 6, pp. 337–347. Available at: https://doi.org/10.5194/amt-6-337-2013.

Rodríguez de la Cruz, D., Sánchez-Reyes, E. and Sánchez-Sánchez, J. (2015) 'A contribution to the knowledge of Cupressaceae airborne pollen in the middle west of Spain', *Aerobiologia*, 31(4), pp. 435–444. Available at: https://doi.org/10.1007/s10453-015-9376-4.

Ruiz-Gil, T. *et al.* (2020) 'Airborne bacterial communities of outdoor environments and their associated influencing factors', *Environment International*, 145, p. 106156. Available at: https://doi.org/10.1016/j.envint.2020.106156.

Ruske, S. *et al.* (2018) 'Machine learning for improved data analysis of biological aerosol using the WIBS', *Atmospheric Measurement Techniques*, 11(11), pp. 6203–6230. Available at: https://doi.org/10.5194/amt-11-6203-2018.

Sarda Estève, R. *et al.* (2018) 'Temporal Variability and Geographical Origins of Airborne Pollen Grains Concentrations from 2015 to 2018 at Saclay, France', *Remote Sensing*, 10(12), p. 1932. Available at: https://doi.org/10.3390/rs10121932.

Sarda-Estève, R. *et al.* (2018) 'Temporal Variability and Geographical Origins of Airborne Pollen Grains Concentrations from 2015 to 2018 at Saclay, France', *Remote Sensing*, 10. Available at: https://doi.org/10.3390/rs10121932.

Sarda-Estève, R. *et al.* (2019) 'Variability and Geographical Origin of Five Years Airborne Fungal Spore Concentrations'. Available at: https://doi.org/10.3390/rs11141671.

Sarda-Estève, Roland *et al.* (2019) 'Variability and Geographical Origin of Five Years Airborne Fungal Spore Concentrations Measured at Saclay, France from 2014 to 2018', *Remote Sensing*, 11(14), p. 1671. Available at: https://doi.org/10.3390/rs11141671.

Sarda-Estève, R. *et al.* (2020) 'Atmospheric Biodetection Part I: Study of Airborne Bacterial Concentrations from January 2018 to May 2020 at Saclay, France', *International Journal of Environmental Research and Public Health*, 17(17), p. E6292. Available at: https://doi.org/10.3390/ijerph17176292.

Sauvageat, E. *et al.* (2020) 'Real-time pollen monitoring using digital holography', *Atmospheric Measurement Techniques*, 13(3), pp. 1539–1550. Available at: https://doi.org/10.5194/amt-13-1539-2020.

Savage, N.J. *et al.* (2017) 'Systematic characterization and fluorescence threshold strategies for the wideband integrated bioaerosol sensor (WIBS) using size-resolved biological and interfering particles', *Atmos. Meas. Tech*, 10, pp. 4279–4302. Available at: https://doi.org/10.5194/amt-10-4279-2017.

Savage, Nicole J. *et al.* (2017) 'Systematic characterization and fluorescence threshold strategies for the wideband integrated bioaerosol sensor (WIBS) using size-resolved biological and interfering particles', *Atmospheric Measurement Techniques*, 10(11), pp. 4279–4302. Available at: https://doi.org/10.5194/amt-10-4279-2017.

Savage, N.J. and Huffman, J.A. (2018) 'Evaluation of a hierarchical agglomerative clustering method applied to WIBS laboratory data for improved discrimination of biological particles by comparing data preparation techniques', *Atmos. Meas. Tech*, 11, pp. 4929–4942. Available at: https://doi.org/10.5194/amt-11-4929-2018.

Sessa, R. *et al.* (2002) 'Microbiological indoor air quality in healthy buildings', *The New Microbiologica*, 25(1), pp. 51–56.

Shaffer, B.T. and Lighthart, B. (1997) 'Survey of Culturable Airborne Bacteria at Four Diverse Locations in Oregon: Urban, Rural, Forest, and Coastal', *Microbial Ecology*, 34(3), pp. 167–177. Available at: https://doi.org/10.1007/s002489900046.

Shoute, L.C.T. *et al.* (2018) 'Immuno-impedimetric Biosensor for Onsite Monitoring of Ascospores and Forecasting of Sclerotinia Stem Rot of Canola', *Scientific Reports*, 8(1), pp. 1–9. Available at: https://doi.org/10.1038/s41598-018-30167-5.

Siqueira, V.M. *et al.* (2011) 'Filamentous Fungi in Drinking Water, Particularly in Relation to Biofilm Formation', *International Journal of Environmental Research and Public Health*, 8(2), pp. 456–469. Available at: https://doi.org/10.3390/ijerph8020456.

Skjøth, C.A. *et al.* (2007) 'The long-range transport of birch (Betula) pollen from Poland and Germany causes significant pre-season concentrations in Denmark', *Clin. Exp. Allergy*, 37, pp. 1204–1212. Available at: https://doi.org/10.1111/j.1365-2222.2007.02771.x.

Skjøth, C.A. *et al.* (2021) 'Air Pollution Affecting Pollen Concentrations through Radiative Feedback in the Atmosphere', *Atmosphere*, 12(11), p. 1376. Available at: https://doi.org/10.3390/atmos12111376.

Spiers, A.G. (1985) 'Factors affecting basidiospore release by Chondrostereum purpureum in New Zealand', *European Journal of Forest Pathology*, 15(2), pp. 111–126. Available at: https://doi.org/10.1111/j.1439-0329.1985.tb00874.x.

Stanley, S., W.R.K.,. P, (2009) 'WIBS-4 Bioaerosol Sensor: User Manual'.

Swanson, B.E. and Huffman, J.A. (2018) 'Development and characterization of an inexpensive single-particle fluorescence spectrometer for bioaerosol monitoring', *Opt. Express*, 26, p. 3646. Available at: https://doi.org/10.1364/oe.26.003646.

Targonski, P.V., Persky, V.W. and Ramekrishnan, V. (1995) 'Effect of environmental molds on risk of death from asthma during the pollen season', *Journal of Allergy and Clinical Immunology*, 95(5), pp. 955–961. Available at: https://doi.org/10.1016/S0091-6749(95)70095-1.

Toprak, E. and Schnaiter, M. (2013) 'Fluorescent biological aerosol particles measured with the Waveband Integrated Bioaerosol Sensor WIBS-4: laboratory tests combined with a one year field study', *Atmospheric Chemistry and Physics*, 13(1), pp. 225–243. Available at: https://doi.org/10.5194/acp-13-225-2013.

Tournas, V.H. (2005) 'Spoilage of vegetable crops by bacteria and fungi and related health hazards', *Critical Reviews in Microbiology*, 31(1), pp. 33–44. Available at: https://doi.org/10.1080/10408410590886024.

Trapero-Casas, A., Navas-Cortés, J.A. and Jiménez-Díaz, R.M. (1996) 'Airborne ascospores of Didymella rabiei as a major primary inoculum for Ascochyta blight epidemics in chickpea crops in southern Spain', *European Journal of Plant Pathology*, 102(3), pp. 237–245. Available at: https://doi.org/10.1007/BF01877962.

Troutt, C. and Levetin, E. (2001) 'Correlation of spring spore concentrations and meteorological conditions in Tulsa, Oklahoma', *International Journal of Biometeorology*, 45(2), pp. 64–74. Available at: https://doi.org/10.1007/s004840100087.

Tummon, F., Adamov, S., *et al.* (2021) 'A first evaluation of multiple automatic pollen monitors run in parallel', *Aerobiologia* [Preprint]. Available at: https://doi.org/10.1007/s10453-021-09729-0.

Tummon, F., Arboledas, L.A., *et al.* (2021) 'The need for Pan-European automatic pollen and fungal spore monitoring: A stakeholder workshop position paper', *Clinical and Translational Allergy*, 11(3), p. e12015. Available at: https://doi.org/10.1002/clt2.12015.

Twohy, C.H. *et al.* (2016) 'Abundance of fluorescent biological aerosol particles at temperatures conducive to the formation of mixed-phase and cirrus clouds', *Atmos. Chem. Phys*, 16, pp. 8205–8225. Available at: https://doi.org/10.5194/acp-16-8205-2016.

Vélez-Pereira, A.M. *et al.* (2019) 'Logistic regression models for predicting daily airborne Alternaria and Cladosporium concentration levels in Catalonia (NE Spain', *Int. J. Biometeorol*, 63, pp. 1541–1553.

Vélez-Pereira, A.M. *et al.* (2021) 'Spatial distribution of fungi from the analysis of aerobiological data with a gamma function', *Aerobiologia*, 37(3), pp. 461–477. Available at: https://doi.org/10.1007/s10453-021-09696-6.

de Weger, L.A. *et al.* (2016) 'The long distance transport of airborne Ambrosia pollen to the UK and the Netherlands from Central and south Europe', *International Journal of Biometeorology*, 60(12), pp. 1829–1839. Available at: https://doi.org/10.1007/s00484-016-1170-7.

World Health Organization. Occupational and Environmental Health Team (2006) *WHO Air quality guidelines for particulate matter, ozone, nitrogen dioxide and sulfur dioxide : global update 2005 : summary of risk*

assessment. WHO/SDE/PHE/OEH/06.02. World Health Organization. Available at: https://apps.who.int/iris/handle/10665/69477 (Accessed: 29 September 2021).

Xie, W. *et al.* (2020) 'The source and transport of bioaerosols in the air: A review', *Frontiers of Environmental Science & Engineering*, 15(3), p. 44. Available at: https://doi.org/10.1007/s11783-020-1336-8.

Yue, S. *et al.* (2016) 'Springtime precipitation effects on the abundance of fluorescent biological aerosol particles and HULIS in Beijing', *Scientific Reports*, 6(June), pp. 1–10. Available at: https://doi.org/10.1038/srep29618.

Zang, L. *et al.* (2019) 'Roles of Relative Humidity in Aerosol Pollution Aggravation over Central China during Wintertime', *International Journal of Environmental Research and Public Health*, 16(22), p. 4422. Available at: https://doi.org/10.3390/ijerph16224422.

Zbîrcea, L.-E. *et al.* (2023) 'Relationship between IgE Levels Specific for Ragweed Pollen Extract, Amb a 1 and Cross-Reactive Allergen Molecules', *International Journal of Molecular Sciences*, 24(4), p. 4040. Available at: https://doi.org/10.3390/ijms24044040.

Zhang, M. *et al.* (2021) 'Sensitivities to biological aerosol particle properties and ageing processes: potential implications for aerosol–cloud interactions and optical properties', *Atmospheric Chemistry and Physics*, 21(5), pp. 3699–3724. Available at: https://doi.org/10.5194/acp-21-3699-2021.

Chapter 3 – Results & Discussion

In recent years, there has been a growing interest in real-time monitoring of PBAPs, including pollen and fungal spores, due to their significant impact on health and climate. These results evaluated the performance of the WIBS in sampling and detecting ambient concentrations of fungal spores and pollen, comparing it to the conventional Hirst volumetric method (Hirst, 1952). Long-term pollen and fungal spore monitoring data evaluate trends in distribution and how they are influenced by climate change and environmental factors (Fernández-Rodríguez *et al.*, 2018). Pollen and fungal spore data have been correlated to study the ambient air at Saclay, Paris (Sarda Estève *et al.*, 2018; Sarda-Estève *et al.*, 2019). In recent years, automated pollen monitoring stations have complemented traditional PBAP monitoring using advanced imaging and sensor technologies to provide real-time pollen data from the WIBS (Savage *et al.*, 2017). These results can serve as the foundation for scientific research on PBAP-related environmental concerns.

3.1 Traditional monitoring of Pollen and Fungal spores

Traditional monitoring of pollen and fungal spores was undertaken from 21st April to 15 June 2017, a traditional Hirst volumetric trap was used to record ambient concentrations of PBAP. A total of 47 types of pollen and 27 types of fungal spores were identified. The most abundant pollen types were seen to be Quercus (28%), Poaceae (27%), Urticaceae (19%), Pinus (9%), Castanea (3%), Cupressaceae-Taxaceae (3%), Sambucus (2%), Rumex (2%), and Platanus (1%). These primary pollen types of samples made up 94% of the total pollen count. The most prevalent fungal spore types included Ascospores (55%), Cladosporium (31%), Tilletiopsis (4%), Basidiospores (3%), and Helicomyces (3%), contributing to 96% of the total fungal spore count. Ascospores and Cladosporium spores alone contributed to more than 85% of the total fungal spore count. This prevalence of Ascospores and Cladosporium spores is consistent with previous studies (Sarda-Estève *et al.*, 2019).

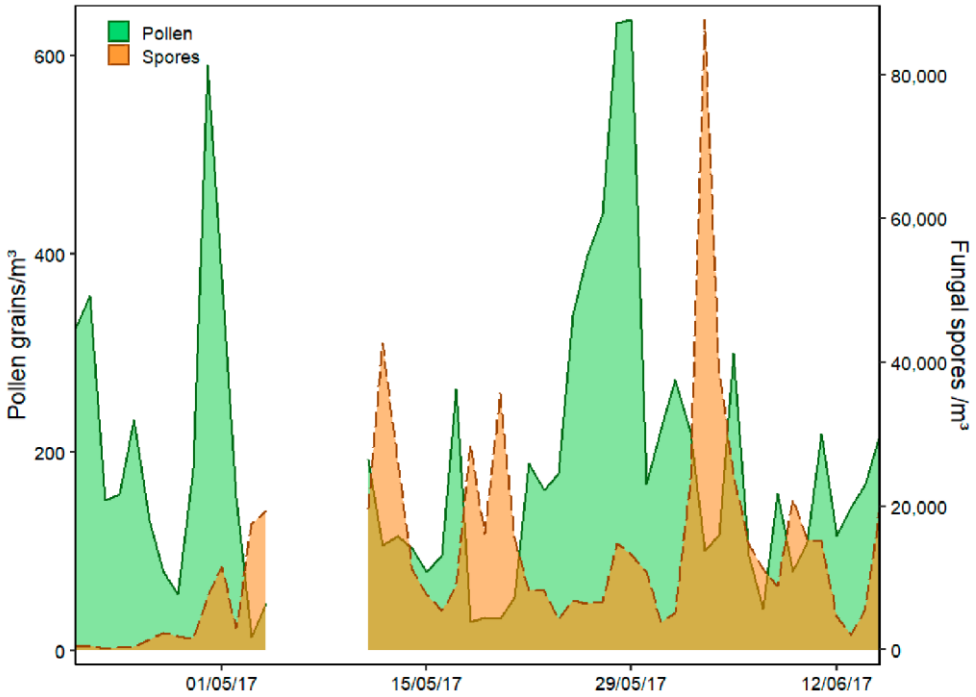

Figure 3.1. Time-series data represents daily pollen and fungal spore concentration measurements obtained using the Hirst. The dataset has been refined to exclude days with missing WIBS data.

Throughout the monitoring period, the ambient pollen concentrations reached peak levels of approximately ~600 grains/m^3 on two distinct occasions. Firstly, on the 29th of April, this was due to exceptionally high concentrations of Quercus pollen. Subsequently, another peak occurred on the 28th–29th of May, attributed to elevated levels of Poaceae and Urticaceae pollen. A smaller peak (200 grains/m^3) was also noted on the 11th of May, which was associated with high concentrations of Pinus pollen, as shown in Figure 3.1.

In contrast, four fungal spore peaks exceeded 30,000 spores/m^3 during the sampling period. The first peak, on the 12th of May, was driven by high concentrations of both Ascospores and Cladosporium spores. The subsequent consecutive peaks on the 18th and 20th of May were primarily due to elevated levels of Ascospores. Lastly, the highest daily fungal spore concentration was recorded on the 3rd of June, reaching nearly 85,000 spores/m^3, with Ascospores accounting for over 70% of the total daily concentration.

For more comprehensive data on the interannual, seasonal, and daily variability of the total pollen grain and fungal spore concentrations at Saclay, two previous investigations have provided comprehensive coverage. These studies encompassed 4-5 years of monitoring data, including the 2017 period examined in this study. Recent monitoring efforts in Saclay have also included the measurement of ambient bacterial concentrations, which can help identify the sources and trends of airborne bacteria in the region (Sarda-Estève *et al.*, 2018, 2019, 2020). These studies provide valuable information on the long-term trends and patterns of airborne allergens and pollutants in the Saclay region, which can help inform public health interventions and improve air quality. The data can also be used to develop predictive models and early warning systems for airborne allergens and pollutants, which can help mitigate their impact on human health.

As for fungal spores, 15 days with concentrations exceeding 2500 spores/m^3 were classified as "high" because the concentration levels were determined either by referencing existing literature values or by considering the predominant constituent families. Days with high concentrations were defined as those between 2000–4000 spores/m^3 with these values of >20,000 spores/m^3 far exceeding that. Since there is limited literature on recommended values for total Ascospores, this threshold primarily relies on Cladosporium spore concentrations (Vélez-Pereira *et al.*, 2021) It has been observed that Cladosporium spores exhibit higher seasonal background levels compared to other types of spores (Vélez-Pereira *et al.*, 2019, 2021; Martinez-Bracero *et al.*, 2022).

In comparison, there were four distinct periods during which fungal spore concentrations exceeded 30,000 spores/m^3. The first peak, on 12th May, resulted from high concentrations of both Ascospores and Cladosporium spores. The subsequent consecutive peak days on May 18th and 20th were predominantly due to high concentrations of Ascospores. Lastly, the highest daily fungal spore concentration, nearly 85,000 spores/m^3, was recorded on 3rd June, with Ascospores contributing to over 70% of the total daily concentration.

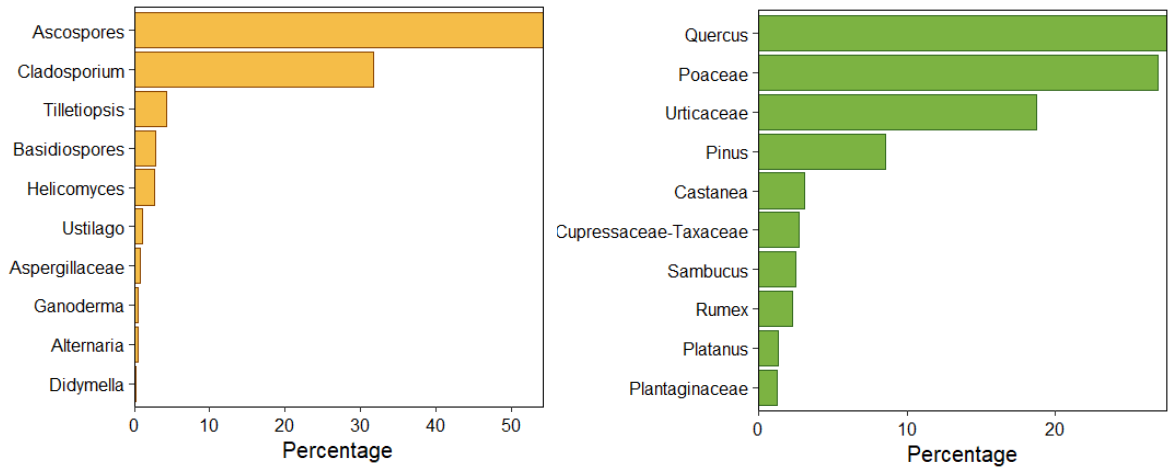

Figure 3.2. Distribution of Fungal Spore Types by Percentage.

Bar charts, also known as bar plots, are a widely used type of data visualization used to display categorical data, making them particularly effective for comparing and representing variables that fall into distinct groups in this case PBAPs. Bar charts help illustrate the distribution, frequency, or relationship between different categories of the dataset. The bar chart categories are displayed on the vertical axis (y-axis), and the bars extend horizontally. Each type of pollen and fungal spores are labelled along this axis. The x-axis represents the percentage frequencies associated with each category. The length or height of each bar is proportional to the percentage value it represents. Figure 3.2 illustrates the highly variable nature of fungal spores and pollen by concentration by percentage. The bars in a bar chart are coloured yellow for fungal spores and green for pollen. This graph illustrates a straightforward and effective way to convey the PBAP categorical data visually. As for fungal spores, Ascospores and Cladosporium were the most abundant types found in the air. The figure also indicates that Poaceae pollen, Cladosporium and Alternaria spores were the major allergenic pollen and fungal spore taxa identified. Quercus pollen was the dominant pollen type at the beginning of the campaign, while Poaceae and Urticaceae dominated the remainder of the campaign as the spring season ended and the summer season began.

In June 2017, a notable episode of high concentration of fungal spores was observed, coinciding with sweltering and dry weather conditions for that season. During 2017, the temperature in the Saclay region was approximately 1.5% higher than the average seasonal

temperatures for that year. Notably, June experienced even higher temperatures, with a deviation of +5% from average records, coupled with drier conditions. The association between airborne ascospore concentrations and relative humidity has been firmly established in prior studies (Flint and Thomson, 2000, Hollins *et al.*, 2004, Spiers, 1985). Cladosporium and basidiospores displayed a noteworthy positive correlation with temperature. This observation aligns with previous research indicating that these types of spores thrive in dry weather conditions and under higher temperatures where his observation aligns with previous studies indicating that air temperature's impact is significantly enhanced by the presence of water, mainly through rain showers, which can lead to a subsequent increase in bioaerosol concentrations after several hours (Huffman *et al.*, 2013; Pace *et al.*, 2019). For a more comprehensive exploration of recorded trends, peak days will be discussed further.

3.2 WIBS determination of ambient fluorescent particles

Utilising the excitation and emission ranges of the WIBS (discussed in the methodology chapter) an understanding of the prominent fluorescent types with the Saclay data set was determined. Figure 3.3 highlights the fraction of each fluorescent component within total fluorescent aerosols namely: "A," "B," "BC," "AB," and "ABC". Other types, such as "AC" and "C," contributed minimally to the fluorescent portion (less than 0.5%) and, as a result, to the overall aerosols. The scarcity of these particle types, particularly AC, has been widely reported in other WIBS campaigns and laboratory research (Hand *et al.*, 2014; Hernandez *et al.*, 2016).

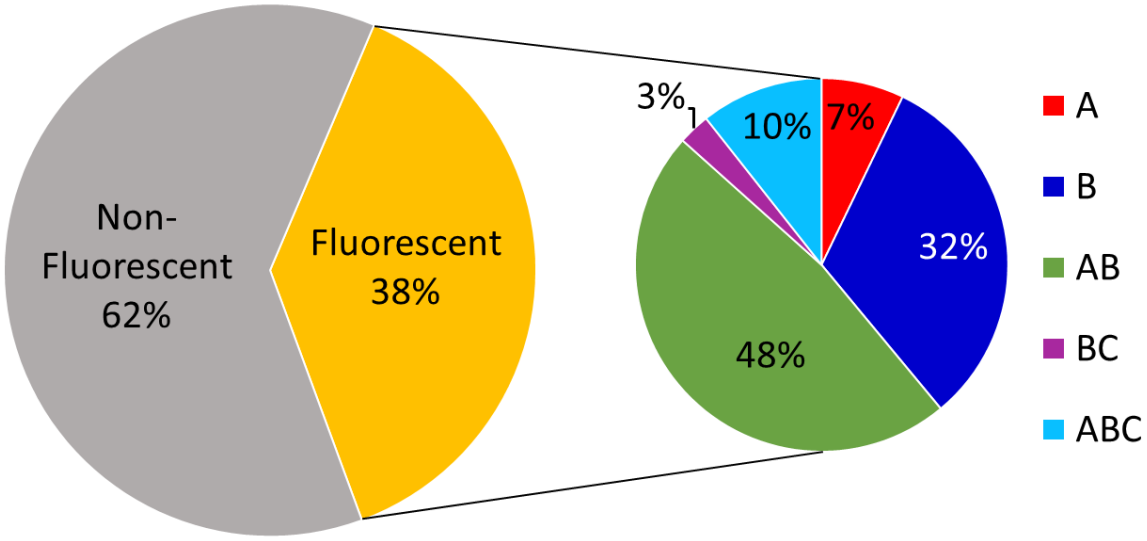

Figure 3.3. The distribution of WIBS particles categorized by the Perring nomenclature (% of total fluorescent particles) is illustrated as a pie chart.

The pie chart is a circular graph used to represent data that is divided into two categorical segments of fluorescent and non-fluorescent particles. These segments, or sectors, are proportional to the values they represent within the whole PBAP dataset with a majority of non-fluorescent particles of 62%. Pie charts are particularly useful for illustrating the composition or distribution of the subset of categories relative to the total. Each slice in the subset is assigned to the Perring nomenclature as a percentage of total fluorescent particles sized proportionally to the value it represents within the total 38%. Different colours are used to differentiate between slices and to distinguish the categories. These colours are accompanied by a label to indicate the category they represent and, in most cases, the exact percentage or value they represent concerning the whole.

The fluorescent fraction of the overall aerosol population was further subdivided into one of seven traditional particle types. This breakdown of particle classes is important for researchers and scientists studying aerosols and their properties. The figure shows seven different particle classes, each identified by a specific combination of letters (A, B, and C) from the Perring nomenclature. These classes likely represent different types of fluorescent aerosol particles.

The percentage contribution indicates the proportion of each particle class within the total population of fluorescent particles. This information is critical for understanding the relative prevalence of different particle types within the sample. The most prominent particle class in this dataset is "AB," which accounts for nearly half (48%) of the total fluorescent particles (Figure 3.3). This suggests that AB-type particles are the most prevalent in the sampled aerosol. The pie chart highlights the diversity of particle classes present in the sample. While AB and B together make up the majority (79%) of the fluorescent particles, smaller fractions of ABC, A, BC, C, and AC are also present. This diversity indicates a complex mixture of aerosol particles. The last two classes, C and AC, have contributions of less than 0.5%. These are considered trace components and are of relatively minor importance within this specific sample. This distribution data can have significant implications for aerosol research. Understanding the composition of aerosols is crucial for various applications for air quality monitoring including climate studies. The precision of the instrument is important when interpreting these results. The instrument's ability to distinguish between different particle classes may vary, and this can affect the accuracy of the percentage contributions.

The fraction presented in Figure 3.3 is often associated with bacterial or fungal origins (Hernandez *et al.*, 2016, Savage *et al.*, 2017). As approximately half of the fluorescent particles were classified as AB, this segment contained roughly 5-20 times higher particle concentrations than most other categories (BC= 2%, A= 8%, ABC=10%). Intriguingly, B-type particles were the second most common particle type (32%). Although this particle fraction has been connected to anthropogenic sources (Gabey *et al.*, 2011a; Toprak and Schnaiter, 2013; Twohy *et al.*, 2016), it has also been linked to particles containing riboflavin (Savage *et al.*, 2017) and detected as a minor fraction in some fungal spore and pollen species. However, a study noted that due to B particles' minor contribution to bioaerosol fraction, any atmospheric sampling with a dominant presence of B-type particles should be carefully examined for potential interferents (M. Hernandez *et al.*, 2016). Saclay's semi-urban location and proximity to Paris, a megacity, maybe a source of various anthropogenic emissions, potentially explaining the high concentrations of B particles observed. Similar observations have been made in other urban areas compared to rural locations (Gabey *et al.*, 2011).

In terms of particle prevalence, ABC (10%) and A (8%) have also been associated with biologically derived particles (Hernandez *et al.*, 2016; Savage and Huffman, 2018).

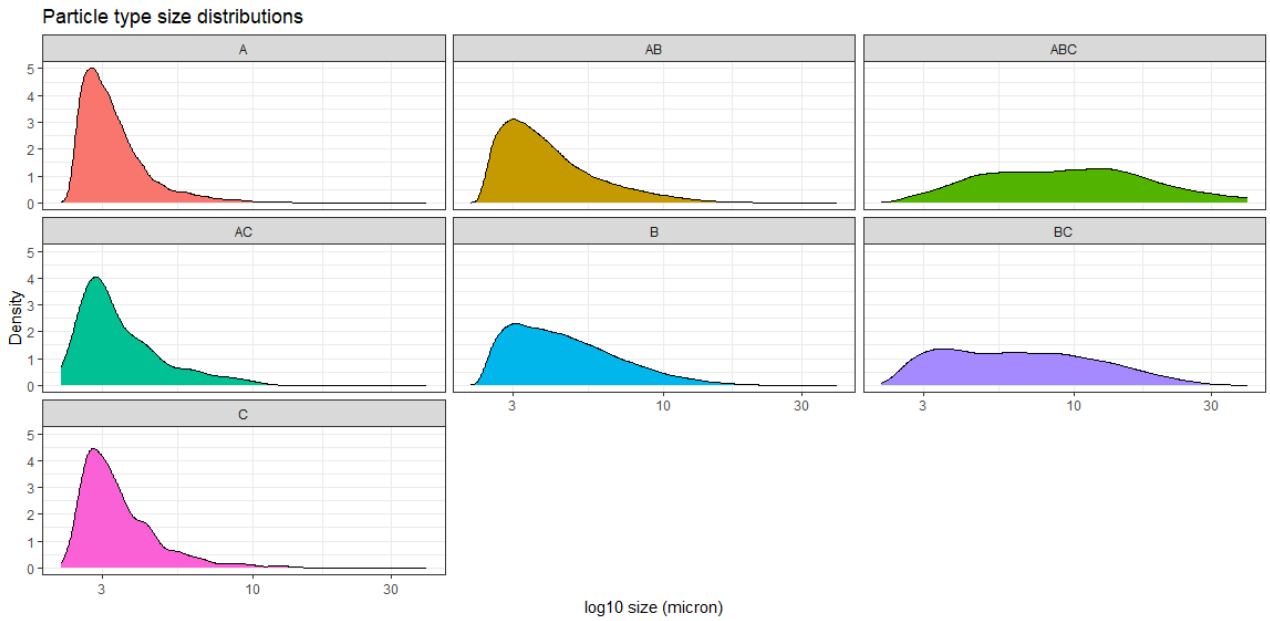

Figure 3.4. Particle type size distribution for each of the WIBS categories.

The figure above displays normalised concentration on the y-axis and size on the x-axis revealing several interesting observations. The term "distribution" describes the size and density of different particle types, including ABC, AB, and A-type particles. The size and density of each particle type can illustrate the variance within each particle category. For example, ABC-type particles were seen to peak with a bimodal profile the largest mode could be indicative of pollen-like particles. Equally, BC is seen to have larger particles and this category has also been linked to pollen-like particles in this size range. AB and A-type particles were seen to contain a high concentration of small particles of <10 μm.

Figure 3.5 represents image plots of the main fluorescence WIBS categories. The left panel of the figure illustrates the daily concentrations concerning size, where each area within the red dotted line represents one day. The right panel shows the size vs. asymmetry factor distribution of the largest contributors to the fluorescent particle trends. The colour bar represents concentrations observed during the campaign, with red indicating high particle concentrations and bluish/purple denoting lower overall aerosol concentrations.

Unfortunately, the sampling period experienced multiple power outages, evident in the plot. It is intriguing to note that despite efforts to minimise the influence of interfering fluorescing anthropogenic aerosols the presence of these anthropogenic particles may also be exhibited in the FL2 (B) channel of the instrument. This has been noted in the literature by (Savage *et al.*, 2017). Thus, while the WIBS instrument was developed as a bioaerosol sensor the WIBS system could be valuable as a comprehensive air-quality monitor capable of detecting anthropogenic and biological aerosols. However, it is essential to note that further investigation is necessary to assess this potential, particularly in complex ambient environments. Future studies should evaluate the system's performance in detecting smaller particle sizes using lower gain WIBS modes. ABC particles are seen in far lower concentrations (blue/green colours) but have a wider size distribution which may be linked to pollen at the larger size regions. 'A type' particles were seen to be generally smaller in size ranges than those of the other categories.

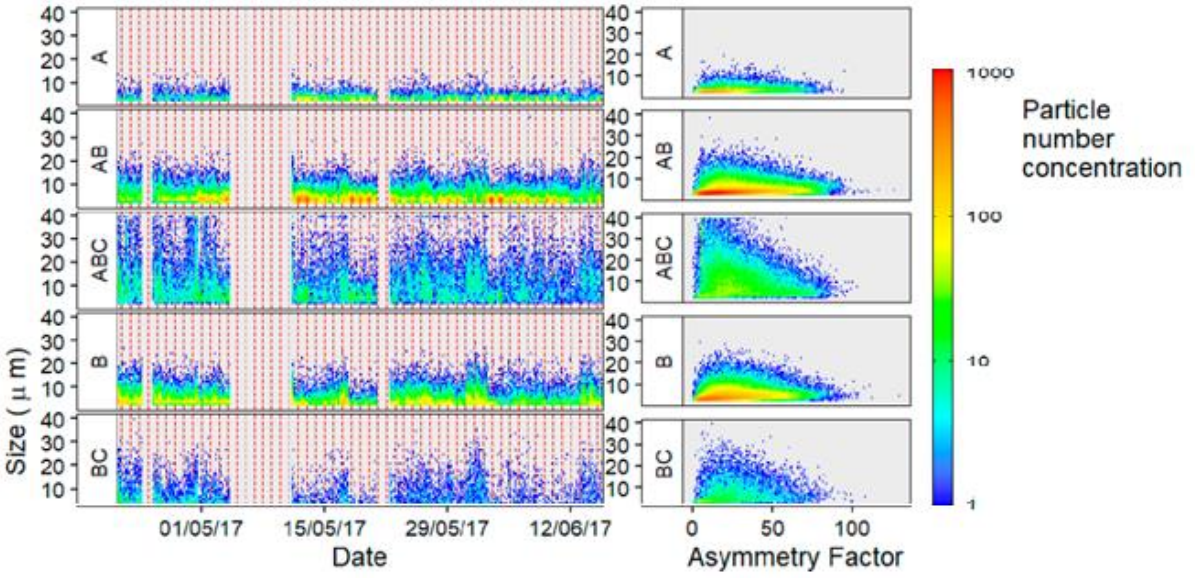

Figure 3.5. Asymmetry factor distribution for the most significant fluorescent particle distribution

By comparing the AF and size distributions of each particle type, we can discern the variability within each category of particles. ABC-type particles were observed to peak at more extensive size ranges, with a median AF value of 25. This characteristic could suggest a resemblance to pollen-like particles. Larger AF values greater than 50 and less than 100 indicated rod-like particles (Kaye

et al., 1991, 2005) It is important to note that the AF parameter is not rigorously a shape factor like those used in other aerosol calculations (DeCarlo *et al.,* 2004; Zelenyuk *et al.,* 2006) and only roughly related to a measure of particle sphericity. These low AF values within all the categories indicate spherical AB particles that could be of fungal origin (Gabey *et al.*, 2010). These observations were made in the context of earlier laboratory studies that utilized different WIBS versions to classify PBAP (Perring *et al.*, 2015).

From a previous study, the WIBS device recorded average concentrations of supermicron fluorescent particles in the air (>1 μm), revealing concentrations that ranged from 2.1 ± 0.8 to 8.7 ± 2.2 × 10^4 particles m^{-3} and accounted for up to 24% of the total supermicron particle number. Notable variations were observed in size distributions and fluorescent properties in different regions and attributed to geographically diverse bioaerosol in a previous study (Perring *et al.*, 2015). The observations were compared with model predictions of fungal and bacterial loading, and the prescribed particle sizes were smaller than the observed fluorescent aerosol.

3.3 Hirst values versus WIBS

A comparison between the WIBS and the Hirst instrumentation was undertaken as a part of this work. Such a comparison poses some challenges due to the WIBS and the Hirst differing operating principles. The WIBS and Hirst systems have distinct sampling capabilities and limitations, which need to be considered when comparing their results. One issue highlighted by previous investigations is the undercounting of particles that are either too large or too small for efficient collection by a particular instrument (Healy *et al.*, 2014a). This means that some particles may not be accurately counted by either system, leading to potential discrepancies in the data. The WIBS can detect particles as small as 0.5 μm, making it suitable for monitoring small bioaerosols such as bacteria. On the other hand, the Hirst system relies on microscopic

analysis and is operator-dependent. It is less efficient at monitoring particles smaller than approximately 2 μm in size (Fernández-Rodríguez *et al.*, 2018).

As a result of these differences, the WIBS and Hirst systems sampled different numbers of FAP, fungal spores, and pollen grains. By facilitating a meaningful comparison between the two methods, the collected fluorescent data from the WIBS was pre-processed by removing particles smaller than 2 μm before analysis. This step helps align the size range of the particles analysed by both systems, enabling a more accurate comparison of the FAP data with fungal spore and pollen concentrations recorded by the Hirst system.

It is critical to acknowledge that removing particles smaller than 2 μm from the WIBS data may result in the exclusion of relevant information regarding smaller bioaerosols. However, this pre-processing step allows for a more direct comparison between the WIBS and Hirst measurements within the overlapping size range, reducing the impact of the systems' inherent differences on the analysis and interpretation of the results.

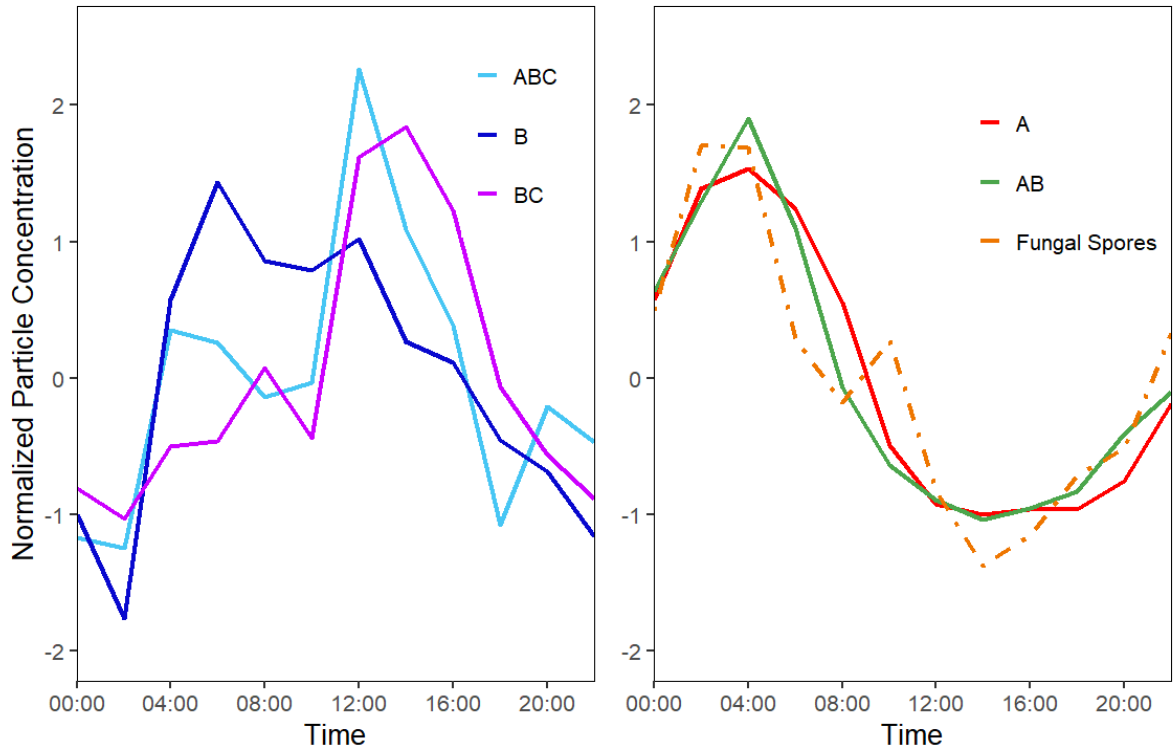

Figure 3.6. Normalised Diurnal Fungal spore and WIBS categories plot.

The diurnal plots above are graphical representations of data that show how the normalised particle concentration values change over a day. These plots are used to illustrate trends that occur within the 24-hour day-night cycle. In a diurnal plot, the x-axis represents the time of day in hours from 00:00 to 24:00. The y-axis represents the variable of normalised particle concentration. Examining the average daily cycles for the categorised WIBS groups provides a deeper understanding of the potential sources of PBAP fractions. Figure 3.6 demonstrates that the average hourly patterns for A and AB particles peak at 5 a.m. in the early morning and rise beginning in the late afternoon at 4 p.m. These trends are consistent with those observed for fungal spores in prior research (Feeney *et al.*, 2018; Healy *et al.*, 2014). This relationship is further substantiated when considering the overall diurnal pattern of fungal spore concentration. The average daily variation in ambient fungal spore levels mirrors the patterns seen in A and AB particles. The diurnal plot gains further credence when the total fungal spore diurnal trend is compared. The average daily trend in ambient fungal spore concentration

sampled by the Hirst is seen to mirror the trends seen in A and AB particles. In comparison, contrasting trends were noted for B, BC, and ABC types with peaks occurring during the middle of the day possibly indicating an anthropogenic source due to traffic.

3.3.1. Comparison of Fungal Spore Concentrations with WIBS fluorescent categories

Corrplots, short for correlation plots, are visual representations of the correlation between variables in a dataset. Correlation measures the statistical relationship between each of the variables, indicating how they are related and to what extent they move together. A correlation matrix is a table that displays the correlation coefficients between multiple variables in a dataset. The values in the matrix represent the strength and direction of the correlations. A common way to visualize a correlation matrix is to use a heatmap, where colours are used to represent the strength of the correlations. A direct analysis (via corrplot, R) of fungal spores counts vs. the concentrations of WIBS fluorescent categories (A, AB, ABC etc.) was undertaken to further scrutinize the proposed link between fungal spores counted via the direct impaction device and that outputted by the WIBS. Each variable elevated is plotted on an axis in a correlation plot (below), and the person colouration coefficients are plotted in the corresponding squares on the graph relating to the variables in question. If there is a positive correlation between two variables, a value close to 1 will be returned. Conversely, if there is a negative correlation, the person correlation will tend towards -1. To further highlight the correlations, a colour scale was also included to indicate the strength of the correlation coefficient. For example, in this case, the shade of blue indicates a stronger positive correlation, while the shade of red indicates a stronger negative correlation. Correlation plots are a powerful tool for visualising and understanding the relationships between variables in the dataset and are essential in data visualisation and analysis.

Within the corrplot fungal spore counts were broken into two cohorts. The Total grouping relates to total fungal counts while Less_Clad is the total fungal spore excluding Cladosporium. *Cladosporium* spores have been shown in previous studies to be miscounted by the WIBS (Healy *et al.*, 2014b; O'Connor *et al.*, 2015; Fernández-Rodríguez *et al.*, 2018). In particular, the WIBS has shown an inability to fully characterize sharp increases in Cladosporium species. Several reasons have been proposed for this observation, from the physical aspects of Cladosporium (it can be released in clusters) leading to increased wall loss to photophysical properties of the fungal spore inhibiting the absorption of light by bio-fluorophores within the cell. Thus, an analysis to see if a similar finding within this was undertaken. In this case, strong associations were exhibited for the WIBS instrument and both spore values (Total and Less_Clad) yielding an r of 0.97. Thus, Cladosporium has a diminished influence on the total fungal counts, with a very similar trend seen for both cohorts. Other fungal spore categories present in the total count may have a stronger relationship with the WIBS measurements, counteracting the diminishing effect of Cladosporium.

Figure 3.7 shows a Pearson correlation coefficient of 0.79 for total fungal spores compared to A and AB types, indicating a strong correlation between them. An excellent correlation between AB and A types also suggests a potential relationship between both types and fungal spore concentrations, which supports previous observations made by previous studies (Healy *et al.*, 2012; Hernandez *et al.*; 2016, Savage *et al.*, 2017). In contrast, negative correlations were observed for B, C, and BC types, while no significant relationship was found for type ABC particles.

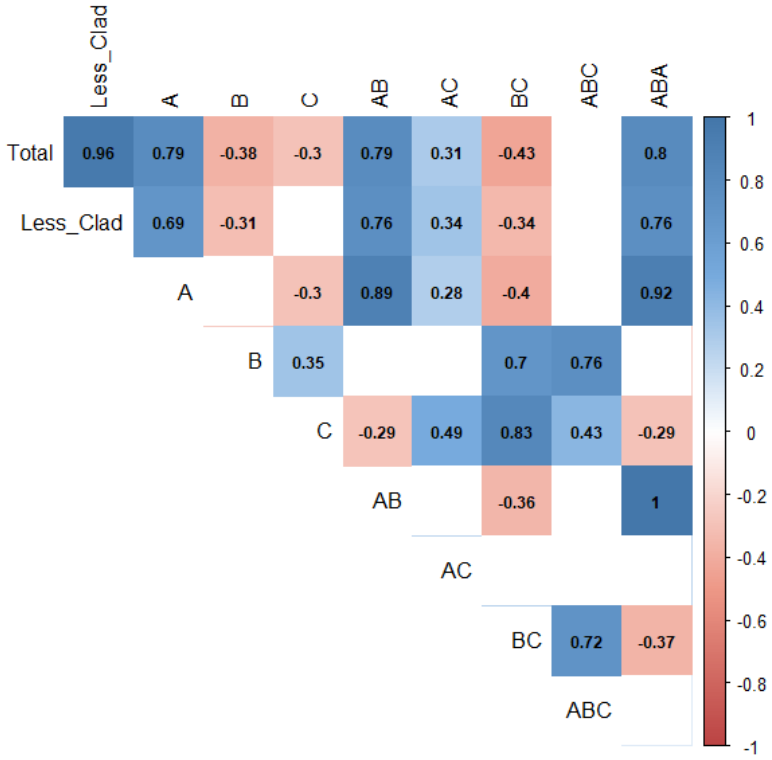

Figure 3.7. Pearson correlation between fluorescent particle types and fungal spore concentrations. The colour bar indicates positive (blue) and negative (red) correlations.

.

The figure above shows the greatest linear correlation was found for fungal spore concentrations and when A and AB particle categories were combined. The trend of A+AB particles was seen to closely mimic that of the observed fungal spore concentration, producing an R^2 value of approximately 0.65. Taking the two dominant fungal spore types into account, it was noted that Ascospores followed similar trends to A+AB particles less than 5 µm in size (r =0.84), whereas Cladosporium concentrations were seen to resemble A particle trends less than 10 µm in size (r =0.68). Although good agreement was seen for Cladosporium spores and A particles, a notable decrease in correlation is apparent when compared to the performance of Ascospores. As a result, several of the previously discussed concerns could be contributing to this slight reduction in Cladosporium sensitivity.

However, several interferents can also contribute to the fluorescent particle signals monitored by the WIBS. Natural processes can affect the measured fluorescence of bioaerosols. Atmospheric

ageing and water uptake have been shown to directly influence the fluorescence signal and intensity of bioaerosols (Gabey *et al.*, 2011; Pan *et al.*, 2021). Moreover, many studies have particularly highlighted the potential interference caused by anthropogenic aerosols. These include polycyclic aromatic hydrocarbons (PAH), humic-like substances (HULIS), mineral dust, secondary organic aerosols and black carbon (Yue *et al.*, 2016; Savage *et al.*, 2017). These substances not of biological origin, have been shown in previous studies to contribute to the fluorescence signals. In efforts to limit the effect of potentially interfering aerosols, the initial fluorescent threshold was increased from 3σ to 6σ and 9σ. Increasing the fluorescent threshold in this manner has been shown to significantly reduce the interference from non-biological aerosols but not affect the relative fraction of bioaerosols detected by the WIBS (Savage *et al.*, 2017).

By increasing the fluorescent threshold from 3σ to 9σ, a marked improvement was noted in the correlation between A-type fluorescent particles and total fungal spore concentrations, as illustrated in Figure 3.8 below.

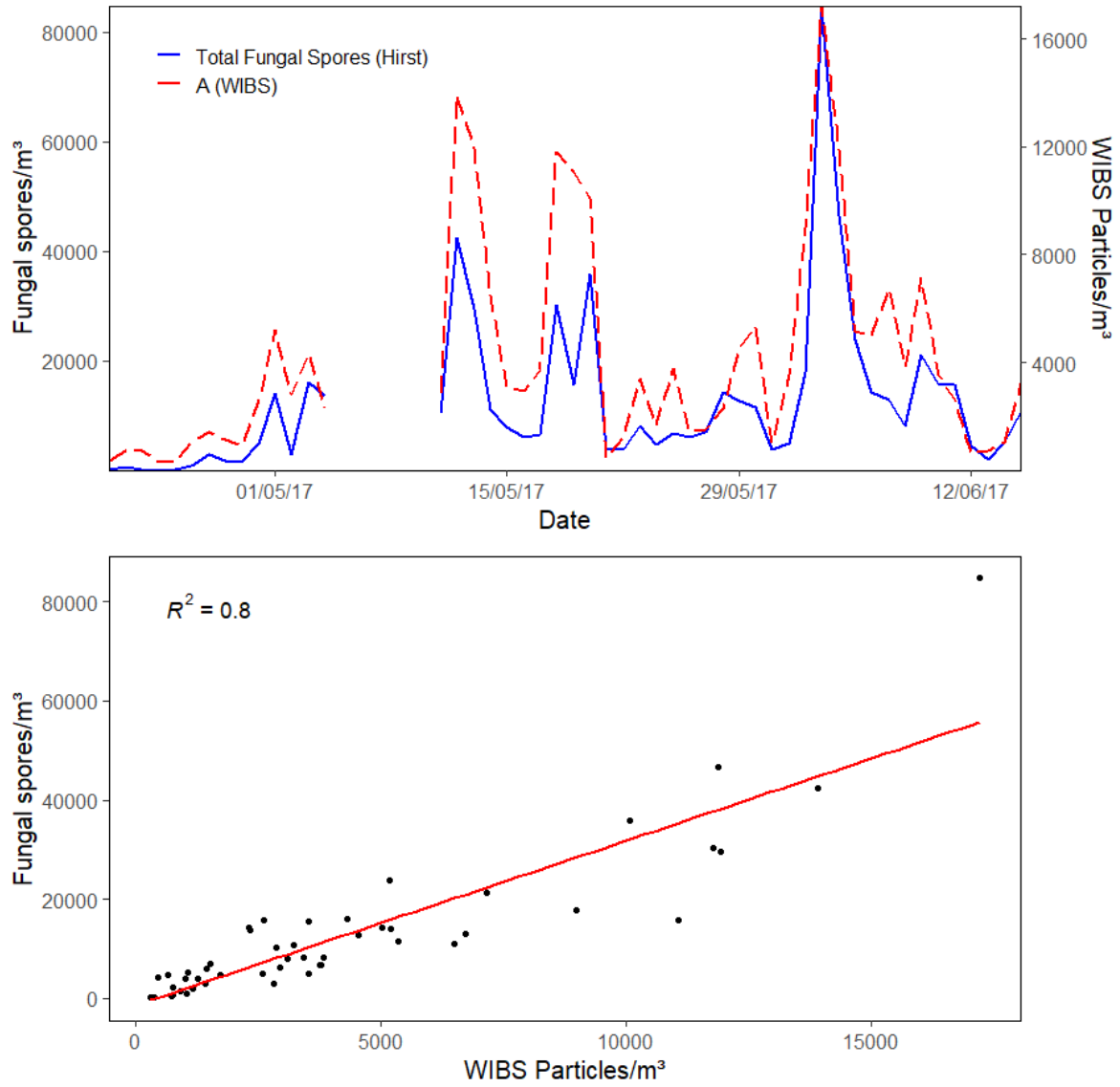

Figure 3.8. (A) time series of Hirst fungal spore counts and WIBS A (9σ) type particles (Daily) and (B) Hirst fungal spore counts and WIBS A-type particles (Daily).

The R^2 for total fungal spores increased from 0.64 (3 σ) to 0.8 (9σ). By increasing the fluorescent threshold, many remaining AB-type particles were shifted to the A-type category, thus giving similar results to the originally combined A and AB particle fraction with the presumed removal of interfering components. Any remaining interferents are likely to be very highly fluorescent anthropogenic or biological aerosols. For example, bacteria have also been shown to contribute significantly to A particle fractions (Hernandez *et al.*, 2016) and although many are removed as a result of size filtering the FAP (<2µm), larger bacteria of up to 5µm

that would not be counted microscopically could be contributing to the A particle fraction at these higher fluorescent thresholds.

3.3.2. Comparison of Pollen Concentration with WIBS Fluorescent Categories

Similar to the fungal spore analysis above a correlation between Pollen and WIBS Fluorescent Categories was undertaken. In the initial correlation analysis for pollen, it was observed that total pollen concentrations exhibited the strongest correlation with B, and BC-type particles displayed significant correlations. Prior research has indicated that both B and BC particle classes can indicate pollen grains (Hernandez *et al.*, 2016). Given the more extensive particle size ranges observed for these particle classes, it is plausible that both could be linked to pollen grains.

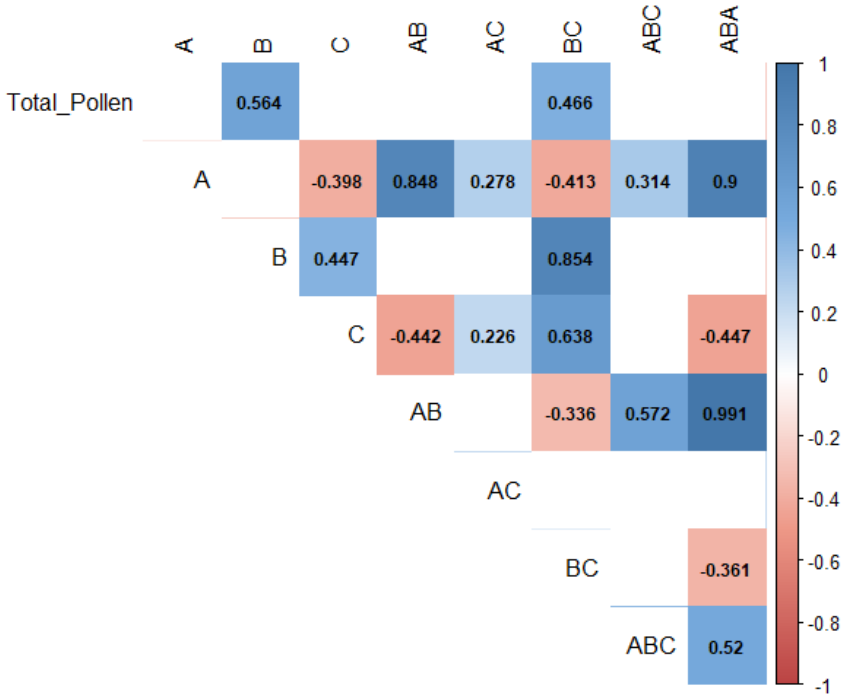

Figure 3.9. Pearson correlation between fluorescent particle types and pollen concentrations. The colour bar indicates positive (blue) and negative (red) correlations.

The correlation plot displays the Pearson correlation between various types of fluorescent particles and Total Pollen in Figure 3.9 in assessing the strength and direction of the linear

relationship. Previous WIBS studies have established that while ambient pollen grains exhibit high fluorescence intensity across all three channels, they display the highest fluorescence in the FL2 and FL3 channels (O'Connor *et al.*, 2014). Consequently, to enhance the precision of identifying pollen-type FAPs, a range of sizes and FL2/FL3 filters were applied to the WIBS data. The conditions that best represented total pollen entailed isolating particles larger than 2 µm with FL2 and FL3 fluorescence exceeding 1300, resulting in an R^2 value of 0.6, as depicted in Figure 3.10. The main deviation between the two scatter plots can be seen around 29/05/17. The scatter plot of the regression in the top right-hand corner relates to the removal of these potential outliers, their exclusion yields a more robust association ($R^2 = 0.81$).

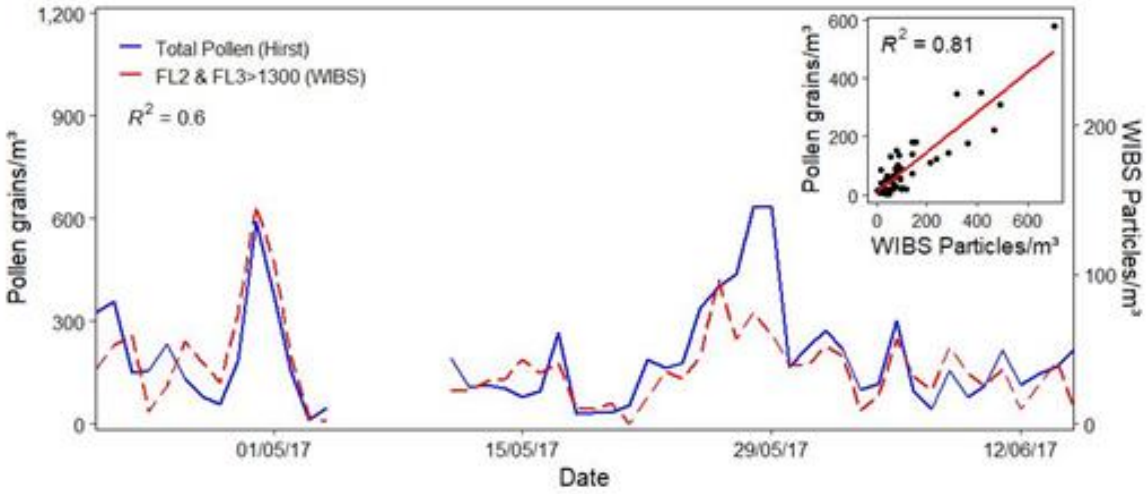

Figure 3.10. Daily temporal progression and incorporated linear regression of Hirst aggregate pollen against WIBS particle concentrations featuring FL2 and FL3 intensities surpassing 1300.

Overall, the isolated FAPs mirror the patterns of the recorded total pollen concentrations for most of the monitoring period, yet they do not adequately account for the peaks on the 11th (Pinus pollen) and 28th–29th (Poaceae pollen) of May. Notably, both Pinus and Poaceae are characterized by having some of the largest pollen grains among the recorded pollen types. The WIBS has demonstrated heightened effectiveness in capturing smaller particles, yet it encounters challenges in efficiently detecting more significant pollen types due to the relatively modest flow rate employed, often resulting in under-sampling (O'Connor *et al.*,

2014; Lieberherr *et al.*, 2021). Consequently, comparative investigations often reveal lower "pollen" concentrations registered by the WIBS compared to the Hirst (Tummon, Adamov, *et al.*, 2021). Additionally, larger particles such as Poaceae and other substantial pollen varieties can undergo inevitable losses due to sedimentation within the inlet system, further contributing to under-sampling, and likely contributing to the observed total pollen concentrations.

3.4 Impact of Meteorological Factors on PBAPs and their Geographic Source

Influence of Meteorological parameters on particle concentrations and geographical origin

Meteorological conditions are the driving force for the production and subsequent release of both pollen grains and fungal spores and have been thoroughly discussed throughout aerobiological studies (Emberlin, 1994, Norris-Hill, 1997, Pérez-Badia *et al.*, 2013). Spearman correlation analysis was carried out to determine any notable association between ambient daily pollen and fungal spore concentrations with weather (Table 3.1).

Table 3.1. Spearman´s rank Correlation between daily Pollen/Spore types, WIBS fluorescent category concentrations and Weather Parameters.

Pollen/Spore Type	Temp	Wind_S	Wind_D	Pres	RH	Rain
Total Pollen	**0.42****	-0.02	**-0.3***	-0.14	**-0.45***	-0.2
Quercus	**-0.51****	-0.12	0.14	-0.2	0.1	0.2
Urticaceae	**0.79****	0.01	**-0.3***	0.19	-0.33	-0.33
Poaceae	**0.89****	0.01	-0.34	0.06	**-0.34***	-0.26
Trees/Shrubs	**-0.09***	-0.1	-0.07	-0.25	-0.25	0.01
Total Fungal Spores	0.22	0.17	0.02	-0.29	**0.47****	0.32
Ascospores	-0.09	0.2	0.08	-0.3	**0.70****	**0.44***
Cladosporium	**0.53****	0.12	-0.13	-0.22	0.1	0.09
Basidiospores	**0.71****	-0.02	-0.13	0.03	-0.27	-0.24
Alternaria	0.45	0.03	0.1	-0.32	-0.25	0.06
A	0.39	0.12	-0.02	-0.2	**0.29****	**0.17**
AB	0.03	0.04	0.06	**-0.32***	**0.58****	**0.39****
ABC	**-0.38****	-0.11	-0.1	-0.21	0.05	0.19
AC	**-0.37****	0.16	0.24	-0.02	0.05	0.07
B	0.04	**-0.36***	**-0.20***	0	**-0.29***	-0.03
BC	**-0.23***	-0.18	**-0.12***	0.03	**-0.27***	-0.05
C	-0.26	0	-0.05	**0.08****	**-0.4****	-0.24

**Significance at the 95% level, **significance at the 99% level*

The results depicted in the table above show that a negative correlation was observed between total pollen and relative humidity. Similar associations have been reiterated in multiple studies and are largely affiliated with the reduced rate of anthesis as relative humidity increases (Hart, Wentworth and Bailey, 1994; de La Guardia *et al.*, 1998).

Conversely, the opposite was observed for the relationship between total fungal spores and Ascospores with relative humidity, a positive correlation with rain was also observed. The relationship between airborne concentrations of ascospores and relative humidity is well established (Li and Kendrick, 1995; Lim *et al.*, 1998; Elbert *et al.*, 2007; Hernández Trejo *et al.*, 2012), and it is generally accepted that during periods of higher relative humidity and following periods of rainfall, the concentration of ascospores increases. Cladosporium and basidiospores saw

a significant positive correlation with temperature which corroborates previous findings of these spore types favouring dry weather and higher temperatures (Spiers, 1985; Flint and Thomson, 2000; Troutt and Levetin, 2001; Hollins *et al.*, 2004b). This was also noted for Total pollen which saw a moderate correlation with temperature (r =0.42).

Investigating the correlation between WIBS FAPs and weather further validates the initial link between A and AB particles with fungal spores discussed in the first iteration of this study (Markey *et al.*, 2022). Initial investigations comparing the WIBS FAPs and fungal spore concentrations, saw a significant correlation between total fungal spores and A and AB-type WIBS particles achieving R^2 values of 0.8. The significant positive correlation seen for A/AB particles and rain and relative humidity mirrors that seen for fungal spores. This is largely driven by the high contribution of ascospores to the total fungal spore concentrations – equating to over 50% of spore concentrations seen during the campaign.

With regards to the WIBS particles, the influence of wind speed became increasingly significant and negatively correlated with increasing particle size greater than 5µm in size. This could be attributed to the stark differences in instrument flow rate and sampling efficiencies as previously discussed in the preceding study (Markey *et al.*, 2022). This could further explain why the WIBS failed to account for several peaks in larger bioaerosol concentrations such as Poaceae pollen – which was under-sampled by the WIBS because of these conditions. The higher efficiency of the WIBS for sampling smaller particles could also explain why fungal spore detection seemed to marginally outperform pollen detection when comparing the WIBS FAPs to the Hirst concentrations.

Wind is an important release and transport mechanism for both fungal spores and pollen, to better understand the transport of airborne bioaerosols over Saclay the ZeFir source receptor model was used. The wind rose diagram, shown in Figure 3.11, provides information on the statistical

probability and distribution of the prevailing winds experienced during the sampling period. In this case, the prevailing wind was more strongly seen originating from the western half of the windrows.

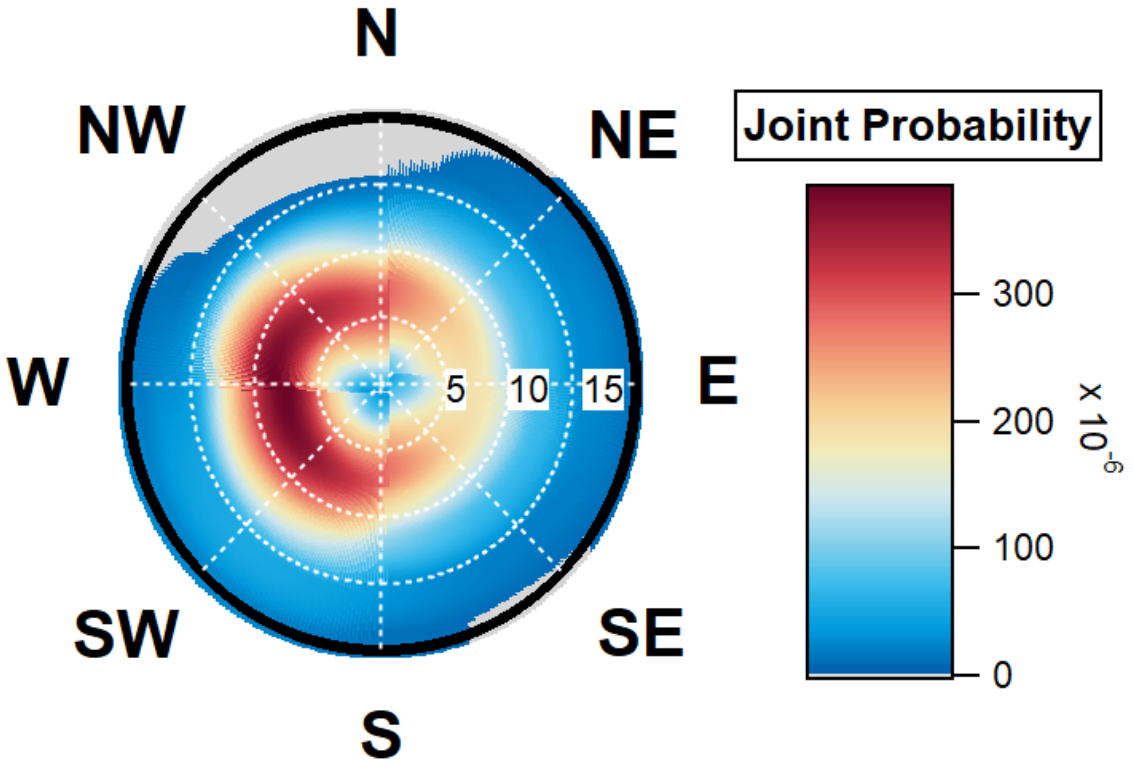

Figure 3.11. Wind rose of prevailing winds during the sampling period. White circles represent a wind speed scale in kilometres per hour (4 km/h, 8 km/h, 12 km/h, 16 km/h).

As shown in Figure 3.12, ambient total pollen concentrations (pollen grain/m^3) did not originate from the prevailing wind direction, instead coming from an easterly direction with Poaceae and Urticaceae also following an easterly direction at strong wind speeds greater than 15 km/h. This trend was also observed for the combined herbaceous pollen types – which were largely dominated by Urticaceae pollen. However, although a similar easterly origin was observed from total tree and shrub pollen, the primary origin for Quercus (which represents approximately 30% of all pollen samples) came from a south-easterly to the south-westerly direction, at moderate wind speeds ranging from 10 to 20 km/h. The multi-directional origin may indicate several point sources as varying wind speeds and directions of the pollen grains are associated with their concentrations across the different pollen types. This explains why trees and shrub pollen have a combined

weighted origin from the east due to the influence of summer tree and shrub taxa following Quercus pollination.

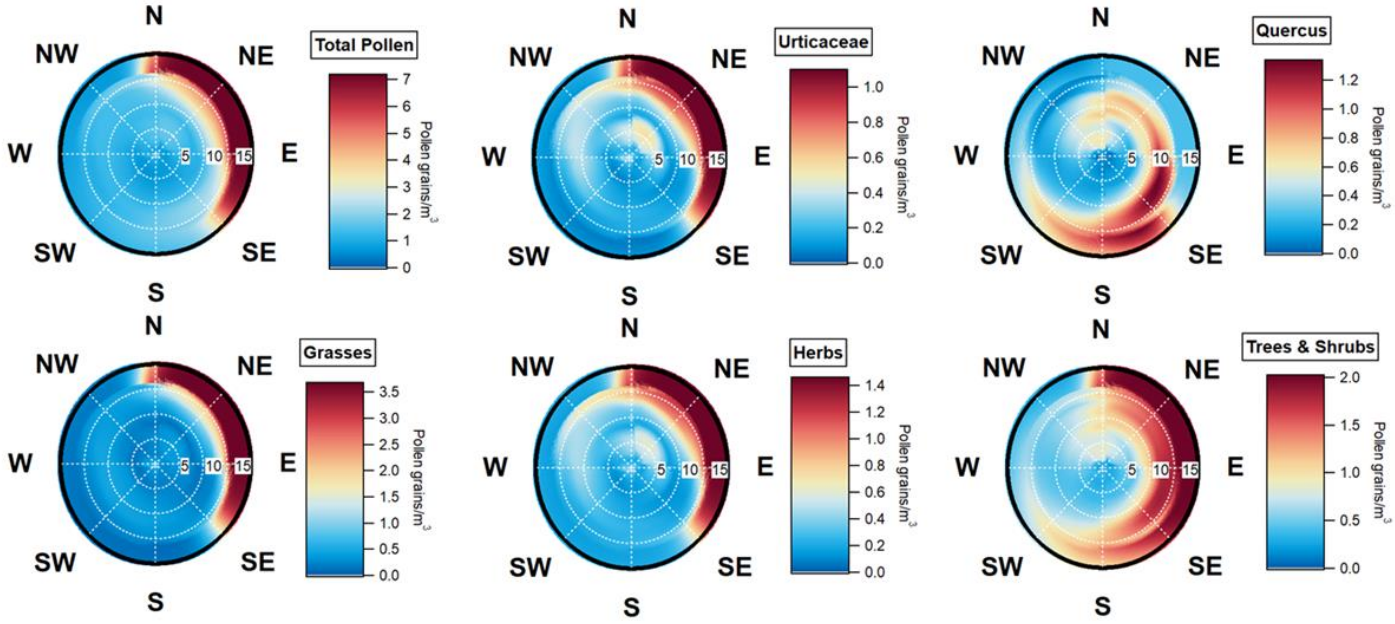

Figure 3.12. Origin of Total pollen at the sampling site. The colour scale represents the estimated concentration (Pollen grains/m^3) white gridlines represent a wind speed scale in kilometres per hour (5 km/h, 10 km/h, 15 km/h,20 km/h).

The geographical origin of ambient atmospheric fungal spores (particles/m^3), highlighted in Figure 3.13, shows a North-westerly direction at a wind speed of greater than 5 km/h but less than 15 km/h. Here we can note that Ascospores also follow a north-westerly order, likely leading to the directional origin of total spores due to their high concentrations. Conversely, Cladosporium, Alternaria and basidiospores originated from a strong North-easterly direction with Cladosporium and Alternaria also possessing a second source from a southern direction, at a wind speed of greater than 5 km/h.

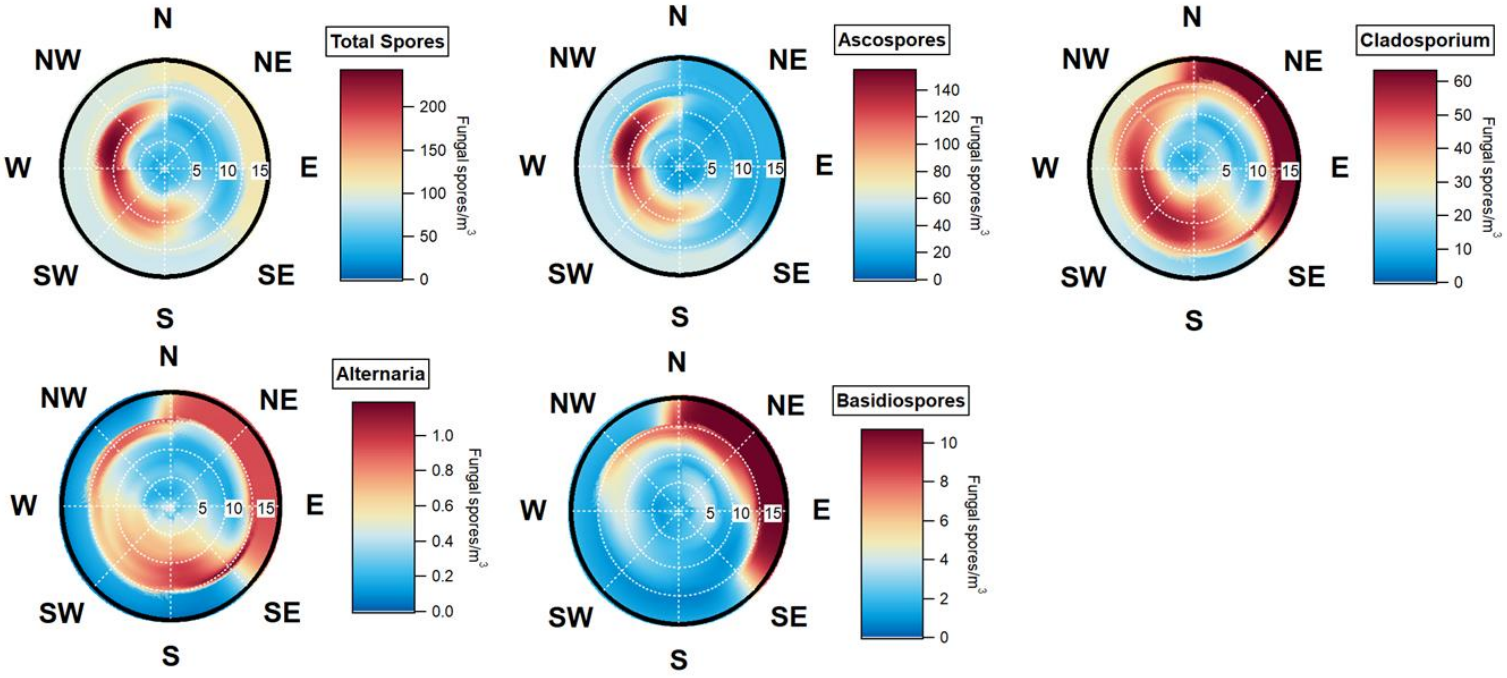

Figure 3.13. Origin of Total fungal spores, Ascospores and Cladosporium, Alternaria and Basidiospores spores at sampling site. The colour scale represents the estimated concentration (Spores/m^3) white gridlines represent a wind speed scale in kilometres per hour (5 km/h, 10 km/h, 15 km/h,20 km/h).

Further land-cover analysis of potential fungal spore and pollen sources can allow for a more comprehensive understanding of their local specific geographical origins as is shown in Figure 3.14 using Corine Land Cover (CLC) 2018. The 30 km surrounding the sampling site is largely dominated by urban and industrial landscapes. However, several broad-leaved forests, coniferous forests, and plenty of non-irrigated arable land mainly to the South/southeast of the sampling site. In the case of herb and grass pollen, it is possible that Poaceae and Urticaceae pollen was transported along the air masses from natural grasslands and national forests situated close to Paris such as Forêt Domaniale de Meudon and Verrières Forest, both of which are situated to the north-east of the sampling site. The sample can be said for tree and shrub pollen which could have originated from similar sources as well as a nearby Arboretum (de la Vallée aux Loups), also positioned in a North-easterly direction from the sampling site. The source of Quercus pollen likely

originated from the nearby forests located to the southeast of the sampling site such as Châtaigneraie du château de Corbeville. In comparison, the geographical origin of total and major fungal spore types likely originated from the non-irrigated arable land situated to the northeast and southwest of the Saclay site. Ascospores and Cladosporium spores represent the vast majority of the fungal spores sampled and are associated with agricultural concerns by infecting crops (Jordan, 1990; MCCARTNEY and LACEY, 1990; Trapero-Casas, Navas-Cortés and Jiménez-Díaz, 1996; Tournas, 2005; Jesús Aira *et al.*, 2012; Shoute *et al.*, 2018), as such they likely originated from areas containing crops such was the arable land surrounding the site.

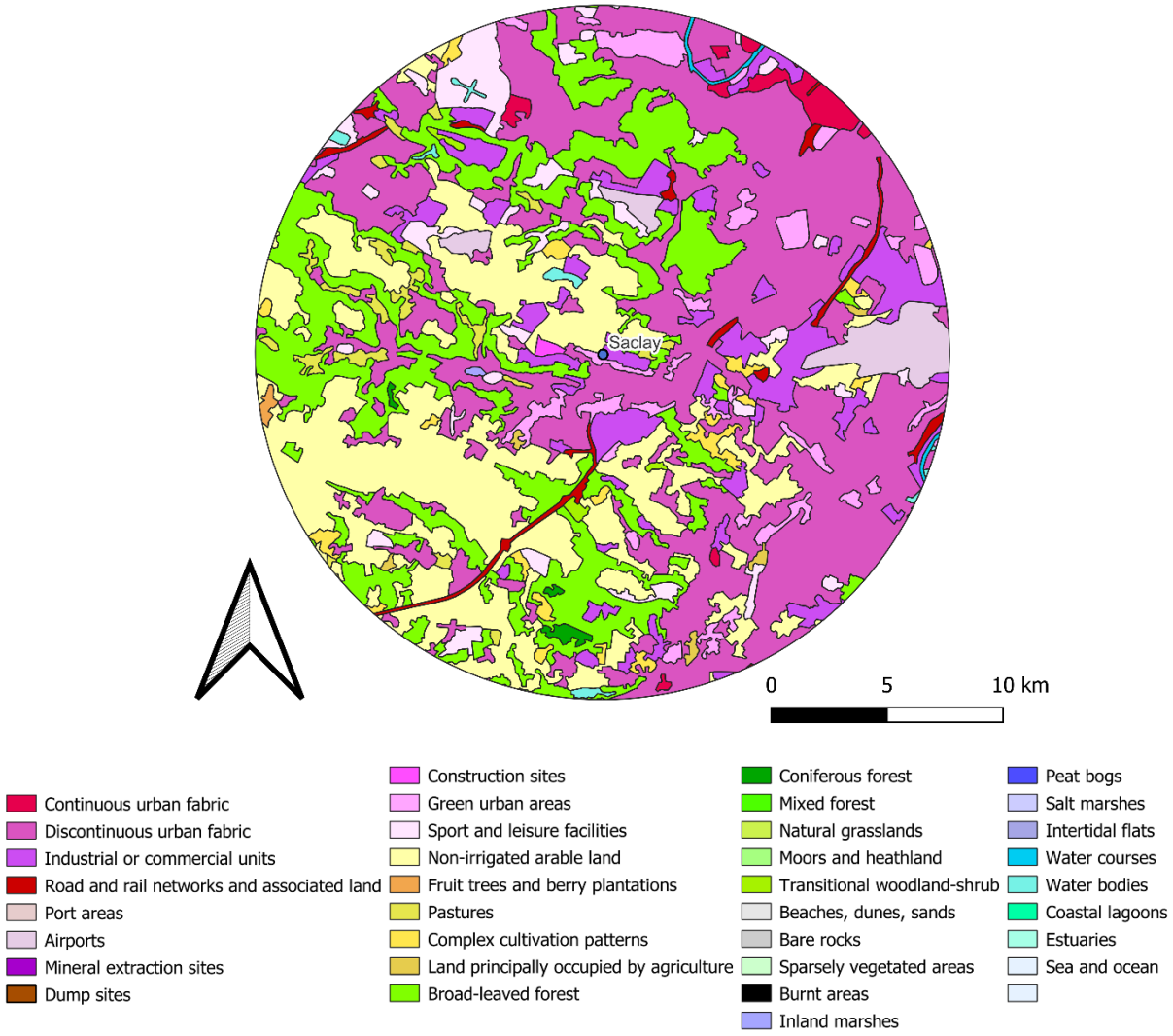

Figure 3.14. Landcover map of the 30km surrounding the sampling site (CLC, 2018).

3.5 K-Means Clustering

K-means clustering was harnessed to refine the connection between the initial A and AB (3σ) particle combination for fungal spores in Table 3.2. Implementing this intra-categorical k-means clustering accomplished a more advanced filtration of A+AB-type particles. This process yielded clusters that could offer a more accurate reflection of fungal spore concentrations compared to a mere sum of all A+AB particles. Nine clusters were identified through the analysis of A and AB particles. Cluster 4 and 8 exhibited the most robust alignment with fungal spores, resulting in an R^2 value of 0.8 (Figure 3.15). These clusters showcased representative size ranges from 2 to 7 µm and 2 to 8 µm, respectively.

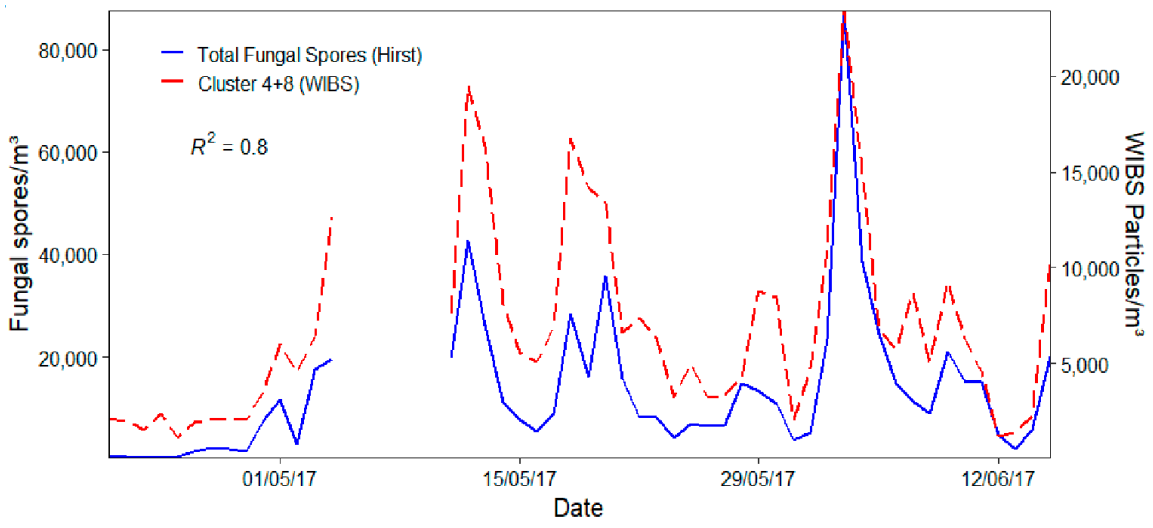

Figure 3.15. Daily temporal trends of Hirst fungal spore concentrations compared to resultant WIBS K-means clusters (4 + 8).

While K-means clustering has been previously used with WIBS data, it has often been outperformed by computationally intensive unsupervised methods like Hierarchical clustering and, more recently, supervised methods like gradient boosting (Ruske *et al.*, 2018). These methods require substantial computational resources and are often limited to supercomputers due to the high-resolution datasets generated by WIBS. The analysis of such data represents a potential bottleneck for the real-time deployment of the WIBS, mainly if the necessary computational power

is not readily available or affordable. On the other hand, K-means clustering demands less processing time and computational power than other clustering methods, making it a favourable alternative. Previous studies have overlooked the potential of K-means clustering for WIBS data analysis due to the tendency to produce similarly sized clusters. However, recent research has demonstrated the potential of this method in differentiating several pollen taxa using data obtained from another fluorescence-based bioaerosol sensor (Swanson and Huffman, 2018).

Table 3.2. Comparative Analysis of Outcomes from K-means Clustering and Particle Filtering Methods.

Pollen/Fungal spore	**K-Means Clustering Results**			**Original Particle Filtering**		
	Conditions	**Pearson Correlation Coefficient (r)**	**R^2**	**Conditions**	**Pearson Correlation Coefficient (r)**	**R^2**
Total Pollen	K-means Cluster 1+2 of particles with FL2 and FL3>1300	0.75	0.6	particles with FL2 and FL3>1300	0.73	0.5
Trees and Shrub Pollen	K-means Cluster 1+3 of particles with FL2 and FL3>1300	0.76	0.6	ABC Particles (9σ) >25µm	0.88	0.8
Total Fungal Spores	K-means Cluster 5+3 of A+AB (3σ) particles	0.88	0.8	A+AB (3σ) particles	0.80	0.7
				A (9σ) particles	0.88	0.8

The results in Table 3.2 represent a comparison between two different methods of clustering and analysing pollen and fungal spore data. Pearson analysis was used to assess the relationship between pollen/fungal spores and WIBS data. Spearman is more commonly used as a non-parametric approach. This was excluded since it can be influenced by monotonic relationships. Pearson has been used frequently when comparing traditional sampling methods to real-time methods in this manner although sometimes they are used interchangeably (Matthias-Maser, Gruber and Jaenicke, 1996; Galán *et al.*, 2000; Skjøth *et al.*, 2007).

The Table illustrates that the k-means clustering method for analysing total pollen data provides a slightly better correlation (r = 0.75) compared to the original particle filtering method (r = 0.73). The R-squared values (R^2) for both methods indicate that they both explain a substantial portion of the variance in the data, but the k-means method (R^2 = 0.6) outperforms the original particle filtering method (R^2 = 0.5).

For total fungal spores, the K-Means clustering method demonstrates a higher Pearson Correlation Coefficient (r = 0.88) compared to the original particle filtering method (r = 0.85), indicating a stronger linear relationship between the clustered data points. Furthermore, the k-means method also has a higher R-squared value (R^2 = 0.8) suggesting that it provides a better fit to the data and explains more of the variance in the fungal spore data.

In both cases, k-means clustering appears to yield slightly better results in terms of correlation and explaining variance when compared to the original particle filtering method. However, it's important to consider the practical implications and context of these results to determine which method is more suitable for the specific analysis or research goals. Additionally, factors such as computational efficiency, ease of implementation, and interpretability should also be considered when choosing between these two methods.

The same k-means technique was applied to WIBS particles exhibiting FL2 and FL3 fluorescence intensity surpassing 1300, a factor correlated with total pollen, initially yielding an R^2 of 0.5. This k-means clustering produced three distinct clusters. The particle sizes within Cluster 2 ranged from 2 to 30 µm, with a median size of 17 µm. As discussed, variations in the anticipated pollen count were observed during periods of high concentration, attributed to discrepancies in instrument sampling efficiencies.

Alternative approaches, including cluster analysis, have demonstrated their capability to distinguish between FAPs (Crawford *et al.*, 2015). On the other hand, K-means demands less processing time and computational power than other clustering methods, rendering it an appealing alternative. Prior studies have dismissed the potential of k-means clustering for WIBS data analysis due to its tendency to generate groups of similar sizes. However, this approach has recently demonstrated promise in distinguishing several pollen taxa using data from another fluorescence-based bioaerosol sensor (Robinson *et al.*, 2013).

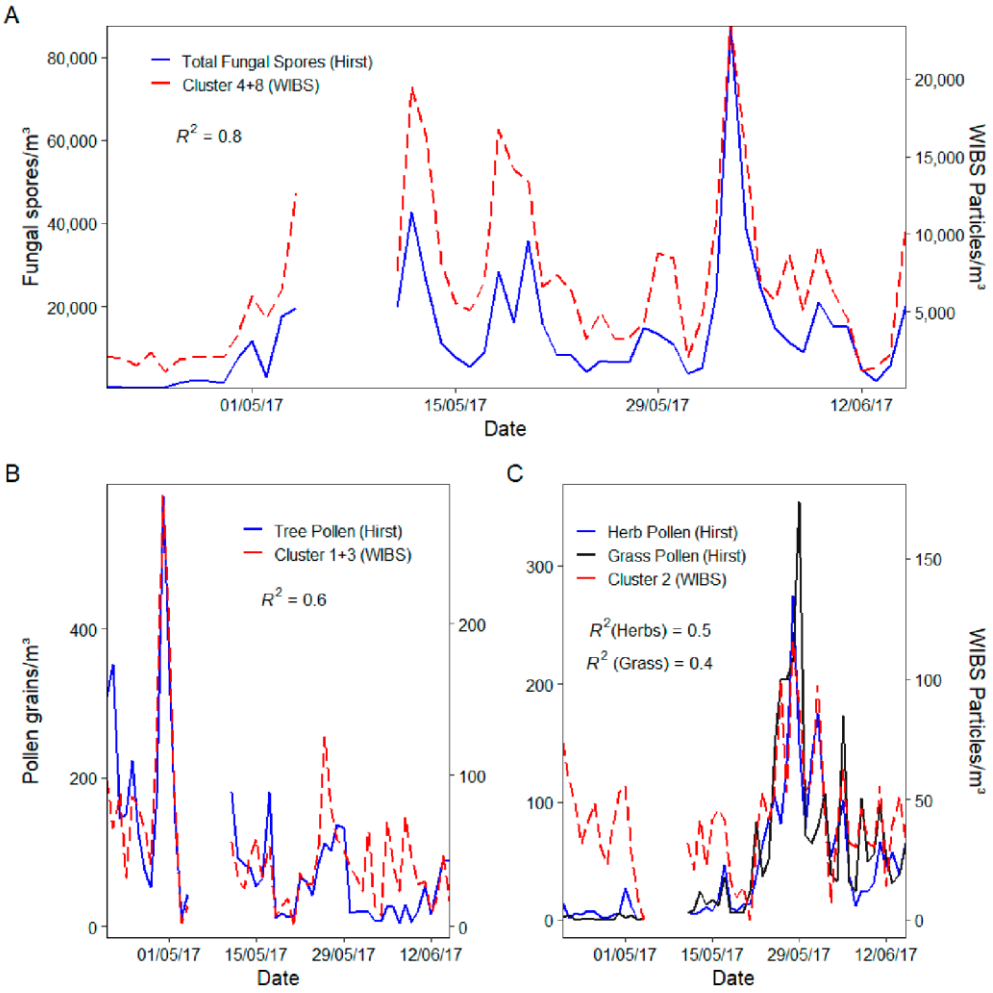

Figure 3.16. illustrates the following daily time series comparisons: (A) The daily time series plots the Hirst fungal spore concentrations with corresponding WIBS K-means clusters (4 + 8). (B) The daily time series displays the Hirst tree pollen concentrations alongside the associated WIBS K-means clusters (1 + 3). (C) The daily time series showcases the Hirst grass/herb pollen concentrations in correlation with the WIBS K-means clusters (2).

In Figure 3.16, the same k-means methodology was applied to WIBS particles characterized by FL2 and FL3 fluorescence intensities exceeding 1300, which have previously demonstrated a correlation with total pollen concentrations, resulting in an initial R^2 value of 0.5. The k-means clustering process led to the identification of three distinct clusters. Interestingly, these clusters exhibited effective discrimination between various pollen types. Cluster 2 displayed a noteworthy correlation with dominant grass and herb pollen types, yielding R^2 values of 0.4 and 0.5, respectively. The particle sizes within Cluster 2 ranged from 2 to 30 μm, with a median size of 17 μm, which could potentially indicate the presence of Urticaceae pollen. Anomalies in the expected pollen count were observed during periods of elevated concentration, attributed to variations in instrument sampling efficiencies, as previously discussed. Similarly, Clusters 1 and 3 exhibited a robust association with tree and shrub pollen, resulting in an R^2 value of 0.6 (as depicted in Figure 3.16). Cluster 3 particles had a median size of 22 μm and displayed a particularly strong correlation with Quercus pollen ($R^2 = 0.61$), representing approximately 30% of all sampled pollen during the campaign.

References

Adams, R.I. *et al.* (2016) 'Ten questions concerning the microbiomes of buildings', *Building and Environment*, 109, pp. 224–234. Available at: https://doi.org/10.1016/j.buildenv.2016.09.001.

Aerosol Technology: Properties, Behavior, and Measurement of Airborne Particles, 2nd Edition | Wiley (no date) *Wiley.com*. Available at: https://www.wiley.com/en-ie/Aerosol+Technology%3A+Properties%2C+Behavior%2C+and+Measurement+of+Airborne+Particles%2C+2nd+Edition-p-9781118591970 (Accessed: 7 July 2023).

Alzate, F. *et al.* (2015) 'Atmospheric pollen and spore content in the urban area of the city of Medellin, Colombia', *Hoehnea*, 42, pp. 09–19. Available at: https://doi.org/10.1590/2236-8906-52/2013.

de Ana, S.G. *et al.* (2006) 'Seasonal distribution of Alternaria, Aspergillus, Cladosporium and Penicillium species isolated in homes of fungal allergic patients', *Journal of Investigational Allergology & Clinical Immunology*, 16(6), pp. 357–363.

Andersen, A.A. (1958) 'NEW SAMPLER FOR THE COLLECTION, SIZING, AND ENUMERATION OF VIABLE AIRBORNE PARTICLES, 12', *Journal of Bacteriology*, 76(5), pp. 471–484.

Bauer, H. *et al.* (2002) 'The contribution of bacteria and fungal spores to the organic carbon content of cloud water, precipitation and aerosols', *Atmos. Res*, 64, pp. 109–119. Available at: https://doi.org/10.1016/S0169-8095(02)00084-4.

Beck, J.M., Young, V.B. and Huffnagle, G.B. (2012) 'The microbiome of the lung', *Translational Research: The Journal of Laboratory and Clinical Medicine*, 160(4), pp. 258–266. Available at: https://doi.org/10.1016/j.trsl.2012.02.005.

Belizario, J.A., Lopes, L.G. and Pires, R.H. (2021) 'Fungi in the indoor air of critical hospital areas: a review', *Aerobiologia*, 37(3), pp. 379–394. Available at: https://doi.org/10.1007/s10453-021-09706-7.

Brock, C.A. *et al.* (2021) 'Ambient aerosol properties in the remote atmosphere from global-scale in situ measurements', *Atmospheric Chemistry and Physics*, 21(19), pp. 15023–15063. Available at: https://doi.org/10.5194/acp-21-15023-2021.

Burrows, S.M. *et al.* (2009) 'Bacteria in the global atmosphere – Part 2: Modeling of emissions and transport between different ecosystems', *Atmospheric Chemistry and Physics*, 9(23), pp. 9281–9297. Available at: https://doi.org/10.5194/acp-9-9281-2009.

Cascade Impactor - an overview | ScienceDirect Topics (no date). Available at: https://www.sciencedirect.com/topics/chemistry/cascade-impactor (Accessed: 28 June 2023).

Cheek, E. *et al.* (2021) 'Portable air purification: Review of impacts on indoor air quality and health', *Science of The Total Environment*, 766, p. 142585. Available at: https://doi.org/10.1016/j.scitotenv.2020.142585.

Chen, Q. and Hildemann, L.M. (2009) 'The effects of human activities on exposure to particulate matter and bioaerosols in residential homes', *Environmental Science & Technology*, 43(13), pp. 4641–4646. Available at: https://doi.org/10.1021/es802296j.

Cho, E.-M. *et al.* (2019) 'Distribution and Influencing Factors of Airborne Bacteria in Public Facilities Used by Pollution-Sensitive Population: A Meta-Analysis', *International Journal of Environmental Research and Public Health*, 16(9), p. 1483. Available at: https://doi.org/10.3390/ijerph16091483.

Crawford, I. *et al.* (2015) 'Evaluation of hierarchical agglomerative cluster analysis methods for discrimination of primary biological aerosol', *Atmos. Meas. Tech*, 8, pp. 4979–4991. Available at: https://doi.org/10.5194/amt-8-4979-2015.

D'Amato, G. (2000) 'Urban air pollution and plant-derived respiratory allergy', *Clinical and Experimental Allergy*, 30(5), pp. 628–636.

D'Amato, G. *et al.* (2007) 'Allergenic pollen and pollen allergy in Europe', *Allergy*, 62(9), pp. 976–990. Available at: https://doi.org/10.1111/j.1398-9995.2007.01393.x.

Després, VivianeR. *et al.* (2012) 'Primary biological aerosol particles in the atmosphere: a review', *Tellus Series B Chemical and Physical Meteorology B*, 64, p. 15598. Available at: https://doi.org/10.3402/tellusb.v64i0.15598.

Dixon, J.M., Taniguchi, M. and Lindsey, J.S. (2005) 'PhotochemCAD 2: a refined program with accompanying spectral databases for photochemical calculations', *Photochemistry and Photobiology*, 81(1), pp. 212–213. Available at: https://doi.org/10.1562/2004-11-06-TSN-361.

Douwes, J. *et al.* (1999) 'Fungal extracellular polysaccharides in house dust as a marker for exposure to fungi: relations with culturable fungi, reported home dampness, and respiratory symptoms', *The Journal of Allergy and Clinical Immunology*, 103(3 Pt 1), pp. 494–500. Available at: https://doi.org/10.1016/s0091-6749(99)70476-8.

DOUWES, J. *et al.* (2003) 'Bioaerosol Health Effects and Exposure Assessment: Progress and Prospects', *The Annals of Occupational Hygiene*, 47(3), pp. 187–200. Available at: https://doi.org/10.1093/annhyg/meg032.

D'Ovidio, M. *et al.* (2021) 'Pollen and Fungal Spores Evaluation in Relation to Occupants and Microclimate in Indoor Workplaces', *Sustainability*, 13, p. 3154. Available at: https://doi.org/10.3390/su13063154.

Elbert, W. *et al.* (2007) 'Contribution of fungi to primary biogenic aerosols in the atmosphere: Wet and dry discharged spores, carbohydrates, and inorganic ions', *Atmospheric Chemistry and Physics*, 7(17), pp. 4569–4588. Available at: https://doi.org/10.5194/acp-7-4569-2007.

Emberlin, J. (1994) 'The Effects of Patterns in Climate and Pollen Abundance on Allergy', *Allergy*, 49, pp. 15-20,. Available at: https://doi.org/10.1111/j.1398-9995.1994.tb04233.x.

Ewa Brągoszewska, Magdalena Bogacka, and Krzysztof Pikoń (2020) 'Effectiveness and Eco-Costs of Air Cleaners in Terms of Improving Fungal Air Pollution in Dwellings Located in Southern Poland—A Preliminary Study'. Available at: https://www.mdpi.com/2073-4433/11/11/1255 (Accessed: 10 July 2023).

Feeney, P. *et al.* (2018) 'A comparison of on-line and off-line bioaerosol measurements at a biowaste site', *Waste Management*, 76, pp. 323–338. Available at: https://doi.org/10.1016/j.wasman.2018.02.035.

Fennelly, M.J. *et al.* (2018) 'Review: The Use of Real-Time Fluorescence Instrumentation to Monitor Ambient Primary Biological Aerosol Particles (PBAP)', *Atmosphere*, 9(1), p. 1. Available at: https://doi.org/10.3390/atmos9010001.

Fernández-Rodríguez, S., Tormo-Molina, R., Lemonis, N., Clot, B., O'Connor, D.J., *et al.* (2018) 'Comparison of fungal spores concentrations measured with wideband integrated bioaerosol sensor and Hirst methodology', *Atmos. Environ*, 175, pp. 1–14. Available at: https://doi.org/10.1016/j.atmosenv.2017.11.038.

Fernández-Rodríguez, S., Tormo-Molina, R., Lemonis, N., Clot, B., O'Connor, D. J., *et al.* (2018) 'Comparison of fungal spores concentrations measured with wideband integrated bioaerosol sensor and Hirst methodology', *Atmospheric Environment*, 175(May 2017), pp. 1–14. Available at: https://doi.org/10.1016/j.atmosenv.2017.11.038.

Flint, K.M. and Thomson, S. V. (2000) 'Seasonal infection of the weed dyer's woad by a Puccinia sp. rust used for biocontrol, and effects of temperature on basidiospore production', *Plant Disease*, 84(7), pp. 753–759. Available at: https://doi.org/10.1094/PDIS.2000.84.7.753.

Franchitti, E. *et al.* (2020) 'Methods for Bioaerosol Characterization: Limits and Perspectives for Human Health Risk Assessment in Organic Waste Treatment', *Atmosphere*, 11(5), p. 452. Available at: https://doi.org/10.3390/atmos11050452.

Gabey, A.M. *et al.* (2010) 'Measurements and comparison of primary biological aerosol above and below a tropical forest canopy using a dual channel fluorescence spectrometer', *Atmos. Chem. Phys*, 10, pp. 4453–4466. Available at: https://doi.org/10.5194/acp-10-4453-2010.

Gabey, A.M. *et al.* (2011) 'The fluorescence properties of aerosol larger than 0.8 μ in urban and tropical rainforest locations', *Atmos. Chem. Phys*, 11, pp. 5491–5504. Available at: https://doi.org/10.5194/acp-11-5491-2011.

Gabey, A. M. *et al.* (2011) 'The fluorescence properties of aerosol larger than 0.8 μ in urban and tropical rainforest locations', *Atmospheric Chemistry and Physics*, 11(11), pp. 5491–5504. Available at: https://doi.org/10.5194/acp-11-5491-2011.

Gajewska, J. *et al.* (2022) 'Fungal and oomycete pathogens and heavy metals: an inglorious couple in the environment', *IMA Fungus*, 13(1), p. 6. Available at: https://doi.org/10.1186/s43008-022-00092-4.

Galán, C. *et al.* (2007) 'Spanish Aerobiology Network (REA): Management and Quality Manual; Servicio de Publicaciones Universidad de Córdoba'. Edited by Ed.

Gollakota, A.R.K. *et al.* (2021) 'Bioaerosols: Characterization, pathways, sampling strategies, and challenges to geo-environment and health', *Gondwana Research*, 99, pp. 178–203. Available at: https://doi.org/10.1016/j.gr.2021.07.003.

Gravesen, S. (1979) 'Fungi as a cause of allergic disease', *Allergy*, 34, pp. 135–154.

Griffin, D.W., Westphal, D.L. and Gray, M.A. (2006) 'Airborne microorganisms in the African desert dust corridor over the mid-Atlantic ridge, Ocean Drilling Program, Leg 209', *Aerobiologia*, 22(3), pp. 211–226. Available at: https://doi.org/10.1007/s10453-006-9033-z.

Gubanova, D.P. *et al.* (2021) 'Time Variations in the Composition of Atmospheric Aerosol in Moscow in Spring 2020', *Izvestiya, Atmospheric and Oceanic Physics*, 57(3), pp. 297–309. Available at: https://doi.org/10.1134/S0001433821030051.

Guercio, V. *et al.* (2021) 'Exposure to indoor and outdoor air pollution from solid fuel combustion and respiratory outcomes in children in developed countries: a systematic review and meta-analysis', *Science of The Total Environment*, 755, p. 142187. Available at: https://doi.org/10.1016/j.scitotenv.2020.142187.

Hand, J.L. *et al.* (2014) 'Journal of Geophysical Research : Atmospheres Aerosols across the United States', *Journal of Geophysical Research : Atmospheres*, 119, pp. 832-849,. Available at: https://doi.org/10.1002/2014JD022495.Received.

Hart, M.L., Wentworth, J.E. and Bailey, J.P. (1994) 'The effects of trap height and weather variables on recorded pollen concentration at leicester', *Grana*, 33(2), pp. 100–103. Available at: https://doi.org/10.1080/00173139409427840.

Healy, D.A. *et al.* (2012) 'A laboratory assessment of the Waveband Integrated Bioaerosol Sensor (WIBS-4) using individual samples of pollen and fungal spore material', *Atmospheric Environment*, 60, pp. 534–543. Available at: https://doi.org/10.1016/j.atmosenv.2012.06.052.

Healy, D.A. *et al.* (2014a) 'Ambient measurements of biological aerosol particles near Killarney, Ireland: a comparison between real-time fluorescence and microscopy techniques', *Atmospheric Chemistry and Physics*, 14(15), pp. 8055–8069. Available at: https://doi.org/10.5194/acp-14-8055-2014.

Healy, D.A. *et al.* (2014b) 'Ambient measurements of biological aerosol particles near Killarney, Ireland: A comparison between real-time fluorescence and microscopy techniques', *Atmospheric Chemistry and Physics*, 14(15), pp. 8055–8069. Available at: https://doi.org/10.5194/acp-14-8055-2014.

Hernandez, M. *et al.* (2016) 'Chamber Catalogues of Optical and Fluorescent Signatures Distinguish Bioaerosol Classes', *Atmospheric Measurement Techniques*, 9, pp. 3283-3292,. Available at: https://doi.org/10.5194/amt-9-3283-2016.

Hernandez, Mark *et al.* (2016) 'Chamber catalogues of optical and fluorescent signatures distinguish bioaerosol classes', *Atmospheric Measurement Techniques*, 9(7), pp. 3283–3292. Available at: https://doi.org/10.5194/amt-9-3283-2016.

Hernández Trejo, F. *et al.* (2012) 'Airborne ascospores in Mérida (SW Spain) and the effect of rain and other meteorological parameters on their concentration', *Aerobiologia*, 28(1), pp. 13–26. Available at: https://doi.org/10.1007/s10453-011-9207-1.

Hernandez-Ceballos, M.A. *et al.* (2013) 'Analysis of atmospheric dispersion of olive pollen in southern Spain using SILAM and HYSPLIT models', *Aerobiologia*, 30(3), p. 239.

Hirst, J.M. (1952) 'An Automatic Volumetric Spore Trap', *Annals of Applied Biology*, 39(2), pp. 257–265. Available at: https://doi.org/10.1111/j.1744-7348.1952.tb00904.x.

Hollins, P.D. *et al.* (2004a) 'Relationships between airborne fungal spore concentration of Cladosporium and the summer climate at two sites in Britain', *International Journal of Biometeorology*, 48(3), pp. 137–141. Available at: https://doi.org/10.1007/s00484-003-0188-9.

Hollins, P.D. *et al.* (2004b) 'Relationships between airborne fungal spore concentration of Cladosporium and the summer climate at two sites in Britain', *International Journal of Biometeorology*, 48(3), pp. 137–141. Available at: https://doi.org/10.1007/s00484-003-0188-9.

Horner, H.T. (2009) 'Fluorescing World of Plant Secreting Cells. By Victoria V. Roshchina.', *The Quarterly Review of Biology*, 84(1), pp. 110–111. Available at: https://doi.org/10.1086/598302.

Huang, H. *et al.* (2015) 'Wind-mediated horseweed (Conyza canadensis) gene flow: Pollen emission, dispersion, and deposition', *Ecology and evolution*, 5, pp. 2646–58. Available at: https://doi.org/10.1002/ece3.1540.

Huffman, J.A. *et al.* (2013) 'High concentrations of biological aerosol particles and ice nuclei during and after rain', *Atmospheric Chemistry and Physics*, 13(13), pp. 6151–6164. Available at: https://doi.org/10.5194/acp-13-6151-2013.

Jesús Aira, M. *et al.* (2012) 'Cladosporium airborne spore incidence in the environmental quality of the Iberian Peninsula', *Grana*, 51(4), pp. 293–304. Available at: https://doi.org/10.1080/00173134.2012.717636.

Jordan, B.M.M. (1990) 'cepae , leaf blotch pathogens of leek and onion . 11 . Infection of host plants'.

Kawashima, S. *et al.* (2007) 'An algorithm and a device for counting airborne pollen automatically using laser optics', *Atmospheric Environment*, 41, pp. 7987–7993. Available at: https://doi.org/10.1016/j.atmosenv.2007.09.019.

Kellogg, C.A. *et al.* (2004) 'Characterization of aerosolized bacteria and fungi from desert dust events in Mali, West Africa', *Aerobiologia*. Available at: https://doi.org/10.1023/B:AERO.0000032947.88335.bb.

Kruglyakova, E., Mirskaya, E. and Agranovski, I.E. (2022) 'Bioaerosol Release from Concentrated Microbial Suspensions in Bubbling Processes', *Atmosphere*, 13(12), p. 2029. Available at: https://doi.org/10.3390/atmos13122029.

Kwaśny, M. *et al.* (2023) 'Fluorescence Methods for the Detection of Bioaerosols in Their Civil and Military Applications', *Sensors*, 23(6), p. 3339. Available at: https://doi.org/10.3390/s23063339.

de La Guardia, C.D. *et al.* (1998) 'An aerobiological study of Urticaceae pollen in the city of Granada (S. Spain): Correlation with meteorological parameters', *Grana*, 37(5), pp. 298–304. Available at: https://doi.org/10.1080/00173139809362682.

Latif, R. *et al.* (2021) 'First report et al. of Didymella americana causing leaf blight on Lily [Lilium hybrida (Longiflorum x Asiatic)] in India', *Indian Phytopathology*, 74(3), pp. 855–857. Available at: https://doi.org/10.1007/s42360-021-00386-4.

Li, D.W. and Kendrick, B. (1995) ‘A year-round study on functional relationships of airborne fungi with meteorological factors’, *International Journal of Biometeorology*, 39(2), pp. 74–80. Available at: https://doi.org/10.1007/BF01212584.

Li, J. *et al.* (2020) ‘Size-resolved dynamics of indoor and outdoor fluorescent biological aerosol particles in a bedroom: A one-month case study in Singapore’, *Indoor Air*, 30(5), pp. 942–954. Available at: https://doi.org/10.1111/ina.12678.

Lieberherr, G. *et al.* (2021) ‘Assessment of real-time bioaerosol particle counters using reference chamber experiments’, *Atmospheric Measurement Techniques*, 14(12), pp. 7693–7706. Available at: https://doi.org/10.5194/amt-14-7693-2021.

Lim, S.H. *et al.* (1998) ‘Outdoor airborne fungal spores in Singapore’, *Grana*, 37(4), pp. 246–252. Available at: https://doi.org/10.1080/00173139809362674.

Luo, Y. *et al.* (2021) ‘The effects of indoor air pollution from solid fuel use on cognitive function among middle-aged and older population in China’, *Science of The Total Environment*, 754, p. 142460. Available at: https://doi.org/10.1016/j.scitotenv.2020.142460.

Madhwal, S. *et al.* (2020) ‘Ambient bioaerosol distribution and associated health risks at a high traffic density junction at Dehradun city, India’, *Environmental Monitoring and Assessment*, 192(3), p. 196. Available at: https://doi.org/10.1007/s10661-020-8158-9.

Mandal, J. and Brandl, H. (2011) ‘Bioaerosols in Indoor Environment - A Review with Special Reference to Residential and Occupational Locations’, *The Open Environmental & Biological Monitoring Journal*, 4(1). Available at: https://benthamopen.com/ABSTRACT/TOEBMJ-4-83 (Accessed: 10 July 2023).

Markey, E. *et al.* (2022) ‘A Modified Spectroscopic Approach for the Real-Time Detection of Pollen and Fungal Spores at a Semi-Urban Site Using the WIBS-4+, Part I’, *Sensors*, 22(22), p. 8747. Available at: https://doi.org/10.3390/s22228747.

Martinez-Bracero, M. *et al.* (2022) ‘Airborne Fungal Spore Review, New Advances and Automatisation’, *Atmosphere*, 13(2), p. 308. Available at: https://doi.org/10.3390/atmos13020308.

Maya-Manzano, J.M. *et al.* (2021) ‘Spatial and temporal variations in the distribution of birch trees and airborne Betula pollen in Ireland’, *Agricultural and Forest Meteorology*, 298–299, p. 108298. Available at: https://doi.org/10.1016/j.agrformet.2020.108298.

MCCARTNEY, H.A. and LACEY, M.E. (1990) ‘The production and release of ascospores of Pyrenopeziza brassicae on oilseed rape’, *Plant Pathology*, 39(1), pp. 17–32. Available at: https://doi.org/10.1111/j.1365-3059.1990.tb02471.x.

McNabola, A. *et al.* (2011) ‘Analysis of the relationship between urban background air pollution concentrations and the personal exposure of office workers in Dublin, Ireland, using baseline separation techniques’, *Atmospheric Pollution Research*, 2(1), pp. 80–88. Available at: https://doi.org/10.5094/APR.2011.010.

Monroy-Colín, A. *et al.* (2020) ‘HYSPLIT as an environmental impact assessment tool to study the data discrepancies between Olea europaea airborne pollen records and its phenology in SW Spain’, *Urban Forestry & Urban Greening*, 53, p. 126715. Available at: https://doi.org/10.1016/j.ufug.2020.126715.

Moulin, C. *et al.* (1997) ‘Control of atmospheric export of dust from North Africa by the North Atlantic Oscillation’, *Nature*, 387(6634), pp. 691–694. Available at: https://doi.org/10.1038/42679.

Nazaroff, W.W. (2016) ‘Teaching indoor environmental quality’, *Indoor Air*, 26(4), pp. 515–516. Available at: https://doi.org/10.1111/ina.12309.

Nevalainen, A., Täubel, M. and Hyvärinen, A. (2015) ‘Indoor fungi: companions and contaminants’, *Indoor Air*, 25(2), pp. 125–156. Available at: https://doi.org/10.1111/ina.12182.

Norris-Hill, J. (1997) 'The Influence of Ambient Temperature on the Abundance of Poaceae Pollen', *Aerobiologia (Bologna*, 13, pp. 91-97,. Available at: https://doi.org/10.1007/BF02694424.

O'Connor, D.J. *et al.* (2014) 'Using the WIBS-4 (Waveband Integrated Bioaerosol Sensor) Technique for the On-Line Detection of Pollen Grains', *Aerosol Science and Technology*, 48(4), pp. 341–349. Available at: https://doi.org/10.1080/02786826.2013.872768.

O'Connor, D.J., Daly, S.M. and Sodeau, J.R. (2015) 'On-line monitoring of airborne bioaerosols released from a composting/green waste site', *Waste Management*, 42, pp. 23–30. Available at: https://doi.org/10.1016/j.wasman.2015.04.015.

O'Gorman, C.M. and Fuller, H.T. (2008) 'Prevalence of culturable airborne spores of selected allergenic and pathogenic fungi in outdoor air', *Atmos. Environ*, 42, pp. 4355–4368. Available at: https://doi.org/10.1016/j.atmosenv.2008.01.009.

Pace, L. *et al.* (2019) 'Temporal variations in the diversity of airborne fungal spores in a Mediterranean high altitude site', *Atmospheric Environment*, 210, pp. 166–170. Available at: https://doi.org/10.1016/j.atmosenv.2019.04.059.

Pan, Y. Le *et al.* (2021) 'Atmospheric aging processes of bioaerosols under laboratory-controlled conditions: A review', *Journal of Aerosol Science*, 155(January), p. 105767. Available at: https://doi.org/10.1016/j.jaerosci.2021.105767.

Patel, T.Y. *et al.* (2018) 'Variation in airborne fungal spore concentrations among five monitoring locations in a desert urban environment', *Environmental Monitoring and Assessment*, 190(11), p. 634. Available at: https://doi.org/10.1007/s10661-018-7008-5.

Pearson, C. *et al.* (2015) 'Exposures and health outcomes in relation to bioaerosol emissions from composting facilities: a systematic review of occupational and community studies', *Journal of Toxicology and Environmental Health. Part B, Critical Reviews*, 18(1), pp. 43–69. Available at: https://doi.org/10.1080/10937404.2015.1009961.

Pérez-Badia, R. *et al.* (2013) 'Dynamics and Behaviour of Airborne Quercus Pollen in Central Iberian Peninsula', *Aerobiologia (Bologna*, 29, pp. 419-428,. Available at: https://doi.org/10.1007/s10453-013-9294-2.

Perring, A.E. *et al.* (2015) 'Airborne observations of regional variation in fluorescent aerosol across the United States', *Journal of Geophysical Research: Atmospheres*, 120(3), pp. 1153–1170. Available at: https://doi.org/10.1002/2014JD022495.

Pfaar, O. *et al.* (2017) 'Defining pollen exposure times for clinical trials of allergen immunotherapy for pollen-induced rhinoconjunctivitis - an EAACI position paper', *Allergy*, 72(5), pp. 713–722. Available at: https://doi.org/10.1111/all.13092.

Pöhlker, C., Huffman, J.A. and Pöschl, U. (2012) 'Autofluorescence of atmospheric bioaerosols – fluorescent biomolecules and potential interferences', *Atmospheric Measurement Techniques*, 5(1), pp. 37–71. Available at: https://doi.org/10.5194/amt-5-37-2012.

Post, W., Heederik, D. and Houba, R. (1998) 'Decline in lung function related to exposure and selection processes among workers in the grain processing and animal feed industry', *Occupational and Environmental Medicine*, 55(5), pp. 349–355. Available at: https://doi.org/10.1136/oem.55.5.349.

R Core Team (2017) 'R: A Language and Environment for Statistical Computing'. Foundation for Statistical Computing; Vienna, Austria, 2017.

Robinson, N.H. *et al.* (2013) 'Cluster analysis of WIBS single-particle bioaerosol data', *Atmos. Meas. Tech*, 6, pp. 337–347. Available at: https://doi.org/10.5194/amt-6-337-2013.

Rodríguez de la Cruz, D., Sánchez-Reyes, E. and Sánchez-Sánchez, J. (2015) 'A contribution to the knowledge of Cupressaceae airborne pollen in the middle west of Spain', *Aerobiologia*, 31(4), pp. 435–444. Available at: https://doi.org/10.1007/s10453-015-9376-4.

Ruiz-Gil, T. *et al.* (2020) 'Airborne bacterial communities of outdoor environments and their associated influencing factors', *Environment International*, 145, p. 106156. Available at: https://doi.org/10.1016/j.envint.2020.106156.

Ruske, S. *et al.* (2018) 'Machine learning for improved data analysis of biological aerosol using the WIBS', *Atmospheric Measurement Techniques*, 11(11), pp. 6203–6230. Available at: https://doi.org/10.5194/amt-11-6203-2018.

Sarda Estève, R. *et al.* (2018) 'Temporal Variability and Geographical Origins of Airborne Pollen Grains Concentrations from 2015 to 2018 at Saclay, France', *Remote Sensing*, 10(12), p. 1932. Available at: https://doi.org/10.3390/rs10121932.

Sarda-Estève, R. *et al.* (2018) 'Temporal Variability and Geographical Origins of Airborne Pollen Grains Concentrations from 2015 to 2018 at Saclay, France', *Remote Sensing*, 10. Available at: https://doi.org/10.3390/rs10121932.

Sarda-Estève, R. *et al.* (2019) 'Variability and Geographical Origin of Five Years Airborne Fungal Spore Concentrations'. Available at: https://doi.org/10.3390/rs11141671.

Sarda-Estève, Roland *et al.* (2019) 'Variability and Geographical Origin of Five Years Airborne Fungal Spore Concentrations Measured at Saclay, France from 2014 to 2018', *Remote Sensing*, 11(14), p. 1671. Available at: https://doi.org/10.3390/rs11141671.

Sarda-Estève, R. *et al.* (2020) 'Atmospheric Biodetection Part I: Study of Airborne Bacterial Concentrations from January 2018 to May 2020 at Saclay, France', *International Journal of Environmental Research and Public Health*, 17(17), p. E6292. Available at: https://doi.org/10.3390/ijerph17176292.

Sauvageat, E. *et al.* (2020) 'Real-time pollen monitoring using digital holography', *Atmospheric Measurement Techniques*, 13(3), pp. 1539–1550. Available at: https://doi.org/10.5194/amt-13-1539-2020.

Savage, N.J. *et al.* (2017) 'Systematic characterization and fluorescence threshold strategies for the wideband integrated bioaerosol sensor (WIBS) using size-resolved biological and interfering particles', *Atmos. Meas. Tech*, 10, pp. 4279–4302. Available at: https://doi.org/10.5194/amt-10-4279-2017.

Savage, Nicole J. *et al.* (2017) 'Systematic characterization and fluorescence threshold strategies for the wideband integrated bioaerosol sensor (WIBS) using size-resolved biological and interfering particles', *Atmospheric Measurement Techniques*, 10(11), pp. 4279–4302. Available at: https://doi.org/10.5194/amt-10-4279-2017.

Savage, N.J. and Huffman, J.A. (2018) 'Evaluation of a hierarchical agglomerative clustering method applied to WIBS laboratory data for improved discrimination of biological particles by comparing data preparation techniques', *Atmos. Meas. Tech*, 11, pp. 4929–4942. Available at: https://doi.org/10.5194/amt-11-4929-2018.

Sessa, R. *et al.* (2002) 'Microbiological indoor air quality in healthy buildings', *The New Microbiologica*, 25(1), pp. 51–56.

Shaffer, B.T. and Lighthart, B. (1997) 'Survey of Culturable Airborne Bacteria at Four Diverse Locations in Oregon: Urban, Rural, Forest, and Coastal', *Microbial Ecology*, 34(3), pp. 167–177. Available at: https://doi.org/10.1007/s002489900046.

Shoute, L.C.T. *et al.* (2018) 'Immuno-impedimetric Biosensor for Onsite Monitoring of Ascospores and Forecasting of Sclerotinia Stem Rot of Canola', *Scientific Reports*, 8(1), pp. 1–9. Available at: https://doi.org/10.1038/s41598-018-30167-5.

Siqueira, V.M. *et al.* (2011) 'Filamentous Fungi in Drinking Water, Particularly in Relation to Biofilm Formation', *International Journal of Environmental Research and Public Health*, 8(2), pp. 456–469. Available at: https://doi.org/10.3390/ijerph8020456.

Skjøth, C.A. *et al.* (2007) 'The long-range transport of birch (Betula) pollen from Poland and Germany causes significant pre-season concentrations in Denmark', *Clin. Exp. Allergy*, 37, pp. 1204–1212. Available at: https://doi.org/10.1111/j.1365-2222.2007.02771.x.

Skjøth, C.A. *et al.* (2021) 'Air Pollution Affecting Pollen Concentrations through Radiative Feedback in the Atmosphere', *Atmosphere*, 12(11), p. 1376. Available at: https://doi.org/10.3390/atmos12111376.

Spiers, A.G. (1985) 'Factors affecting basidiospore release by Chondrostereum purpureum in New Zealand', *European Journal of Forest Pathology*, 15(2), pp. 111–126. Available at: https://doi.org/10.1111/j.1439-0329.1985.tb00874.x.

Stanley, S., W.R.K.,. P, (2009) 'WIBS-4 Bioaerosol Sensor: User Manual'.

Swanson, B.E. and Huffman, J.A. (2018) 'Development and characterization of an inexpensive single-particle fluorescence spectrometer for bioaerosol monitoring', *Opt. Express*, 26, p. 3646. Available at: https://doi.org/10.1364/oe.26.003646.

Targonski, P.V., Persky, V.W. and Ramekrishnan, V. (1995) 'Effect of environmental molds on risk of death from asthma during the pollen season', *Journal of Allergy and Clinical Immunology*, 95(5), pp. 955–961. Available at: https://doi.org/10.1016/S0091-6749(95)70095-1.

Toprak, E. and Schnaiter, M. (2013) 'Fluorescent biological aerosol particles measured with the Waveband Integrated Bioaerosol Sensor WIBS-4: laboratory tests combined with a one year field study', *Atmospheric Chemistry and Physics*, 13(1), pp. 225–243. Available at: https://doi.org/10.5194/acp-13-225-2013.

Tournas, V.H. (2005) 'Spoilage of vegetable crops by bacteria and fungi and related health hazards', *Critical Reviews in Microbiology*, 31(1), pp. 33–44. Available at: https://doi.org/10.1080/10408410590886024.

Trapero-Casas, A., Navas-Cortés, J.A. and Jiménez-Díaz, R.M. (1996) 'Airborne ascospores of Didymella rabiei as a major primary inoculum for Ascochyta blight epidemics in chickpea crops in southern Spain', *European Journal of Plant Pathology*, 102(3), pp. 237–245. Available at: https://doi.org/10.1007/BF01877962.

Troutt, C. and Levetin, E. (2001) 'Correlation of spring spore concentrations and meteorological conditions in Tulsa, Oklahoma', *International Journal of Biometeorology*, 45(2), pp. 64–74. Available at: https://doi.org/10.1007/s004840100087.

Tummon, F., Adamov, S., *et al.* (2021) 'A first evaluation of multiple automatic pollen monitors run in parallel', *Aerobiologia* [Preprint]. Available at: https://doi.org/10.1007/s10453-021-09729-0.

Tummon, F., Arboledas, L.A., *et al.* (2021) 'The need for Pan-European automatic pollen and fungal spore monitoring: A stakeholder workshop position paper', *Clinical and Translational Allergy*, 11(3), p. e12015. Available at: https://doi.org/10.1002/clt2.12015.

Twohy, C.H. *et al.* (2016) 'Abundance of fluorescent biological aerosol particles at temperatures conducive to the formation of mixed-phase and cirrus clouds', *Atmos. Chem. Phys*, 16, pp. 8205–8225. Available at: https://doi.org/10.5194/acp-16-8205-2016.

Vélez-Pereira, A.M. *et al.* (2019) 'Logistic regression models for predicting daily airborne Alternaria and Cladosporium concentration levels in Catalonia (NE Spain', *Int. J. Biometeorol*, 63, pp. 1541–1553.

Vélez-Pereira, A.M. *et al.* (2021) 'Spatial distribution of fungi from the analysis of aerobiological data with a gamma function', *Aerobiologia*, 37(3), pp. 461–477. Available at: https://doi.org/10.1007/s10453-021-09696-6.

de Weger, L.A. *et al.* (2016) 'The long distance transport of airborne Ambrosia pollen to the UK and the Netherlands from Central and south Europe', *International Journal of Biometeorology*, 60(12), pp. 1829–1839. Available at: https://doi.org/10.1007/s00484-016-1170-7.

World Health Organization. Occupational and Environmental Health Team (2006) *WHO Air quality guidelines for particulate matter, ozone, nitrogen dioxide and sulfur dioxide : global update 2005 : summary of risk*

assessment. WHO/SDE/PHE/OEH/06.02. World Health Organization. Available at: https://apps.who.int/iris/handle/10665/69477 (Accessed: 29 September 2021).

Xie, W. *et al.* (2020) 'The source and transport of bioaerosols in the air: A review', *Frontiers of Environmental Science & Engineering*, 15(3), p. 44. Available at: https://doi.org/10.1007/s11783-020-1336-8.

Yue, S. *et al.* (2016) 'Springtime precipitation effects on the abundance of fluorescent biological aerosol particles and HULIS in Beijing', *Scientific Reports*, 6(June), pp. 1–10. Available at: https://doi.org/10.1038/srep29618.

Zang, L. *et al.* (2019) 'Roles of Relative Humidity in Aerosol Pollution Aggravation over Central China during Wintertime', *International Journal of Environmental Research and Public Health*, 16(22), p. 4422. Available at: https://doi.org/10.3390/ijerph16224422.

Zbîrcea, L.-E. *et al.* (2023) 'Relationship between IgE Levels Specific for Ragweed Pollen Extract, Amb a 1 and Cross-Reactive Allergen Molecules', *International Journal of Molecular Sciences*, 24(4), p. 4040. Available at: https://doi.org/10.3390/ijms24044040.

Zhang, M. *et al.* (2021) 'Sensitivities to biological aerosol particle properties and ageing processes: potential implications for aerosol–cloud interactions and optical properties', *Atmospheric Chemistry and Physics*, 21(5), pp. 3699–3724. Available at: https://doi.org/10.5194/acp-21-3699-2021.

Chapter 4 - Conclusion

The WIBS was stationed in Saclay from 21st April to 5th June 2017 to assess its capability to detect, count, and distinguish between pollen and fungal spores. The device was positioned alongside the traditional Hirst instrument to compare ambient levels of pollen and fungal spores. The particles isolated by the WIBS strongly correlated with overall ambient pollen ($R^2 = 0.6$) and total fungal spore ($R^2 = 0.8$) concentrations. However, deviations were noted during elevated pollen levels, primarily when the pollen grains were found to be more significant. This was ascribed to the variance in the sampling efficiencies of the two instruments for different particle sizes, which resulted from inconsistent flow rates.

Traditional monitoring of pollen and fungal spores was conducted using a Hirst volumetric trap. It identified 47 types of pollen and 27 types of fungal spores. The most common pollen types were Quercus, Poaceae, and Urticaceae, while Ascospores and Cladosporium dominated the fungal spores. Fungal spore peaks exceeded 30,000 spores/m^3 on several occasions, primarily driven by Ascospores and Cladosporium. This data contributes to long-term trend analysis of allergens and pollutants in the Saclay region, aiding public health interventions and air quality improvement. High fungal spore concentrations were linked to dry and hot weather in June 2017. The study also highlighted the influence of temperature and relative humidity on PBAP concentrations. Ascospores correlated with humidity, while Cladosporium and basidiospores showed a positive correlation with temperature, consistent with prior research. The role of rain in increasing bioaerosol concentrations was also significant.

The study found that approximately 38% of particles in the Saclay monitoring campaign were classified as fluorescent. Concentrations of supermicron fluorescent particles in the air varied, ranging from 2.1×10^4 to 8.7×10^4 particles per cubic meter. These variations were attributed to

geographically diverse bioaerosols. Despite the primary focus on bioaerosols, the WIBS system showed potential for detecting anthropogenic aerosols, though further investigation is needed, especially in complex ambient environments.

Real-time monitoring systems for PBAPs, including those based on WIBS or similar technologies can enable rapid response to changing environmental conditions, especially concerning the presence of allergens or pathogens in the air. The time-consuming nature of this data analysis from WIBS or related systems in handling large volumes of real-time data can be challenging. Automation and advancements in data processing techniques, including machine learning algorithms for pattern recognition, can potentially play a role in streamlining this process.

Real-time monitoring devices provide immediate and continuous data updates, making them highly valuable for applications where timely information is essential. The distinction between "real-time" and "almost real-time" often lies in the latency or delay in data reporting. Real-time devices which provide instant data updates, typically with minimal delays, allow for a more immediate response when collecting data. It's fundamental to understand the operational characteristics of these systems with the temporal requirements of the monitoring campaign. Advances in technology continue to enhance the capabilities of real-time sensors, aiming to provide more accurate and timely data for future aerobiology studies. The current discussion surrounding the performance of the KH-3000 and the recognition of the BAA500 as a more precise device contribute valuable insights to the progress of real-time monitoring.

The comparison between the WIBS and Hirst instrumentation involved addressing the differences in their operating principles and sampling capabilities. The WIBS can detect smaller particles (as small as 0.5 μm), including bacteria, while the Hirst system relied on microscopic analysis and was found to be less efficient for particles smaller than about 2 μm. The difference in particle size

detection led to variations in counts of FAP, fungal spores, and pollen grains between the two systems. To enable a meaningful comparison, the WIBS data was pre-processed by removing particles smaller than 2 μm. While this pre-processing step might have excluded data about smaller bioaerosols, it aligns the size range of particles analysed by both systems, which allowed for a more accurate comparison of FAP data with fungal spore and pollen concentrations measured by the Hirst system.

In the diurnal plots, the average hourly patterns for A and AB particles peaked in the early morning and late afternoon, consistent with fungal spore patterns observed in previous research. These patterns were similar to those observed in the diurnal variation of fungal spore concentration recorded by the Hirst system. In contrast, B, BC, and ABC particles exhibited different diurnal patterns, with peaks during the middle of the day, possibly indicating an anthropogenic source. Correlation plots were used to visually represent the relationships between variables. Strong associations were found between the WIBS instrument and both total fungal spore concentrations and fungal spore concentrations excluding Cladosporium. While good agreement was observed for Cladosporium spores and A particles, a slight decrease in correlation was noted, suggesting that Cladosporium sensitivity might be lower due to various factors.

For pollen analysis, strong correlations were found between total pollen concentrations and ABC, B, and BC types of particles. The best conditions for identifying pollen-type FAPs involved isolating particles larger than 2 μm with specific fluorescence intensities (FL2 and FL3) exceeding 1300. The data from the WIBS closely mirrored the patterns in total pollen concentrations for most of the monitoring period. However, larger pollen types, such as Pinus and Poaceae, were not as effectively captured by the WIBS. Additionally, substantial pollen varieties might have undergone losses due to sedimentation within the inlet system, further contributing to under-sampling. Fluorescence measurements of PBAPs face challenges in terms of interferences and uncertainty

introduced by anthropogenic emissions. Each fluorophore species exhibits a unique fluorescence spectrum, allowing for effective differentiation of biological particles from other FAPs based on their specific excitation-emission matrix. The limitations of excitation and emission wavebands in the WIBS underscore the need for the development of a multi-waveband instrument. The approach of cluster analysis has demonstrated an improved ability to distinguish various FAPs. Integrating additional particle properties, such as size and morphology, can enhance the discrimination of fluorescent particles with different emission mechanisms and mitigate interferences.

The primary focus is on the application of K-means clustering to the A and AB (3σ) particle combinations associated with fungal spores. The results indicated that K-means clustering provided slightly better correlations and explained more variance in the data for both total pollen and total fungal spores, as compared to the original particle filtering methods. This suggests that K-means clustering is a promising alternative for data analysis in this context.

In conclusion, the research findings are encouraging, demonstrating that the WIBS can effectively differentiate between distinct types of biological aerosols, including pollen and fungal spores. The strong agreement observed with ambient pollen concentrations suggests that future sensor development efforts could potentially lead to improved bioaerosol detection capabilities. Further studies should be conducted between air quality and meteorological parameters in the context of bioaerosol monitoring in Ireland. At present, Met Éireann and Dr David O'Connor at DCU are using the Swissens Poleno Jupiter with an advanced optical particle measurement laser capable of assessing both pollen/ fungal spores and various airborne pollutants in the atmosphere. It operates concurrently with traditional monitoring methods, facilitating the comparison of results. Integrated AI in the unit has the potential to promptly identify, measure, and count individual pollen particles, quickly providing results for possible submission in dispersion models for Irish forecasts. These

insights have the potential to benefit various fields, including environmental monitoring, public health, and atmospheric science.